

Copyright is owned by the Author of the thesis. Permission is given for a copy to be downloaded by an individual for the purpose of research and private study only. The thesis may not be reproduced elsewhere without the permission of the Author.

Synthetic Test Patterns and Compression Artefact Distortion Metrics for Image Codecs

Amal Punchihewa

2009

Synthetic Test Patterns and Compression Artefact Distortion Metrics for Image Codecs

A thesis presented in partial fulfilment of the requirements for the degree of Doctor of
Philosophy in Engineering at Massey University, Palmerston North, New Zealand.

Amal Punchihewa

2009

To

My parents, family

&

Those all who supported this endeavour

Acknowledgements

I would like to thank my two supervisors Associate Professor Donald Bailey and Professor Bob Hodgson for their support, encouragement, understanding and patience. Over these years, they provided me with valuable guidance and tools to perform my research. I would also like to thank Dr. Steven Marsland for his comments during my thesis writing.

I would like to thank my family, wife Dilantha and three daughters Chamilka, Minushika and Sashini for their sacrifices during the last seven years.

This work was supported in numerous ways by Massey University, especially the Institute of Information Sciences and Technology and the School of Engineering and Advanced Technology. I appreciate the continued support given by former heads of the Institute of Information Sciences and Technology, Professor Bob Hodgson and Professor Janina Mazierska and also the current head of the School of Engineering and Advanced Technology, Professor Don Cleland. The support extended by them for me to attend conferences enabled twenty two peer reviewed publications in the proceedings of respective conferences solely from my PhD research. The networking at conferences gave me exposure to wider research community in the road to the completion of my PhD research while working as a full time senior staff member of Massey University.

Abstract

This thesis presents a framework of test methodology to assess spatial domain compression artefacts produced by image and intra-frame coded video codecs. Few researchers have studied this broad range of artefacts. A taxonomy of image and video compression artefacts is proposed. This is based on the point of origin of the artefact in the image communication model. This thesis presents objective evaluation of distortions known as artefacts due to image and intra-frame coded video compression made using synthetic test patterns. The American National Standard Institute document ANSI T1 801 qualitatively defines blockiness, blur and ringing artefacts. These definitions have been augmented with quantitative definitions in conjunction with test patterns proposed.

A test and measurement environment is proposed in which the codec under test is exercised using a portfolio of test patterns. The test patterns are designed to highlight the artefact under study. Algorithms have been developed to detect and measure individual artefacts based on the characteristics of respective artefacts. Since the spatial contents of the original test patterns form known structural details, the artefact distortion metrics based on the characteristics of those artefacts are clean and swift to calculate. Distortion metrics are validated using a human vision system inspired modern image quality metric.

Blockiness, blur and ringing artefacts are evaluated for representative codecs using proposed synthetic test patterns. Colour bleeding due to image and video compression is discussed with both qualitative and quantitative definitions for the colour bleeding artefacts introduced. The image reproduction performance of a few codecs was evaluated to ascertain the utility of proposed metrics and test patterns.

Keywords:

Compression, artefacts, coding, multipath, artefact mitigation, image and video quality, subjective assessment, objective assessment, test patterns, blockiness, blur, ringing, colour bleeding, JPEG, JPEG2000, MPEG, colour blur, colour ringing.

Table of Contents

Acknowledgements	4
Abstract	5
<i>Keywords:</i>	5
Table of Contents	6
Publications:.....	9
Chapter 1: Introduction.....	13
1.1 Background Information.....	13
1.1.1 <i>Image Communications</i>	13
1.1.2 <i>Colour Attributes and Coding in Television Broadcasting</i>	14
1.1.3 <i>Overview of JPEG, JPEG2000 and MPEG CODECs</i>	17
1.2 Description of the Problem.....	19
1.3 Motivations for this Thesis	21
1.4 Review of the Use of Synthetic Test Patterns in Compression Distortion Evaluation.....	23
1.5 Thesis Aims and the Scope of Research.....	24
1.6 Proposed Framework and Approach	24
1.7 Summary of Contributions	25
1.8 Organisation of the Thesis	26
Chapter 2: Taxonomy for Image Communication Artefacts	31
2.1 Introduction to Artefacts	31
2.2 Capture Artefacts	33
2.3 Processing Artefacts	34
2.4 Delivery Artefacts.....	36
2.5 Display Artefacts	38
2.6 Human Visual System related Artefacts	39
2.7 Artefact Mitigation Techniques	40
2.7.1 <i>Artefact Mitigation Techniques for Analogue Systems</i>	40
2.7.2 <i>Artefact Mitigation Techniques for Digital Systems</i>	42
2.8 Spatial-domain only Compression Artefacts	43
2.9 Chapter Summary and Conclusions	44
Chapter 3: Review of Image Quality Assessment	46
3.1 Quality of an Image	46
3.2 Picture Quality	47
3.3 Signal Quality.....	48
3.4 Fidelity Metrics.....	48
3.5 Quality Metrics	49
3.6 Methods of Quality Assessment	50
3.6.1 <i>Subjective Test Methods</i>	50
3.6.2 <i>Objective Test Methods</i>	53
3.6.3 <i>Objective Quality Metrics</i>	53
3.6.4 <i>Double-ended Quality Measure</i>	54
3.6.5 <i>Single-ended Quality Measure</i>	55
3.7 Commercial Systems	56
3.8 Structural Similarity Based Image Quality Assessment	56
3.9 Video Quality Experts Group (VQEG)	57
3.10 Discussion and Conclusions	58

Chapter 4: Test Pattern Generation for Compression Artefacts.....	60
4.1 General Philosophy of Synthetic Test Pattern Design.....	60
4.2 Blocking Artefact.....	61
4.2.1 Qualitative Definition.....	61
4.2.2 First Generation – Test Pattern ‘sine-squared grey scale –diagonal’.....	62
4.2.3 Second Generation – Test Pattern ‘sine-squared grey scale – radial’.....	64
4.2.4 Possibility for Sequence Generation.....	65
4.3 Blur and Ringing Artefacts	66
4.3.1 Qualitative Definition.....	67
4.3.2 First Generation – Test Pattern ‘monochrome rings’.....	68
4.3.3 Second Generation – Test Pattern ‘colour rings’.....	70
4.3.4 Possibility for Sequence Generation.....	73
4.4 Colour Bleeding Artefact.....	73
4.4.1 Qualitative Definition.....	74
4.4.2 First Generation - Test Pattern ‘colour rings’.....	77
4.4.3 Second Generation – Test Pattern ‘honeycomb’.....	78
4.4.4 Luminance Modulation.....	79
4.4.5 Colour Attribute Transformation.....	81
4.4.6 Random Test Pattern Generation.....	84
4.4.7 Possibility for Sequence Generation.....	85
Chapter 5: Distortion Metrics for Compression Artefacts	86
5.1 Blockiness Artefact Metrics	86
5.1.1 Quantitative Definition of Blockiness.....	86
5.2 Blur and Ringing Artefact Metrics	90
5.2.1 Quantitative Definition of Blur and Ringing.....	91
5.2.2 Algorithm.....	92
5.2.3 Influence of Contrast on Blur and Ringing.....	97
5.3 Colour Bleeding Artefact Metrics	99
5.3.1 Quantitative Definition of Colour Bleeding.....	99
5.3.2 Algorithms.....	101
5.3.3 Spatial Scalability of iso-luminance honeycomb test pattern	104
5.3.4 Components of Colour Bleeding	105
Chapter 6: Evaluation of Metrics for Compression Artefacts	108
6.1 Blockiness Artefact Distortion Metrics	108
6.1.1 Experiment I – Evaluation of Blockiness Distortion Metrics.....	108
6.1.2 Experiment II – Validation of Blockiness Distortion Metric.....	112
6.2 Blur Artefact Distortion Metric	113
6.2.1 Experiment III – Evaluation of Blur Distortion Metric.....	113
6.2.2 Experiment IV – Validation of Blur Distortion Metric.....	114
6.3 Ringing Artefact Distortion Metric	116
6.3.1 Experiment V – Evaluation of Ringing Distortion Metric.....	116
6.3.2 Experiment VI - Validation of Ringing Distortion Metric.....	117
6.4 Colour Bleeding Artefact Distortion Metrics	118
6.4.1 Experiment VII – Evaluation of Colour bleeding metrics.....	118
6.4.2 Experiment VIII – Validation of Colour bleeding metric.....	123
6.5 Chapter Summary and Conclusions	125
Chapter 7: Performance Evaluation of Image Codecs	126
7.1 Benchmarking Codec Implementations.....	126
7.1.1 Experiment –IX Comparison of Blockiness due to JPEG codecs - IrfanView™ Vs Matlab™.....	126
7.1.2 Experiment –X Comparison of Blockiness due to IrfanView™ codecs - JPEG vs. JPEG2000.....	127
7.1.3 Experiment –XI Comparison of Blur due to IrfanView™ JPEG and JPEG2000 codecs	129

7.1.4	<i>Experiment –XII Comparison of Ringing due to IrfanView™ JPEG Vs JPEG2000 codecs.....</i>	<i>130</i>
7.1.5	<i>Experiment –XIII Comparison of Colour Bleeding due to JPEG and JPEG2000 codecs – Using Honeycomb test pattern.....</i>	<i>131</i>
7.1.6	<i>Experiment XIV – Comparison of Colour Bleeding due to JPEG and JPEG2000 codecs random colour circles test pattern.....</i>	<i>135</i>
7.1.7	<i>Experiment XV - Comparison of Colour Ringing and Blur due to JPEG and JPEG2000 codecs - Using Isoluma colour rings test pattern.....</i>	<i>138</i>
7.2	Pre and Post-processing Algorithms.....	141
7.2.1	<i>Experiment - XVI De-blocking in an MPEG-4 codec.....</i>	<i>141</i>
7.3	Integrated Test and Measurement Environment	143
7.3.1	<i>Block Diagram of the Integrated Environment.....</i>	<i>143</i>
7.3.2	<i>Visualisation</i>	<i>144</i>
7.4	Objective Measurement of Artefacts in MPEG-4 and Advanced Codecs.	144
7.5	Chapter Summary and Conclusions	147
	Chapter 8: Summary, Conclusions and Future work	148
8.1	Summary.....	148
8.2	Conclusions	150
8.3	Future Work.....	151
	Chapter 9: References.....	152
	Appendix 1: Ghosting Artefacts: Z-domain Analysis of Ghost Cancellation for Television Signals	172
A-1.1	Background	172
A-1.2	Multi-path Channel Characterisation.....	173
A-1.3	Analysis in the Z-Domain.....	176
A-1.4	Channel Characteristics in the Presence of Echoes	176
A-1.5	Echoes and Ghost Cancellation	183
A-1.6	Characterising the Channel.....	187
A-1.7	Summary and Conclusions	189
	Appendix 2: Test Patterns used in Analogue Television Broadcasting:	191
	Appendix 3: ANSI T1.801.02-1996 Definitions of Compression Artefacts:	196
	Appendix 4: Abbreviations	197
	Appendix 5: Glossary.....	199
	Appendix 6: List of Image and Video Artefacts:	200
	Appendix 7: Vectorscope Graphs:.....	203
	Appendix 8: Test Patterns (uncompressed) that are Designed and Used in this Thesis:.....	205
	Appendix 9: Bibliography:	207

Publications:

Publications prepared during the course of research for this thesis include:

Journal Papers:

- [1] G.A.D. Punchihewa, D.G. Bailey and R.M. Hodgson, "Benchmarking Image Codecs by Assessment of Coded Test Images: The development of Test Images and New Objective Quality Metrics", *Journal of Telecommunications and Information Technology (JTIT2006)*, 1/2006, pp 11-16, 2006.
- [2] A. Punchihewa, J Armstrong, S. Hangai, T Hamamoto, "Components of Colour Distortions due to Image Compression and Influence of Luminance", to be published in *The IEICE Transactions on Image processing*, Japan, 2009.

IEEE and IET Conference papers published in the proceedings:

- [3] G.A.D. Punchihewa, D.G. Bailey and R.M. Hodgson, "The Development of a Synthetic Colour Test Image for Subjective and Objective Quality Assessment of Digital Codecs", *11th Asia Pacific Conference on Communications (APCC2005)*, Perth, Australia, pp. 881-885, 2005.
- [4] G.A.D. Punchihewa, D.G. Bailey and R.M. Hodgson, "The Development of a Novel Image Quality Metric and a Synthetic Colour Test Image for Objective Quality Assessment of Digital Codecs", *The IEEE Telecommunication Conference Region 10, (IEEE Tencon 2005)*, Melbourne, Australia, pp. 1-6, 2005.
- [5] A. Punchihewa, D. Salvador, "An Integrated Environment for Objective Evaluation of Digital Codecs using a Small set of Novel Image Quality Metrics and Synthetic Test Images", *The IEEE International Conference on Information and Automation (ICIA 2005)*, Sri Lanka, pp.1-6, 2005.
- [6] G. A. Punchihewa, "A random colour test pattern generator for objective colour artefact assessment in benchmarking colour image codecs", *The IEEE*

International Conference on Information and Automation (ICIA 2006), Sri Lanka, pp. 307-312, 2006.

- [7] A. Punchihewa, J. Armstrong, "Objective Evaluation of Colour Bleeding Artefact due to Image Codecs", *Proceedings of Visual Information Engineering Conference (VIE 2008)*, Xian, China, pp. 312-317, 2008.

Other peer reviewed papers published in the proceedings of the conferences.

- [8] G.A.D. Punchihewa, J. Armstrong, "Encoder Artefact Assessment for Visual media; An Engineering Approach", *Broadcast Asia Conference (BCA 2008)*, Singapore, pp. 1-6, 2008.
- [9] A. Punchihewa, J. Armstrong, "Benchmarking Video Codecs for Blockiness Compression Artefacts", *Image and Vision Computing New Zealand (IVCNZ 2007)*, Hamilton, New Zealand, pp. 467-472, 2007.
- [10] A. Punchihewa, J. Armstrong, "Objective Evaluation of Intra-Frame Coded Codecs for Blockiness Artefact", *Electronics New Zealand Conference (ENZCon 2007)*, Wellington, New Zealand, pp. 312-317, 2007.
- [11] G.A.D. Punchihewa, D.G. Bailey, and R.M. Hodgson, "Integrated Test and Measurement Environment to Evaluate Codecs for Compression Artefacts", *Broadcast Asia Conference (BCA 2007)*, Singapore, pp. 1-6, 2007.
- [12] G.A.D. Punchihewa, D.G. Bailey, and R.M. Hodgson, "Integrated Test Pattern Generator and Measurement Algorithm for Colour Compression Artefacts in Ubiquitous Spaces", *Image and Vision Computing New Zealand (IVCN 2006)*, Great Barrier Island, New Zealand, pp. 467-472, 2006.
- [13] G.A.D. Punchihewa, D.G. Bailey, and R.M. Hodgson, "Synthetic Colour Test Image for Objective Quality Assessment of Digital Codecs", *Broadcast Asia Conference (BCA2006)*, Singapore, pp. 1-6, 2006.
- [14] A. Punchihewa, D.G. Bailey, and R.M. Hodgson, "Colour Reproduction Performance of JPEG and JPEG2000 Codecs", *8th International Symposium on DSP and Communication Systems, (DSPCS 2005) and 4th Workshop on the Internet, Telecommunications and Signal Processing, (WITSP 2005)*, Noosa Heads, Australia, pp. 312-317, 2005.

- [15] G.A.D. Punchihewa, D.G. Bailey, and R.M. Hodgson, "Objective evaluation of edge blur and ringing artefacts: application to JPEG and JPEG2000 image codecs", *Image and Vision Computing New Zealand (IVCNZ 2005)*, Dunedin, New Zealand, pp. 61-66, 2005.
- [16] G.A.D Punchihewa, D. G. Bailey and R. M. Hodgson, "Objective Quality Assessment of Coded Images: The development of New Quality Metrics", *3rd Workshop on the Internet, Telecommunications and Signal Processing, (WITSP 2004)*, Adelaide, Australia, pp. 1-6, 2004.
- [17] A. Punchihewa, D. G. Bailey, R.M. Hodgson, "MPEG-4 and the challenges of benchmarking its implementations", *Proceedings Image and Vision Computing New Zealand 2004 (IVCNZ'04)*, Akaroa, New Zealand, pp. 71-76, 2004.
- [18] G.A.D. Punchihewa, D.G. Bailey, R.M. Hodgson, "Z-Domain Analysis of Ghost Cancellation for Television Signals", *Proceedings of the 7th International Symposium on Digital Signal Processing for Communication Systems (DSPCS 2003)*, Coolangatta, Australia, pp. 550-556, 2003.
- [19] A. Punchihewa, D.G. Bailey, R.M. Hodgson, "A Survey of Coded Image and Video Quality Assessment", *Proceedings of Image and Vision Computing New Zealand (IVCNZ 2003)*, Palmerston North, New Zealand, pp. 326-331, 2003.
- [20] A. Punchihewa and D.G. Bailey, "Artefacts in Image and Video Systems: Classification and Mitigation", *Proceedings Image and Vision Computing New Zealand (IVCNZ 2002)*, Auckland, New Zealand, pp. 197-202, 2002.
- [21] A. Punchihewa, J. Armstrong, "Objective Evaluation of Components of Colour Distortions due to Image Compression", *The Proceedings of the International Workshop on Image Media Quality (IMQA 2008)*, Kyoto, Japan, pp. 312-317, 2008.
- [22] A. Punchihewa, J. Armstrong, "Effects of Sub-sampling and Quantisation on Colour Bleeding due to Image and Video Compression", *Image and Vision Computing New Zealand (IVCNZ 2008)*, Christchurch, Lincoln, New Zealand, 2008.

- [23] A. Punchihewa, J Armstrong, "Colour Artefacts in JPEG and JPEG2000 Image Codecs" *The Proceedings of the International Conference in Computer Information and Robotic Applications (CIRAS 2007)*, Palmerston North, New Zealand, pp 141-145, 2007.

Chapter 1: Introduction

1.1 Background Information

1.1.1 Image Communications

Image and video communication technologies have been advancing at a rapid pace for the last two decades. MPEG-4 has been deployed in image communication applications yielding higher compression efficiency over MPEG-2 for a given quality [1]. The compression gain is however at the cost of higher encoder and decoder complexities [1]. Ultra high definition television is being researched and developed as a next generation high definition television system. Demonstration systems already operate with image resolution of 4320 x 7680 pixels per frame progressively scanned at 60 frames per second. 10 bits per pixel would result in a raw data rate of 20Gbits/s [2]. The storage and transportation of these signals necessitate a substantial level of compression. There is always need for improved image and video data compression techniques. This need is more pressing with the 3-D television capture and processing now being researched as the next revolution in television broadcasting [3]. Here it is important for the artefacts to be matched between left and right views to minimise stereo fusion instability and viewer fatigue. Scalable and distributed video coding is being researched for future deployments [4], [5]. Thompson Corporate Research has performed an objective assessment using a software scalable video coder (SVC) and observed rate distortion curves [6]. SVC and 3-D television applications demand high performance image and video CODers and DECoders; hereafter referred to as “*codecs*”.

For most digital image and video codecs, increasing bit rate performance has been achieved at the cost of increasing complexity in techniques and implementations. McCann [7], [8] claims that codec development achieves an average reduction in bit rate of 15% per annum. Consumer products that are available today include a broad range of new imaging applications. JPEG and MPEG codecs are in common use in digital photography, digital TV, photographic quality printers and DVDs. Most of these codecs use block-transform based techniques and consequently produce visually

annoying compression artefacts. World Wide Web (WWW), television and multimedia networks also deploy numerous codecs. Both service providers and content providers and end users are using codecs to transfer content between production facilities and to deliver, interact and manage content. However there are problems due to errors in colour, coding and optics related to picture quality, especially from the television engineers' perspective, where the picture quality is well below that of conventional broadcast pictures. Although picture quality evaluation is a complex subject from a professional broadcasters' point of view [9], it needs to be performed to ensure an agreed level of service.

Due to limited bandwidth and storage constraints, the quantity of data needs to be reduced for transporting and storage. Source coders are being deployed for data reduction in communication systems. Codecs have been in use for television since its inception in the 1930s. For example, monochrome television broadcasting has an inherent two to one compression due to the use of interlace scanning. In 1960s, colour television broadcasting was developed to be compatible with monochrome television broadcasting. Analogue colour television broadcasting has six to one compression.

In recent times, it is observed that the time period of system improvement from introduction to maturity of an image codec is about 5~8 years [9]. Furthermore, on average, the long term gain in quality efficiency is about 5~10% per year [9]. Hence, developers need to fine tune and optimise their codecs rapidly to recover the development cost.

1.1.2 Colour Attributes and Coding in Television Broadcasting

In analogue television signal processing, the *RGB* signals are converted to luminance, *Y*, and two colour difference signals, *R-Y* and *B-Y* [10]. The two colour difference signals (*R-Y*) and (*B-Y*) of analogue television broadcasting are weighted and used to modulate a colour sub-carrier using quadrature modulation [11]. The analogue system is commonly called *YUV* (or *YIQ* for the NTSC standard). Equation (1.1) shows the conversion from *RGB* colour space to *YUV* colour space as defined in ITU television standard known as System-B; colour PAL. *R*, *G* and *B* can take values between 0 and 1.

$$\begin{pmatrix} Y \\ U \\ V \end{pmatrix} = \begin{pmatrix} 0.30 & 0.59 & 0.11 \\ -0.15 & -0.29 & 0.44 \\ 0.61 & -0.52 & -0.10 \end{pmatrix} \begin{pmatrix} R \\ G \\ B \end{pmatrix} \quad (1.1)$$

In polar coordinates, the phase angle of the resultant carrier corresponds to the dominant colour, or hue, and the magnitude is the strength of the colour or saturation. These two attributes of colour, *hue* and *saturation*, can be defined as:

$$Hue = \tan^{-1} \left[\frac{V}{U} \right] \quad (1.2)$$

$$Saturation = \sqrt{U^2 + V^2} \quad (1.3)$$

Digital television adopted the colour conversion used in analogue television with some minor changes [12]. The U and V components are scaled to bring their range from -0.5 to 0.5. The Y , and scaled U and V are then digitised to 8 bits, with some footroom and headroom to allow for some values slightly outside the legal range [18]. The digital version is called $YCbCr$.

The research presented in this thesis uses the luminance, Y , hue and saturation colour space as defined in equations (1.1) to (1.3). The main reasons for the selection of this colour space is that it enables the visualisation of the points on a two dimensional display. The instrument to do this is known as vectorscope. The vectorscope plots the U and V (or equivalently Cr and Cb) signals on an X-Y plot, and is used to monitor the hue and saturation. Appendix A.2 shows the standard analogue colour bar test pattern whose digital colour difference signals Cr and Cb are shown in Figure 1.1. Vectorscopes are commonly employed in analogue television broadcasting to monitor colour quality. Reusing this concept within a digital test environment will reduce the learning curve for television broadcast engineers.

Perceptually uniform colour spaces (for example Lab , Luv , etc.) were not explored as they demand higher computational resources.

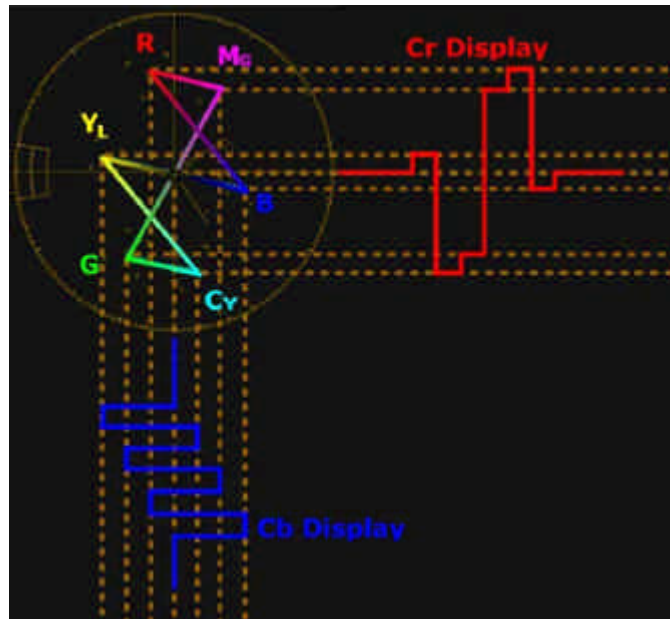


Figure 1.1 Visual display of colour information using colour difference signals Cr and Cb of colour bar test pattern shown in appendix 2 [12]

A vectorscope uses an overlaid reference display, or *graticule*, for visualizing chrominance signals. The graticule of a vectorscope approximately represents saturation as distance from the centre of the circle, and hue as the angle, as shown in Figure 1.2. The standard vectorscope is defined in more detail in Appendix 7.

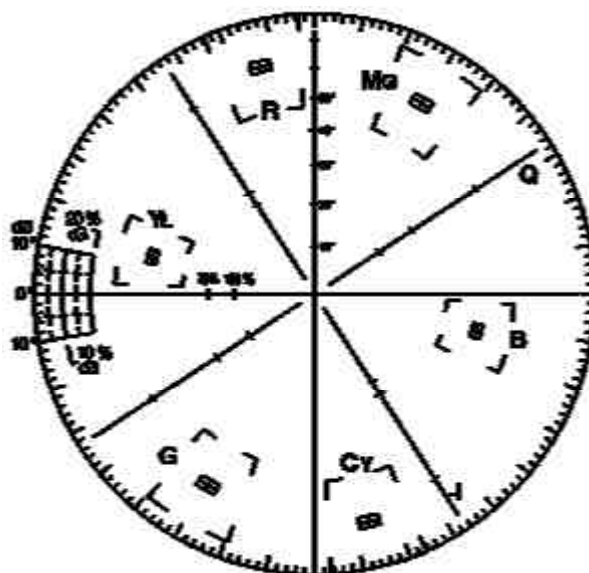


Figure 1.2 The graticule of the vectorscope (reproduced from [15])

Most colour digital codecs use a similar method of colour representation to that used in analogue television. The colour image is first transformed from RGB to colour space $YCbCr$, (or similar, related spaces such as RCT , ICT) based on the application [16]. Then the two chrominance components are sub-sampled and coded separately. In JPEG, using block-based DCT, each of the two chrominance components is then coded separately.

1.1.3 Overview of JPEG, JPEG2000 and MPEG CODECS

Research presented in this thesis used two JPEG codecs, one JPEG2000 codec and a MPEG-1/2/4 codec to carry out experiments. This section presents an overview of design and typical implementation of those image codecs.

Image and video compression is achieved by exploiting the spatial, temporal, spectral and statistical redundancies within the image or video data [17]. While removal of these redundancies does enable data reduction, for typical images lossless compression is limited to a factor of between two and five [18]. Hence, lossy methods are used to further reduce data volume. With lossy compression, the pixel values in the decoded image are only an approximation of the original pixel values – some data has been lost in the compression process, and cannot be recovered.

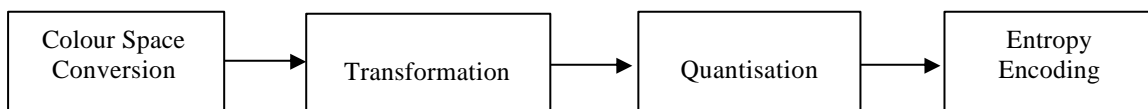


Figure 1.3 Block diagram of a generic image coding system

Figure 1.3 shows a general block diagram of an image compression system. The colour space conversion converts the RGB image to $YCbCr$ (or similar colour space). This has two effects. First, it concentrates the energy into the Y component, enabling better overall compression. Second, since the human visual system has a lower colour resolution, the Cb and Cr components are usually sub-sampled by a factor of two. This immediately gives a factor of two reduction in data volume. Image transformation exploits spatial redundancy by concentrating the image energy into a

few coefficients of the transformed image. These coefficients are then quantised to reduce the number of bits used to represent each coefficient, and reduce the insignificant coefficients to zero. This is where most of the compression is achieved. With quantisation, there is a trade-off between minimising the loss (high quality) and maximising the compression (lower fidelity). This is controlled through changing the quantisation step size, with the control parameter known as ‘quality factor’ [19]. The resulting discrete coefficients are then entropy coded to exploit the statistical distribution of coefficient values, giving typically another factor of two compression [18].

The JPEG standard splits each component the image into a set of non-overlapping 8x8 blocks, which are then transformed using DCT (discrete cosine transform). This size provides a trade-off in concentration of energy locally and the computational overheads. The DCT coefficients are quantised using an 8x8 base step size matrix that has been derived from perceptual studies. This quantisation matrix is scaled by the quality factor to get the actual quantisation level. The coefficients are reordered with a zig-zag scan to place the higher frequency coefficients (those more likely to be 0) at the end, where they can be compressed efficiently with run length coding. The resulting symbols are then encoded using variable length coding (usually Huffman encoding) [19].

The JPEG2000 standard uses the discrete wavelet transform of the complete image for energy compaction. (If the image size is large, the image is divided into smaller sub-images or tiles, with each tile compressed separately.) Many of the high frequency sub-band coefficients are small or quantised to 0, with a strong correlation between the detail levels. This is exploited through a combination of bitplane coding and tree based coding using SPIHT [19] or EBCOT [19] coding schemes. The tree based coding enables spatial scalability, while bitplane coding enables quality scalability (the least significant bits are at the end of the bitstream where they may be truncated).

The MPEG is a series of video coding standards developed by motion picture expert group – a collection of researchers from academia, industry, and other research organisations. In video, both spatial and temporal redundancies are present. Exploiting only spatial redundancies (for example by applying JPEG or JPEG2000 to

each frame) is known as intra-coding. Exploiting temporal redundancies between frames is called inter-frame coding. A frame structure is defined, known as a group of pictures (GOP), which consists of a base intra-coded frame (I), a number of forward predicted inter-coded frames (P), and several bi-directionally predicted inter-coded frames (B) predicted from adjacent I and P frames. For predicted frames, motion within a spatial area (usually 16x16) known as macro-block is determined through motion estimation (local correlation). The motion vectors are encoded, and the prediction subtracted from the input frame, with only the difference transmitted using a JPEG type coding. Many of these differences are small or zero, enabling significant data reduction [20].

The effects of the designs of the codecs on the type of compression artefacts produced will be discussed in chapter 2.

1.2 Description of the Problem

In digital television broadcasting, video streaming and other multimedia communications, image and video are the dominant components. With limited communication bandwidth and storage capacity in terminal devices, it is necessary to reduce the quantity of data or the data rate using digital codecs. The sub-sampling techniques and quantisation used in image and video compression codecs introduce distortions known as artefacts. *The Digital Fact Book* defines artefacts as “particular visible effects, which are a direct result of some technical limitation” [21].

For the purpose of communication we need to acquire, process and deliver information, visual data, including images and video. In a multimedia environment, an image can be described as a two-dimensional representation of a scene or other visual data. Video can simply be treated as a sequence of images but often contains additional information such as timing or synchronization signals. Video also implies correlated audio, which is often included in the video stream. Audio artefacts are beyond the scope of this thesis.

Humans are able to gather large amounts of information quickly from visual input. For this reason, images and video can provide a higher information transfer than other

forms of information such as text, sound and signs. This, combined with the ability to make a high impact, make image and video communications one of the dominant media in today's society.

When an item of visual data is used for a given medium, it is processed based on the constraints of that medium. Since each image or video contains a large quantity of data, delivery and storage generally require high bandwidth and large storage capacities respectively. Generally, most image data contains significant redundancy in the form of high correlation between adjacent pixel values, and between adjacent frames of video. The role of codecs is to exploit this redundancy to reduce the total volume of data.

As the volume of data and processing power increase, while at the same time the available spectrum per user is diminishing, it is important that modern digital communication systems handle the available spectrum efficiently. Despite the massive global deployment of high bandwidth networks and the introduction of broadband local loop access technologies, there still exists a place for image and video compression technologies. Bandwidth will always have a cost and the less service providers can use the better. However, the current standards for compression technologies may not continue to dominate. With increasing processing power available at terminal equipment, it is possible to improve the quality of images and video to be displayed by improving the performance of codecs.

As described in section 1.4, a literature review revealed that though there were two reported attempts to design and develop test patterns, the distortion metrics developed to evaluate compression artefacts were limited to two of the most common artefacts, namely blockiness and mosquito noise. Also there is no world standard related to compression artefact distortion measurements. There is a need for an easy-to-use portfolio of test signals and distortion metrics to assess the performance of a digital codec rapidly. The evaluation process may be complicated by each new generation of codec introducing different artefacts that were not necessarily apparent in previous systems.

1.3 Motivations for this Thesis

Image and video data are compressed for storage and transport. Digital video broadcasting to handheld terminal devices started in 2002. One of the commercial requirements was to provide broadcast audio and video streaming services for portable and mobile usage with acceptable quality [22]. A formal subjective measure of picture quality, such as that applied in traditional television broadcasting, is difficult to apply to measure picture quality in mobile broadcasting. This is due to the fact that the terminal devices used are mobile phones and portable handheld devices show a wide range of specifications in display image size and memory capacity. For these reasons it is useful to have objective measures. Objective measures can be classified into two general methods; one method measures picture quality indirectly by measuring the signal quality and the other method measures picture quality directly [23]. In objective picture quality analysis, natural test images and sequences are used and objective measures are derived to correlate to the perceptual quality as close as possible. Generally, in signal quality analysis, synthetic test patterns are used which are specifically designed to stress and measure the specific distortion mechanism. This is a well established technology for test and measurement, particularly in analogue television broadcasting. However with emerging technologies such as mobile television and Internet Protocol (IP) based television it is necessary to measure the distortions added by the new types of encoders and decoders used in digital television services. Dalton explains the need for objective methods of assessing compression systems, and stresses the time consuming nature of subjective testing [23]. His paper also emphasises the need for a new set of test patterns as the standard test waveforms used in traditional broadcast video systems are unable to stress digital systems. A few important and traditional analogue test waveforms are listed in appendix 2. They are designed to stress video codecs in which amplifiers are the main building block. Traditional, analogue test methods can accurately measure and assess analogue impairments of a video signal. However, with the introduction and development of digital technologies, visually noticeable artefacts are being manifested in ways that are different from analogue artefacts. Digital codecs can reconstruct repetitive data available in existing analogue test patterns with fewer errors. Hence, it is required to define and design a new form of test patterns.

There are many artefact mitigation techniques proposed by researchers which are listed in section 2.7 of chapter 2. However, no rapid objective tools are available to check the effectiveness of those mitigation techniques.

Little research has been reported on the additional colour errors introduced by digital codecs. Coudoux et al. [24], [25], [26] developed post processing algorithms to reduce the colour bleeding artefact. However, there is no objective measure reported for the colour bleeding artefact that can be used to evaluate the performance and effectiveness of colour bleeding mitigation algorithms such as the algorithm proposed in [26]. Yuen and Wu [27] presented an analysis of colour bleeding in their survey on hybrid MC-DPCM-DCT video coding distortions. There had been no attempts to objectively measure the colour bleeding due to coding. This motivated the investigation and the development of test patterns and related artefact metrics to measure colour bleeding due to image and video coding.

MPEG-4 is a new standard for coding multimedia information. It uses shape and texture coding in place of block coding for objects in images. One reason for the use of shape coding is to eliminate the artefacts introduced by strong edges in images. No discussion could be found in the literature about the potential for new forms of artefacts that may be introduced by shape and texture coding.

Although one may perceive that image compression schemes such as JPEG and JPEG2000 are limited to digital still image and content management, these are widely used within the motion picture industry. The digital cinema is distributed over wideband networks after compression using JPEG2000 in intra-frame coded only mode. High quality image transportation requires distortion to be below perceptible levels [31].

The recent exploration of Mars deployed special image capture systems [32]. Due to the large volume of image data, the images and video need to be compressed so as to preserve the integrity of data. The compression schemes deployed in the image acquisition system of the probe also uses a wavelet based compressor similar to JPEG2000 [32], [33]. Therefore, even with the prevalence of video coding, there is still an essential need for assessing the quality of still image codecs.

In summary, there are no objective tools available to carry out rapid testing for compression distortions and colorimetry.

1.4 Review of the Use of Synthetic Test Patterns in Compression Distortion Evaluation

Lambrecht et al. [28] proposed a test methodology that can be used for assessing MPEG coding fidelity. This method produces synthetic test patterns specifically designed to evaluate the features such as luminance rendition, chrominance rendition, edge rendition, blocking effect, isotropy, abrupt scene changes, noise test, text rendition, texture rendition, time aliasing, motion tracking and buffer control. A chessboard pattern of diamonds was used to assess the blocking effects and rotating squares and moving circles for edge rendition. However, in this and subsequent research, Lambrecht did not propose any distortion metrics for common compression artefacts such as blur, ringing and colour bleeding. In his work the test pattern generator had the ability to generate a sequence with moving luminance bars and colour bars for luminance and chrominance rendition.

Fenimore et al. [29], [30] at the National Institute of Standards and Technology (NIST) in the USA developed a test pattern for evaluation of MPEG codecs for mosquito noise. Mosquito noise defined as *distortion concentrated at the edges of objects, and further characterized by its temporal and spatial characteristics. Sometimes associated with movement, characterized by moving artefacts and/or blotchy noise patterns* [30]. NIST wanted to develop such test patterns and metrics for compression rates that typically introduce perceptually negligible artefacts mainly for high quality video [29]. This is important as post processing between the decoder and the display device may highlight the artefacts. Fenimore's test pattern development was designed to stress specific features of compression which uses motion estimation and quantisation [30]. The work reported was limited to an artefact referred to as mosquito noise. Fenimore et al. [29] recognises the services rendered by analogue television test patterns by saying "Evidence of synthetic test patterns' utility is seen in their 50 years of use in the technical evaluation of analogue systems in the studio". They also argue the need for a set of well characterised test patterns and image and video quality metrics. However, no further research has been found from Fenimore in

developing such test patterns and related artefact metrics for other common compression artefacts.

The purpose of this thesis is to investigate, design and develop synthetic test patterns to stress codecs under test. Using the original and reconstructed test patterns, individual intra-frame coded artefacts, that is spatial-domain artefacts, are detected, separated and metrics computed.

In 2000 the Video Quality Expert Group (VQEG) reported that the experimented human vision system based predictive quality metrics did not provide a clear advantage over peak signal to noise ratio (PSNR) measurements though PSNR is a pixel-based global metric calculated on an error image, which is the difference between the original image and the reconstructed image [34]. However, in 2003 the VQEG found more promising results [35], [36]. One example of such a metric is the structural similarity index (SSIM) [37]. This will be described in more detail in chapter 3.

1.5 Thesis Aims and the Scope of Research

The goal of this research is to evaluate the most common spatial-domain compression artefacts resulting from a still image codecs or motion codecs operating in intra-frame coded mode. As the first aim, a library of synthetic test patterns and a random test pattern generator are designed and implemented to achieve the goal. As the second aim, the related artefact metrics for four dominant compression artefacts, namely, blockiness, blur, ringing and colour bleeding are also designed, implemented and validated. The scope of the research was limited to intra-frame coding as motion artefacts require a separate study which would demand much longer time span than was available.

1.6 Proposed Framework and Approach

The framework proposed was to develop test pattern generation algorithms for synthetic test patterns. Each test pattern stimulates the appearance of the associated artefacts. These are then detected and measured enabling the codec to be evaluated.

As shown in Figure 1.4 the test methodology is based on a test pattern generator. The test pattern module includes a library of pre-defined synthetic test patterns and an algorithm for the generation of random test patterns.

Synthetic test patterns offer many advantages over natural test scenes:

- ? Algorithmically generated synthetic test patterns are resolution independent. Hence they can be generated at any image size, aspect ratio and can be colour or monochrome.
- ? The test patterns are entirely known, and free from distortions in the input image, which makes artefact metric evaluation rapid and accurate.
- ? Synthetic test patterns require much less memory than complex natural scenes.
- ? Algorithms can be designed to generate specific test patterns on demand to provide more depth in testing the specific features of a coder.

This approach allows the evaluation of each artefact introduced by the coding process.

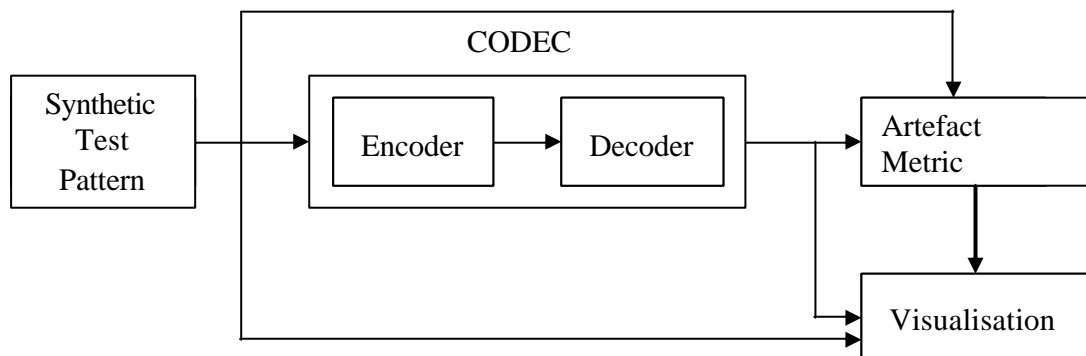


Figure 1.4 Block diagram of the image and video artefact assessment system

1.7 Summary of Contributions

The main contributions of this thesis are:

- ? An extended taxonomy for the sources of artefacts in image and video communication was proposed to facilitate efficient localisation of codec artefacts.

- ? Distinct test patterns were proposed for the efficient measure of the four types of dominant codec artefacts, namely, blockiness, blur, ringing and colour bleeding.
- ? Artefact metrics were designed for blockiness, blur, ringing and colour bleeding artefacts based on qualitative and proposed quantitative definitions of four dominant artefacts due to image compression.
- ? Algorithms were devised to detect, measure and evaluate compression artefact metrics using synthetic test patterns. The proposed algorithms were subsequently validated with a human visual system based modern image quality metric using representative JPEG and JPEG2000 codec implementations.
- ? An integrated test and measurement environment was developed to evaluate image and video codecs and processing systems for distortions due to image and video compression.
- ? The proposed framework was deployed to evaluate the effectiveness of several pre- and post-processing algorithms of image and video compressors and de-compressors.

1.8 Organisation of the Thesis

This thesis introduces tools that are required to objectively evaluate the performance of image and video codecs in an environment where the codec design process is rapid and complex. The contents are structured as shown in Figure 1.5.

Chapter 1: Introduction

This chapter introduces the problem of the evaluation of compression artefacts as the problem to be studied. The author was motivated by his analogue television broadcasting background, the lack of tools to ascertain the effectiveness of mitigation techniques and the lack of any objective evaluation standards for compression artefacts. The proposed approach is to use known reference and purpose-defined test patterns designed to stress the codec. The scope of the research is limited to 'spatial-domain' compression artefacts or 'intra-frame coded' codecs. The chapter also presents an outline of the thesis and a summary of contributions.

Chapter 2: Taxonomy for Image Communication Artefacts

Although the image coding field has been growing rapidly, prior to this work there was only one published taxonomy of image and video artefacts known to the author. This chapter describes a taxonomy of image and video artefacts based on the point of origin within an image communication model. Artefacts due to codecs are one out of the six possible sources that introduce artefacts into images and video. This taxonomy helps to find the origin of artefacts and then mitigation strategies help to prevent the propagation of those artefacts.

Chapter 3: Review of Image Quality Assessment

This chapter reviews the literature on image and video quality assessment methods. Though human vision system based measurement is often used in image and video quality measurement, this thesis does not investigate such methods. An objective method based on signal quality measures was used for over half a century for analogue colour television and so an objective approach is now sought in the digital domain. This chapter reviews two paradigms for image quality measurement; signal quality measurement and picture quality measurement. Measurement of artefact distortions by comparing the reconstructed image with the reference is defined as signal quality measurement. This approach belongs to the class of objective measurements. Previously published attempts to use synthetic test patterns for assessment of artefacts are described. This chapter also describes the philosophy of the research reported here. The signal model of an artefact assessment system involves test pattern generation, detection and separation (classification) of artefacts at the codec output and further computation to generate a parameter representative of the quality performance of the codec.

Chapter 4: Test Pattern Generation for Compression Artefacts

This chapter presents the philosophy of test pattern design. It also defines the blockiness, blur, ringing and colour bleeding artefacts qualitatively. Synthetic test patterns are proposed to stress the codec under test for each artefact. Extension of the

test patterns to test sequences is briefly discussed. A set of synthetic colour test patterns is proposed for measurement of the colour artefacts.

Chapter 5: Distortion Metrics for Compression Artefacts

This chapter defines the blockiness, edge-blur, ringing and colour bleeding artefacts quantitatively. It also presents algorithms to detect, separate and measure individual artefacts based on the artefact distortion characteristics. Distortion metrics represent the degree of distortion. The algorithms developed include routines to detect, separate and then measure the artefact under study. Several blockiness artefact metrics are presented and compared against each other. A computational algorithm for the colour bleeding artefact is not covered in the ANSI T1.801.02 definitions. This chapter defines a coding colour bleeding artefact. It includes the descriptions given by other researchers. An algorithm to detect, separate and then measure the two components of the colour bleeding artefact is explained. Colour bleeding, edge-blur and ringing artefact metrics are also presented.

Chapter 6: Evaluation of Metrics for Compression Artefacts

The efficacy of the proposed algorithms to generate test patterns and distortion metrics were tested using MatlabTM JPEG and IrfanViewTM JPEG codecs. Each codec was exercised with respective synthetic test patterns to evaluate the artefact distortion metrics. It is observed that distortion metrics increase with increase in compression ratio. Artefact detection and measurement algorithms compute only the artefact under study. Hence, the artefact metrics provide a reasonable representation of the compression distortions and are readily calculated. The *colour rings* test pattern with the same luminance can be used to evaluate the colour blur and colour ringing. In colour bleeding measurements, two artefact metrics presented on a virtual vectorscope provide quick measure against the expected hue and saturation values. Each of the four distortion metrics were validated using structural similarity index as a proxy for mean observer score.

Chapter 7: Performance Evaluation of Image Codecs

This chapter discusses the use of the proposed test patterns and metrics for benchmarking. The usefulness is demonstrated by benchmarking a small sample of image codecs for blockiness, edge-blur, ringing and colour bleeding. This chapter also discusses the challenges of detecting and measuring image and video artefacts. These challenges will become more acute with the trend towards the rapid development of codecs. Techniques such as shape coding and texture coding used in the latest coding standards such as MPEG-4 are also discussed briefly. Since video has a temporal dimension, future work is needed to adapt the static test patterns reported here to the generation of test sequences.

Chapter 8: Conclusions and Future Work

This chapter summarises the main conclusions of the research work and proposes future work to extend the metrics for quality measurements. Future work includes an exercise to carry out formal subjective testing for each of the artefacts and an investigation of the possibility of combining them with appropriate weights to form a single metric. The extension of this research into temporal or motion artefacts is already in progress although it is not reported in this thesis.

Appendix – A-1 - Z-domain Analysis

‘Multi-path’ distortion is a critical problem in image communication that occurs when the receiver is presented with both a direct signal and one or more reflected signals due to clutter in the signal path. Multi-path signals generate multiple images on analogue television pictures known as “ghosts”. This appendix reviews techniques for measuring ghosting artefacts and characterising channels in analogue television broadcasting. A new, direct technique based on z-domain analysis of ghosting is proposed and analysed. While the method works in theory, it is overly sensitive to noise and numerical accuracy, limiting its practical application. The method can further be improved by iterating the first solution provided by the proposed method. This chapter is included as it reports on original published work in an area related to the thesis [35].

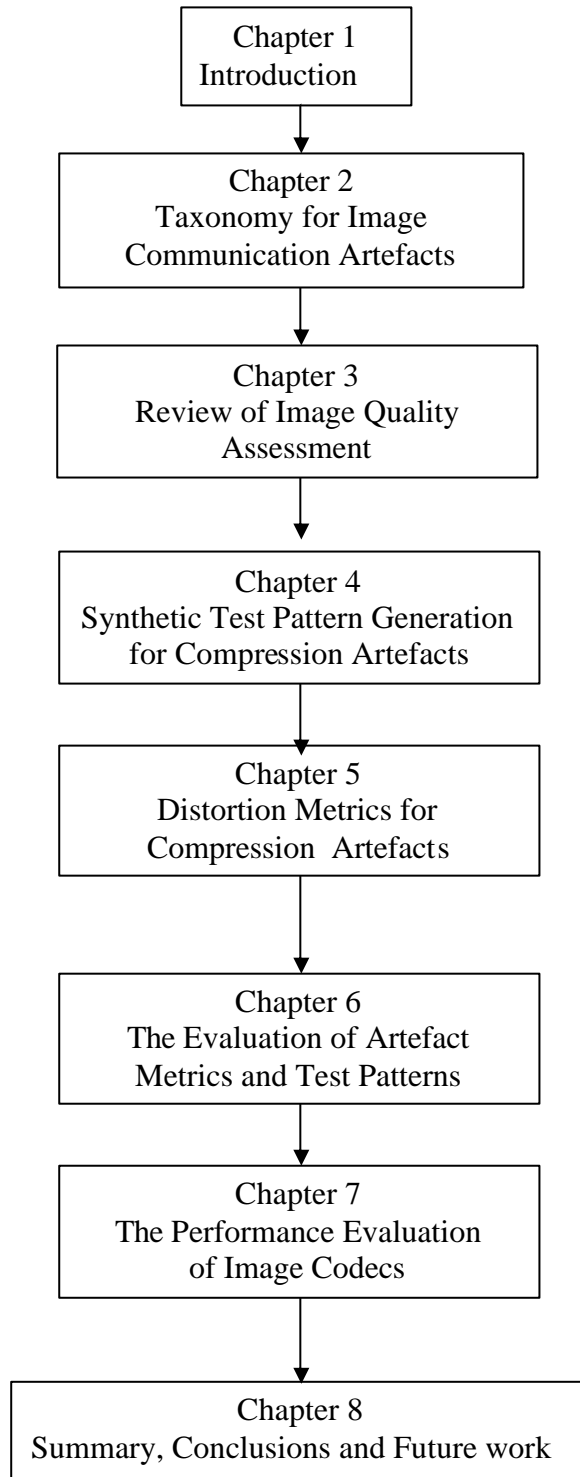


Figure 1.5 Outline of the Thesis

Chapter 2: Taxonomy for Image Communication Artefacts

2.1 Introduction to Artefacts

The only taxonomy of image communication artefacts known to the author was published in 1996 by Wu et al. [39], and was limited to video distortions. Yuen et al. also surveyed video coding distortions in 1998 [27].

In an image and video communication chain, artefacts can be introduced at many points so the sources of artefacts in image communication are reviewed here. Generally, the quality of the image at the receive end depends not only on the image and video itself but also on the use of the received image. If the received end use is for human viewing, then the viewer, viewing conditions, display and the content itself would influence the quality. Therefore, it is important to identify and localise the source of artefacts within the communication chain.

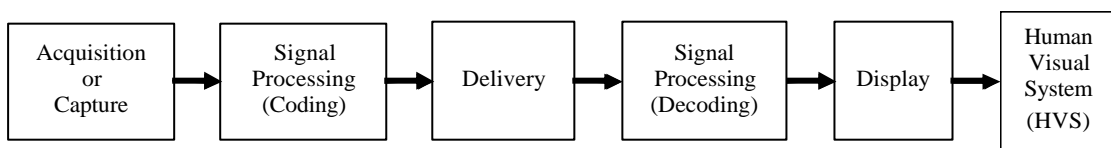


Figure 2.1 Image processing model for visual communication

A common model for the visual communication process is shown in Figure 2.1. In an image and video communication chain, artefacts can be introduced at many points. When visual information is captured, processed and delivered to the final recipient, the displayed image and video may differ from the original. Artefacts are defined [21] as any visible differences that are a direct result of some technical limitation such as bandwidth and storage at any stage of the visual communication process. To define and to attain better focus for the research reported in this thesis a survey was carried out to identify artefacts that can be generated at various stages of image communication.

Image and video artefacts can be broadly classified into five types based on their origin. They are due to capture, processing (coding and decoding), delivery, display and the properties of the human visual system. They occur in both analogue and digital systems. However some artefacts may be more prevalent or visible in one type of system (either analogue or digital). The table 2.1 summarises some of the coding and delivery artefacts.

Table 2-1 Summary of common coding and delivery artefacts found in digital image and video systems [40]

Impairment	Description	Source
Blockiness	Distortion of the image characterized by the appearance of an underlying block structure.	Coding
Blur	Global distortion over the entire image, characterized by reduced sharpness of edges and spatial detail.	Coding
Ringing	Appears as echoes of the hard edges in the picture or a rippling of an edge.	Coding
Colour bleeding	Appears as smearing of colour around colour boundaries.	Coding
Black square blocks	Appears as random block, generally black.	Delivery
Ghosting	One or more delayed versions of the image appear superimposed over the original. Each ghost may appear either to the left or to the right of the original, depending on whether it is a pre or post ghost.	Delivery

Each of the stages within the communication model is considered in turn, listing some of the key artefacts introduced by technical limitations in that stage. While a detailed analysis of many of these artefacts is beyond the scope of this thesis, it is important to outline and classify these artefacts as part of the context for this research.

2.2 Capture Artefacts

Images and video are captured using cameras that comprise of an optical system and a sensor with processing circuitry. Reflected light from the object or scene forms an image on the sensor. Artefacts based on capture will affect both analogue and digital systems as this is at the “front end” of the image acquisition.

Optical imperfections distort the image captured; limited depth of field can defocus parts of the image; non-uniform magnification leads to barrel or pincushion distortion; chromatic aberrations introduce colour fringing and vignetting, a decrease of intensity towards image corners, is due to lenses being faster in the centre than the periphery [40].

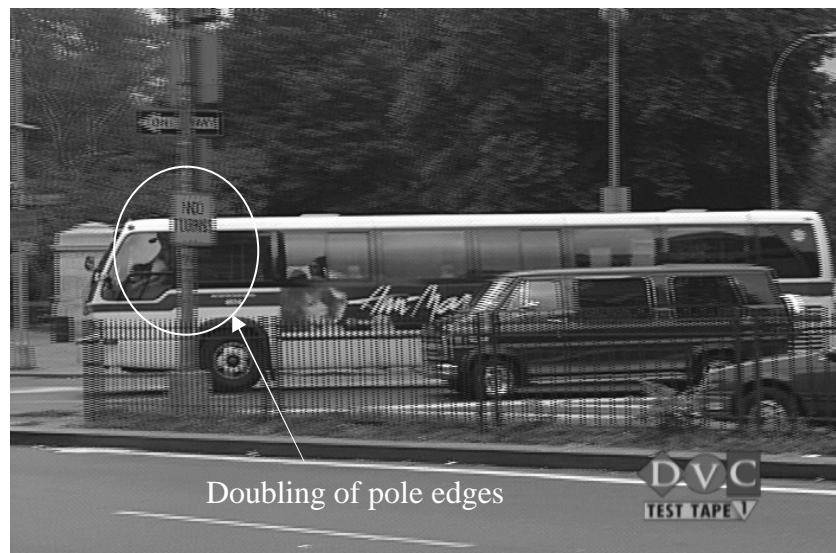


Figure 2.2 Interlace artefact from panning the camera [40]

Capture artefacts may include visible effects due to interlaced scanning (see for example Figure 2.2), both temporal and spatial aliasing, and distortion due to perspective. Area sampling on the sensor limits the resolution and can give rise to contrast inversions at some spatial frequencies. This is a result of the first sidelobe of the sampling frequency response going negative, combined with spatial aliasing. With digital image capture, quantisation introduces additional noise and can give rise to false contouring. The study of these artefacts and their mitigation is important to the development of methods to stop the propagation of these artefacts. This work is

beyond the scope of this research presented in this thesis as the focus here is on evaluation of spatial-domain compression artefacts only.

2.3 Processing Artefacts

Once image or video data is captured it needs to be processed for delivery through the communication medium. This processing is required to meet constraints such as bandwidth limitations imposed by the medium, limited storage and to provide immunity against medium noise. The compression algorithm used, the picture content and compression rate influence the coding artefacts. The greatest technical limitation is the available bandwidth, as this dictates the compression ratio and data rate. In general, artefacts become more visible as the compression ratio is increased.

There is a wide range of coding techniques for exploiting redundancies in images and video. Such coding introduces artefacts; the most common and dominant undesirable visible effects are the results of reduced spatial and temporal resolution.

One technique of managing the large data volume is to divide an input image into blocks of selected size and independently process each sub-image or block. The lack of continuity or coherence between the processing of adjacent blocks can lead to blocking artefacts.[40]. Staircase noise is one form of blocking artefact, which appears when a block includes image edges; with heavy compression the edge is degraded such that it has lower contrast than the block boundaries. Grid noise is another form of artefact where a slight change of image intensity along the block boundary becomes noticeable in areas with slowly varying intensity with position. Corner outliers are visible at the corner points of blocks, where the corner point is either numerically much larger or much smaller than neighbouring pixels. Blockiness can be observed in low bit rate images and video coded with a codec that uses block based processing [40].

Blur and ringing artefacts result from truncation or quantisation of coefficients in the frequency domain. Ringing artefacts typically appear as sharp oscillations along the edges of an object against a relatively uniform background as shown in Figure 2.3.

Any motion of the object in a video results in these oscillations flickering, giving mosquito noise [30].

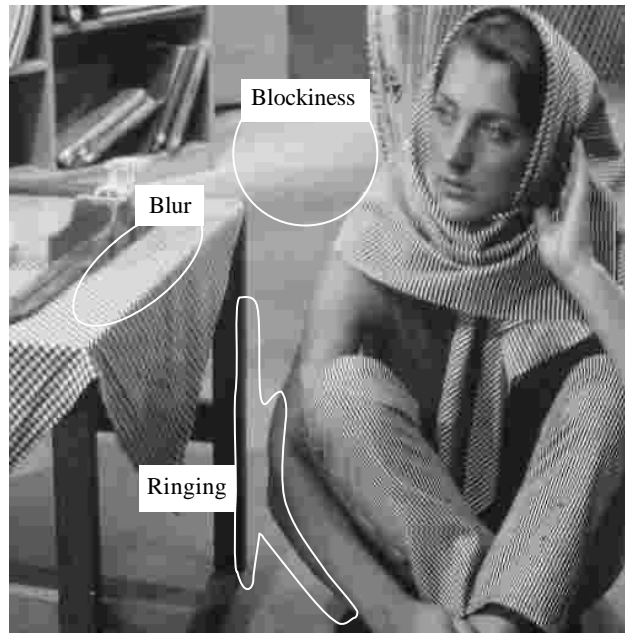


Figure 2.3 Blockiness, ringing and blur artefacts [40]

Colour images have three independent variables to represent the colour information. They can be processed as red, green and blue components or some combination of them depending on the colour space used. In normal or standard definition analogue video, each of three primary colour signals requires a channel with 5MHz bandwidth. Early analogue television standards used a technique of frequency interleaving for compatibility with existing black and white systems. When colour information is frequency interleaved to the same luminance frequency band, this gives a composite signal, which could be delivered over a single channel. This approach can result in cross-colour artefacts for high detailed video signals and cross-luminance artefacts with saturated colours.

When converting a frame from one format to another, scan conversion artefacts may be introduced [41], [42]. An example is line replication artefacts, such as those shown in Figure 2.4. State-of-the-art field rate conversion uses motion-compensated up-conversion to avoid judder artefacts [42].

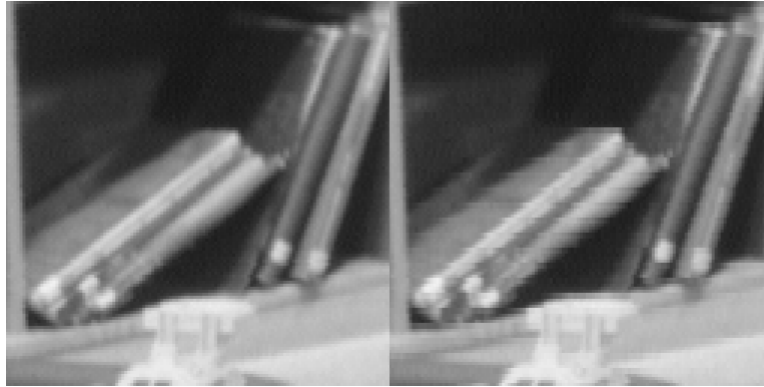


Figure 2.4 Line replication artefact from scan conversion [40]

2.4 Delivery Artefacts

When data is transmitted through a medium, some of the data may be lost, distorted or delivered as multiple overlapping copies of the data due to reflections. When data arrives through many paths in addition to the direct path, the distortion is known as multipath distortion and affects both analogue and digital communications. Multipath distortion or ghosting is a common artefact as seen in Figure 2.5 in an analogue television system [43] and is the most severe artefact in analogue communication. In digital systems, multipath inter-symbol interference is a common propagation distortion and robust modulation schemes such as orthogonal frequency division multiplexing (OFDM) are used to minimise its ill effects [44], [45], [46]. Channel estimation is needed to recover the symbols when the reflections are severe [46].

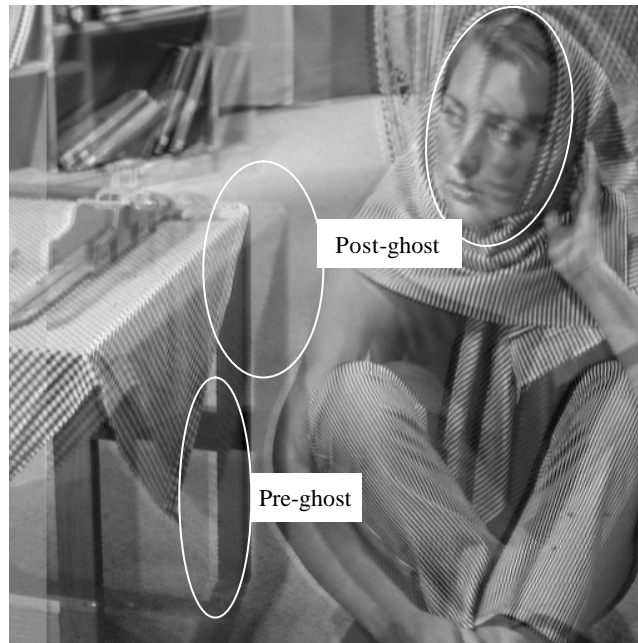


Figure 2.5 Ghosting artefacts [40]

In digital communication systems, data recovery can be achieved without loss when the signal strength is over the threshold of the receiver. However, noise and distortions can result in missing data blocks or packets in digital systems. These errors are often propagated by subsequent processing when predictive coding is used. Motion compensation data is particularly vulnerable to this sort of error propagation.

There is a growing demand for image and video delivery to mobile devices both in industrial and consumer applications. In low bit-rate video telephony service for third generation mobile systems, channel errors can introduce distortions to the video and audio resulting in highly annoying artefacts [47].

The conventional synchronous model of digital video, in which video is reconstructed synchronously at the decoder on a frame-by-frame basis, assumes that the transport is free from delay-jitter. However in modern integrated service packet networks such as the Internet, network delay jitter varies widely resulting in poor quality [48] unless the codec design includes mechanisms to mitigate these effects. Packet based services may also experience missing blocks as shown in Figure 2.6 due to loss of packets between the sender and the destination.

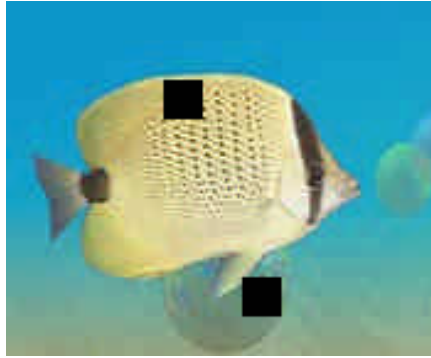


Figure 2.6 The black squares are the effects of missing blocks or data packets [49]

If the delivery is via videotape or other analogue storage medium, there can be synchronisation jitter due to tape stretch or wear, or poor calibration of tape and drum speeds. These delay artefacts appear as a tearing of the lines in the image, as shown in Figure 2.7.



Figure 2.7 Illustration of the effects of synchronisation jitter [40].

2.5 Display Artefacts

Display artefacts are due to poor contrast range, limited ability to reproduce colour, persistence in display devices and flicker resulting from interlaced scanning, resolution limitations, aspect ratio distortions, defective degaussing to remove earth

magnetic effects (see Figure 2.8) and blur and judder resulted from scan rate conversions. Haan and Klompenhouwer [50] published an overview of these flaws in emerging television displays and remedial processing methods.

In analogue television, large area flicker due to low display frequencies and line flicker due to interlaced scanning are visible if the television is not equipped with video up conversion. Though motion-compensated up-conversion is used to reduce flicker artefacts, incorrect motion vectors may introduce objectionable artefacts [42]. With large displays, edge flicker is inevitable when interlaced scanning is used.



Figure 2.8 Distortions due to magnetisation and aspect ratio.

2.6 Human Visual System related Artefacts

The Human visual system (HVS) is a complex image processing system [51], perhaps the most complex known. Visual illusions are artefacts due to limitations within the HVS. The Mach band effect is one form of artefact due to the non-linear response of the human eye to varying intensities [52]. The illusion results from the HVS enhancing the contrast of the edges giving a banding effect from visual overshoot. In motion pictures, the non-visibility of spinning blades is another HVS artefact in the temporal domain. Nadenau has described in details other illusions such as ambiguous, distortion, camouflage, depth illusions and the lateral inhibition and simultaneous contrast in his thesis [53].

Modelling the human visual system is a complex task especially in response to varying image feature orientations, the perception of the image features would differ

from the actual features. This makes modelling the human visual system difficult and research is constantly being carried out to push the frontiers of that knowledge [54].

2.7 Artefact Mitigation Techniques

Many artefact mitigation techniques have been proposed by researchers. However, there is no reliable tool available to evaluate the effectiveness of such mitigation techniques and algorithms. Most researchers either perform informal subjective evaluation or rely on the mean square error if the original image is available. Such methods do not adequately assess the improvement of the specific artefact being mitigated, or the introduction of additional artefacts. A brief account of mitigation techniques for both analogue and digital systems from the survey is presented here.

2.7.1 Artefact Mitigation Techniques for Analogue Systems

Artefacts can be reduced by system design. One example is a colour component signal. In analogue television, when transmission is based on a composite signal, the three components share the same transmission band giving rise to cross-colour and cross-luminance interference or artefacts. Having three separate components for video information, where bandwidth allows, prevents these artefacts. Depending on the colour space used, the three signals are RGB, YUV or YPbPr. Hybrid video systems use components for colour. Digital compression is used on component video prior to storage. Hence for hybrid systems cross-colour, cross-luminance artefact mitigation is at the cost of other processing artefacts such as blockiness from the increased compression needed to compensate for the larger storage requirements. Some researchers have proposed algorithms that detect block boundaries and define a block map for blocking effect and then post-process to minimise the blocking artefacts [55].

Multipath distortion can be mitigated by post processing at the terminal device by transmitting a reference signal [56]. Analogue television broadcast systems can be equipped with a very robust ghost mitigation mechanism where broadcasters transmit a reference signal on one of the blanking lines during the vertical retrace. This signal is used at the receiver to characterise the channel and to perform adaptive filtering. A world standard ghost cancellation signal was defined in the mid nineties and now

high-end receivers in the consumer market are equipped with circuitry conforming to this standard [56], [57]. This mechanism enables ghosting to be almost completely eliminated. Appelhans and Schroder [58] have researched ghost cancellation for mobile television which has increased susceptibility because of the physical motion of the receiver. They have studied three methods: blind equalisation, use of synchronisation signals and use of a low correlation signal. Line synchronisation can detect only short echoes. They have extended the echo detection range by superimposing a correlation signal on the picture signal. Several researchers have proposed new ghost cancellation reference signal designs [59], [60], [61]. While carrying out the research reported here, alternative methods of ghost cancellation were investigated [35]. In 2003 Punchihewa et al. proposed the z-domain analysis presented in Appendix A-1, a theoretically sound but computationally intense method. As the primary focus of this research is on digital compression artefacts, further work was not undertaken to investigate the performance of the proposed method under noisy conditions.

In analogue video, early equipment had only composite interfaces. When colour television signals are to be processed for recording in professional or higher standard formats, luminance and chrominance signals need to be separated. Comb-filters have been deployed for this task for many years. Even high-end consumer television receivers are equipped with comb-filters for cleaner luminance and chrominance signal separation.

For consumer television, field repetition and progressive scanning with field stores would mitigate large area flicker and line flicker. This may result in motion blur or motion judder. To reduce motion artefacts, motion compensated up-conversion techniques are being developed for high-quality consumer displays. The image degradation due to motion compensation artefacts can be suppressed by error concealment. The estimated global image degradation is compared against the concealment level to control the degree of suppression. The concealment levels are based on human perception properties [41]. Edge directional line averaging interpolation techniques reduce edge flicker in interlaced large displays [42].

2.7.2 Artefact Mitigation Techniques for Digital Systems

Many researchers have developed algorithms and techniques to mitigate blocking artefacts. These can be broadly classified into pre-processing [62], [63], post-processing [64], [65], [66], or some combination of the two [67]. The simplest post-processing approach is low pass filtering to blur block boundaries. Statistical estimation and set-theoretic reconstruction methods improve on this by making use of the underlying image statistics. Statistical estimation methods use probabilistic models and maximum a priori probabilities to mitigate blocking artefacts. For an example, set-theoretic reconstruction methods use the convex constraint set or the smoothness constraint set to reconstruct the original image by projection on to the convex set (POCS). The key idea in POCS is to represent every known property of the original image by a closed convex set. The solution is an image that is an element in all sets and can be found by alternating projections onto each set, starting from the blocky image itself [68], [69], [70], [71], [72]. The post-processing algorithms include: the principle of POCS-Projection onto convex sets [64], [70], [73], MRF (Markov random fields) [74], multi-frame constraint sets, maximum-likelihood parameter estimation [75], MAP (maximum a posteriori probability) [64], [76], [77], entropy maximisation [78], Bayesian approaches [79], spatio-temporal concealment using a boundary matching algorithm and mesh-based warping [80], multilayer perception for adaptive processing [81] and spatio-temporal adaptive filtering [80], [81], [82], [83], [84]. One drawback of all of these algorithms is their high computational complexity. Any post-processing should be able to efficiently remove blocking artefacts while preserving dominant edges, retaining the sharpness of the image and not introducing any new artefacts [85].

Carli et al. [86] developed an error concealment technique by data hiding that is used to mitigate missing blocks due to loss of data packets in transmission. Data hiding techniques can be used to control errors and conceal them by transmitting redundant information that can be used at least to partially recover data lost during transmission. In the wavelet transform, embedded data can act as a reference signal for both error detection and concealment. Atzori et al. [80] have developed a spatio-temporal concealment technique using a boundary matching algorithm and a mesh-based warping to conceal errors due to lost data packets in transmission.

Other techniques developed to mitigate the above coding artefacts include; adaptive filtering [82] overlapped block motion compensation [83], the application of singularity detection and wavelet transform [87], [88], wavelet-based sub-band decomposition [89], adaptive lapped transform [90], a modified uniform quantisation scheme that constrains local regularity [91], and wavelet transform modulus maxima [87].

Source coding and channel coding are used in communication to minimise the effects of transmission errors. Source coding techniques are efficient only if the error rate is below an acceptable level (usually in the order of 10^{-6} ~ 10^{-7}). Unequal error protection schemes, forward error correction schemes which assign more channel coding bits adaptively for important source bits, reduce significantly the occurrence of highly annoying audio and video artefacts [47].

The experimental results of Chang et al. [48] indicate that introducing temporal jitter in video rendering without degrading video quality can be managed with a technique called delay cognizant video coding (DCVC). DCVC segments an incoming video into two video flows with different delay attributes. The DCVC decoder operates in an asynchronous reconstruction mode that attempts to maintain image quality in the presence of network delay jitter [48].

In spite of the wide range of artefact mitigation techniques proposed in the literature, no objective method was found to evaluate the effectiveness of proposed mitigation algorithms and techniques. This finding motivated the development of an objective approach to allow the effectiveness of such pre- or post-processing algorithms to be evaluated.

2.8 Spatial-domain only Compression Artefacts

Section 2.1 to 2.7 is an overview of studies related to image communication artefacts. Most of the studies are focused on only one type of artefact. For the research of this thesis compression artefacts have been chosen as the area for study. It was also observed that there are many compression artefacts including blockiness, blur, ringing, colour bleeding, jerkiness, mosquito noise etc. These compression artefacts

can be grouped into spatial domain and spatio-temporal domain compression artefacts. The motion artefacts arising out of compression process are the spatio-temporal compression artefacts. Motion artefacts are dynamic effects and their dependency on human visual processing is under active study [92]. This thesis is limited to a study of compression artefacts in 'intra-frame' coded codecs. This study is not limited to image codecs such as JPEG and JPEG2000, but can be extended to motion codecs operated under "*intra-frame only*" mode.

2.9 Chapter Summary and Conclusions

In this review, an overview of artefacts has been presented with their causes and mitigation in image and video systems. Artefacts are classified into five types based on their origin within the visual communication model. Blockiness, blur, ringing and colour bleeding are the common spatial domain compression artefacts. Blocking artefacts are the result of the independent processing of each block in block-based signal processing. Blur and ringing are artefacts result from truncation or quantisation of coefficients in the frequency domain. Ringing artefacts typically appear as sharp oscillations along the edges of an object against a relatively uniform background. Any motion of the object in a video results in these oscillations flickering, giving mosquito noise.

As the volume of data and processing power increases with time, the usable and available spectrum per user is diminishing. Hence it is important that modern digital communication systems are able to handle the frequency spectrum and storage devices efficiently. With increasing processing power available at terminal equipment, it is possible to improve the quality of images and video to be displayed by mitigating artefacts. However, most existing techniques focus only on single types of artefact and may trade one form of artefact for another. For example, to reduce blockiness low pass filtering is performed resulting the introduction of a blur artefact. Therefore, there is a need for a more comprehensive and systematic approach to artefact reduction and evaluation. Hence the approach to the mitigation of compression distortion would be to improve the performance of codecs. The ranking of the severity of artefacts may change as new codecs are introduced. This is

complicated as each new generation of codec may introduce different artefacts that were not apparent in previous generations.

Though there are many artefact mitigation techniques available, there is no rapid, reliable objective-tool to evaluate the effectiveness of such techniques and algorithms.

Chapter 3: Review of Image Quality Assessment

3.1 Quality of an Image

This chapter reviews the current status of the quality assessment of coded digital images and video. Mobile television and digital video broadcasting to handheld mobile devices started in early 2002. It is a commercial requirement that image and video be of acceptable quality [22]. In the context of artefact distortion evaluation, Farias, defines video quality as “a measure of how good video looks compared to one or more other videos” [93].

Image and video systems are intended to display a picture that accurately represents the scene being captured by the camera. With today’s special effects capabilities, the displayed pictures may differ in an artistically defined manner from the original. None-the-less, at some point in the processing, where the artistic changes are complete, the resulting pictures are to be accurately conveyed to the user with the desired quality of service. There are a number of terms that are used to describe image and video test methods for such systems.

(i) Either signal quality (indirect) or picture quality (direct): Signal quality measurements are made by processing specially designed test signals and are also called indirect measurements. Picture quality measurements are performed on the images and video of interest and are called direct measurements [94].

(ii) Either in-service or out-of-service: In-service measurements are made while the image or video is being displayed, directly by evaluating the image and video contents or indirectly by including test signals with the images and video. With out-of-service testing, appropriate scenes are used for direct measurements and full field test signals are used for indirect measurements [94].

It is important to note that each pair of terms is independent of the other. As an example, in-service testing could use either direct or indirect methods and it could

also be either real or non-real time. Real time tests may be either continuous or sampled.

3.2 Picture Quality

Digital video coding introduces fundamentally different types of impairments than those created by traditional analogue techniques. Coding digital images to exploit the redundancy present almost inevitably results in a loss of quality in the final image or video. This is because when removing redundant information, some essential information is distorted or destroyed, resulting in artefacts, impairments or defects [95]. Frequently the terms ‘impairments’, ‘artefacts’ and ‘defects’ are used synonymously. However, impairments generally refer to a subjective measure of the degradation of data. Artefacts are visible differences or features that may be added to or removed from an image or video resulting from a technical limitation, usually of the coding process. Defects may be introduced anywhere within the communication chain, and are therefore more general than artefacts. These defects influence the human visual system in such a way that the final perceived images differ from the original.

The compression algorithms used, the picture content, and the origin of the source material determine the nature of the coding artefacts. The available bandwidth affects the compression ratio and data rate with artefacts becoming more visible as the compression ratio is increased. Compression-related artefacts such as blockiness and colour bleeding are common at low bit rates. Often defects may be decomposed into features or special characteristics. For example, after MPEG-2 compression [30], [93], images may show varying strengths of blockiness, loss-of-detail, ringing, and mosquito noise features.

For digital video systems, the nature of the source plays a crucial role in determining the amount of compression that is possible and hence the potential severity of the compression artefacts. The operating characteristics of the digital transmission channel used may also be dynamic in relation to bit rate and this will cause the received video quality to vary even when the information content of the input video stream is constant. When digital data is transmitted, some of the data may be lost or

distorted. Any reflections may result in multiple data. Noise and distortions can result in missing data blocks or data packets in digital systems. For low bit-rate video telephony services, it is important to assess the quality of the picture as that affects the total quality of service.

3.3 Signal Quality

Analogue video and uncompressed digital video are evaluated using traditional signal quality tests. These are indirect with respect to the pictures passing through the system. That is, they measure channel response to a series of different high quality test signals. Indirect tests are based on the premise of a linear time invariant system. Video distortions introduced by such a system may be accurately determined by passing suitable test signals through the same system. Such testing is described well in the literature [94], [96] and will not be covered here.

Digital compression systems are non-linear hence the resulting video quality will be a function of the picture content and other time varying attributes of the system. As an example in statistical multiplexing, a higher bit rate is assigned to one programme channel while assigning a lower rate to another. Traditional signals used to test analogue systems are readily compressed when converted to digital so generally do not provide a meaningful measure of video quality through a digital system [23]. Therefore, direct testing of picture quality is required in addition to the signal quality measurements used to assess the linear parts of the system. Direct evaluation of a system is based on the quality changes between the video at the selected test point and the video at the source. The source video may be either a variety of defined, preferably standard program-like picture sequences or general program material.

3.4 Fidelity Metrics

Common measures of the errors in signal processing are mean square error (MSE) and the peak signal to noise ratio (PSNR). There are other measures such as total absolute error (TAE), root mean square error (RMS) and signal to noise ratio (SNR). If the reference signal is x and \hat{x} is the decoded signal or the approximation of x each having N samples, then these metrics are defined as:

$$\text{MSE} = \frac{\sum_{i=1}^N (\hat{x} - x)^2}{N} \quad (3.1)$$

$$\text{PSNR} = \frac{[\max(x)]^2}{\text{MSE}} \quad (3.2)$$

$$\text{TAE} = \sum_{i=1}^N |(\hat{x} - x)| \quad (3.3)$$

$$\text{RMS} = \sqrt{\text{MSE}} \quad (3.4)$$

$$\text{SNR} = \frac{\sum x^2}{\sum (\hat{x} - x)^2} \quad (3.5)$$

3.5 Quality Metrics

The objective signal fidelity measures defined in the previous section (equations 3.1 to 3.5) are often poorly correlated with perceived image quality. For example, dithering, the process of adding noise prior to quantisation to reduce contouring or other alias artefacts will make the mean square error worse but usually improve the subjective appearance of a heavily compressed image.

Due to limitations in the existing quality metrics, it is important to develop new quality metrics that are informed by our knowledge of the Human Visual System (HVS). Impairment metrics have been developed based on a HVS model and an extension of such a vision model [97]. Researchers have presented extensions to the vision model by introducing a segmentation tool to partition the areas of the test sequence into classes. A particular metric is then evaluated on each class to estimate how the particular features of each class are rendered [98].

Researchers have developed metrics to estimate the level of blockiness and have used that indicator to assess the performance of some blockiness reduction algorithms [83],

[99]. Fenimore et al. [30] developed test patterns and metrics for MPEG compressed video.

Different coding schemes introduce different artefacts to the final decoded pictures, making it difficult to design an objective quality model capable of measuring all the artefacts. Tan and Ghanbari [100] proposed a multi-metric model comprising of a perceptual model and a blockiness detector. This approach combines a picture quality model for each kind of known distortion according to the perceptual impact of each type of impairment.

3.6 Methods of Quality Assessment

The International Telecommunications Union (ITU) has defined Quality of Service (QoS) as “The collective effect of service performance which determines the degree of satisfaction of a user of the service” [101], [102], [103] They further note that QoS is a combination of aspects and requires additional description in order to be used in a quantitative sense for technical evaluations. The user is a key element in evaluating a system for the delivery of digital television programs. There are two classes of picture quality assessment methods: subjective and objective. Picture quality, that is in both image and video quality, depends on many factors, such as the properties of the initial capture system and processing, compression, transmission, output device, media and associated viewing conditions [104].

3.6.1 Subjective Test Methods

Subjective experiments, which to date are the only widely recognized method of determining actual perceived quality, are complex and time-consuming both in their preparation and execution. Basic fidelity measures including mean-squared error (MSE), peak signal-to-noise ratio (PSNR) are simple and widely used, but they do not always correlate well with perceived quality. Additionally, these measures require a reference that exists in the form of an “original” to compare with, which restricts their usability. Thus, reliable automatic methods for visual quality assessment are needed. Ideally, such a quality assessment system would “perceive” and measure image or video impairments just like a human being does.

Two approaches can be taken:

(i) The “psychophysical approach”, which is based on models of the human visual system. Their general structure is usually determined by the modelling of visual effects, such as colour appearance, contrast sensitivity, and visual masking, to name a few. Due to their generality, psychophysical metrics can be used in a wide range of video applications; the disadvantage is the high complexity of the underlying vision models. In addition, the visual effects models are best developed at the threshold of visibility, whereas image distortions are often supra-threshold i.e. above the threshold of visibility [23].

(ii) The “engineering approach”, where metrics are defined that makes assumptions about the types of artefacts that are introduced by a specific compression technology or transmission link. Such metrics look for the strength of these distortions in the video and use their measurements to estimate the overall quality [23].

Subjective test methods require human viewers to rate the quality or difference in quality between two images or video clips. In most testing scenarios these two clips differ in that one is the source and the other has been processed in some manner. Subjective assessment can be a costly and time-consuming process and may not yield repeatable results. This type of assessment is particularly necessary in critical situations such as final product evaluation and standardization processes where quality must be assured.

In subjective testing human observers are generally asked to rate video quality in terms of annoyance, where annoyance is a measure of how “bad” the observer thinks the impairment is. The annoyance value correlates with the strength of the impairment (Table 3.1).

Table 3-1 Five point scale of ITU Rec. 500-3 subjective assessment of images [105]

Quality		Impairment	
5	Excellent	5	Imperceptible
4	Good	4	Perceptible, not annoying
3	Fair	3	Slightly annoying
2	Poor	2	Annoying
1	Bad	1	Very annoying

The Mean Opinion Score (MOS) is a subjective error measure and is calculated by averaging the annoyance level for all observers. Double stimulus continuous quality scale (DSCQS) is a method in which source and processed video clips are presented in pairs to observers [106]. The video or image presentation sequence is randomised. Viewers grade the quality of each clip then the data is processed in pairs. Until very recent times subjective measures such as MOS and DSCQS offered the most reliable quality measures.

There is a wide variety of possible methods of subjective evaluation based on the ITU standards BT500 and P910 [107], [108]. In subjective evaluations, test element parameters must be considered, meticulous setup and control are required, many observers must be selected and screened, and the complexity makes it very time consuming. Subjective tests are only applicable for development purposes. They do not lend themselves to operational monitoring, production line testing, troubleshooting or the repeatable measurements required for equipment specifications.

Some issues that arise with subjective assessment include the cost and the fact that these methods cannot be used to monitor video quality in real time or continuously. The process requires special equipment and many people. Traditional analogue objective measurements, while still necessary, are not adequate to measure the quality of systems using digital compression. Thus there is a need for new objective methods incorporating the characteristics of the human visual system including perceptual processes [109].

3.6.2 Objective Test Methods

Objective test methods do not use human subjects, but rather incorporate an analytical evaluation of the video signal. These analyse the video signal in the image space, utilizing knowledge of the human visual system. These methods implement an algorithm that measures image quality, usually based on the comparison of the source and the processed sequences. These algorithms, referred to as “models”, are designed to incorporate the functioning of the human visual system to systematically measure the perceptible degradation occurring in the video imagery. In some situations objective methods may successfully replace the use of subjective assessment. Some impairment metrics have already been developed based on human visual system models. Lambrecht et al. [110] presented a spatio-temporal vision model based on parameters derived from psychophysical experiments.

Several objective quality metrics have been developed for absolute measurement of picture quality and for use in artefact mitigation algorithms. Attempts were made to quantify the quality without reference to the original source. For example, many researchers have proposed algorithms to measure blockiness [111], [112], [113]. Different coding schemes introduce different artefacts making it difficult to design a universal objective quality model.

3.6.3 Objective Quality Metrics

The term “quality metric” is generally applied to any physical or psychophysical measure of image quality. Objective measures of quality are impairment measures and are based on the difference between reference and test images or videos. By definition, fidelity measures require information about the reference video, which can be very restrictive. Quality measures based on impairments are categorized according to the amount of reference information they require. The difference between the reference and the decoded image or video provides an objective measure. Full-reference quality measures require the entire reference video and are not practical for real time transmission applications. Reduced-reference quality measures use a reduced size version of the reference, while non-reference quality measures use no reference at all.

With digital video, a full reference is often not available at the received end to enable the above quality assessment measures to be used. However, digital techniques can enable some data to be embedded with the main stream and this can be used for a partial quality assessment. Two such examples are proposed by Atzori et al.[80] and Carli et al.[86] where embedded data within the coded image acts as a reference signal for both error detection and concealment, that is the process of hiding error.

3.6.4 Double-ended Quality Measure

A dual-ended quality measure compares the input signal with the output signal. To test a compression system, the uncompressed source is compared with the corresponding compressed and then decompressed signal, as shown in Figure 3.1. This allows the encoding system to be tested in a laboratory environment. To be effective the streams used for the test should be designed or chosen to highlight the details of potential artefacts. Dual-ended measurement also prevents the use of video processing techniques like standards conversion, aspect ratio conversion, digital video effects and fades between the source and measurement. Finally, the source material requirement makes dual-ended algorithm impractical for day-to-day quality measurements.

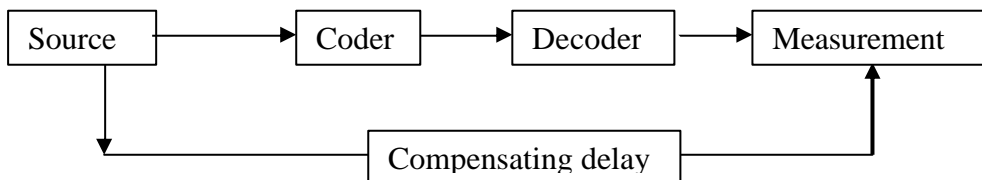


Figure 3.1 Double-ended picture quality measurements [49]

The compensating delay shown must precisely align the input image with the output. This can be accomplished by incorporating rugged, easily identifiable regions into the source images or sequences, from which spatial and temporal alignment information can be retrieved even when the sequence has undergone severe degradation. Double-ended measurement is not well suited to monitoring applications where the source is neither available nor controllable. It is useful as a laboratory tool where these

restrictions pose less of a problem [110]. Hence it can be used for testing codec (coder/decoder) designs.

3.6.5 Single-ended Quality Measure

In most practical transmission applications, internet, broadcast, cable, etc., a reference signal is not available unless stored in the system. A single-ended measure only uses the output signal to calculate the quality measure (Figure 3.2). It is therefore economical and practical. Measurement can be made of any coded data stream from any point in the communication chain. However the use of this method may require knowledge of certain compression parameters to be available in the output stream. The researchers who have developed such measures claim that they are accurate measures. Knee [109] has developed a picture appraisal rating (PAR), a single-ended picture quality measure for MPEG-2. The PAR algorithm calculates how much distortion is added by simply retrieving the MPEG parameters included in the compressed stream. It assumes the source of the encoder is an uncompressed signal. This results in a maximum PAR Figure of 48 dB which is close to maximum signal-to-noise ratio of an 8-bit system. The algorithm finally subtracts the level of artefact calculated from the coding parameters from 48dB to derive the final PAR Figure. The calculations are performed on a picture-by-picture basis [109]. The literature does not explain in any detail how algorithm works. However, based on this argument, different implementations of a given codec will produce the same level of artefacts. This is an invalid assumption, as it can be observed later in chapters 6 and 7 of this thesis where different implementations of the same codec type, such as JPEG and JPEG2000, introduce different levels of artefacts. As the PAR closely correlates to PSNR, PAR is a PSNR estimator rather than a distortion measure. Experiments presented in chapter 7.1.4 show that blockiness distortion does not follow the PSNR. This becomes more complex when codecs such as MPEG-4 introduce pre-processing to mitigate blockiness. Generally, mitigation algorithms transform one form of distortion to another.

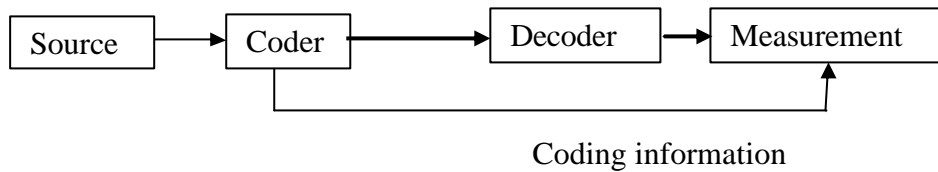


Figure 3.2 Single ended picture quality measurements [49]

3.7 Commercial Systems

There are only a few products developed by industry to measure image and video quality. Most of these have been optimised for the measurement of MPEG-2 data streams. Rohde and Schwarz have developed a digital video quality analyser and monitor, which functions in real time as a no-reference measure i.e. a single ended video quality analysis system [114]. Snell and Wilcox have several products that use the picture appraisal rating (PAR) measure [109]. Tektronix have developed the MPEGscope test system, for analysing transmission impairments in MPEG-2 transport streams [115].

The International Standard Organisation (ISO) is working on an international standard for still image quality evaluation (ISO/DIS 20462-2 [116], [117], [118]), and the ITU has established standard test procedures for subjective video quality evaluations (ITU-T Rec. P.910 [108] and ITU-R Rec. BT.500 [107]). If one metric is compared to another, the results are only meaningful if they are applied to the same dataset under the same test conditions with the same instructions, as was done for example by the Video Quality Experts Group (VQEG) [113],[119].

3.8 Structural Similarity Based Image Quality Assessment

Structural Similarity index (SSIM) is a modern human vision system inspired image quality metric developed by Wang et al. [37]. The SSIM has been shown to correlate better with subjective assessment than PSNR [162]. For this reason, it is used in Chapter 6 as a proxy for subjective assessment when evaluating the artefact metrics developed in this thesis.

The SSIM for pair of images is based on three components [162]: a luminance comparison, a contrast comparison, and a structure comparison. The luminance comparison function between two images I_1 and I_2 ,

$$l(I_1, I_2) = \frac{(2\mathbf{m}_{I_1} \mathbf{m}_{I_2} + C_1)}{(\mathbf{m}_{I_1}^2 + \mathbf{m}_{I_2}^2 + C_1)} \quad (3.6)$$

where μ_I is the mean of image I , and C_1 is a constant to avoid instability with division by zero. The contrast comparison function between the two images is

$$c(I_1, I_2) = \frac{(2\mathbf{s}_{I_1} \mathbf{s}_{I_2} + C_2)}{(\mathbf{s}_{I_1}^2 + \mathbf{s}_{I_2}^2 + C_2)} \quad (3.7)$$

where s_I is the standard deviation of image I , and C_2 is again a constant to avoid instability with low contrast images. The structure comparison function is

$$s(I_1, I_2) = \frac{(\mathbf{s}_{I_1 I_2} + C_2/2)}{(\mathbf{s}_{I_1} \mathbf{s}_{I_2} + C_2/2)} \quad (3.8)$$

The SSIM is then given as the product of these three terms [162]:

$$SSIM(I_1, I_2) = \frac{(2\mathbf{m}_{I_1} \mathbf{m}_{I_2} + C_1)(2\mathbf{s}_{I_1 I_2} + C_2)}{(\mathbf{m}_{I_1}^2 + \mathbf{m}_{I_2}^2 + C_1)(\mathbf{s}_{I_1}^2 + \mathbf{s}_{I_2}^2 + C_2)} \quad (3.9)$$

3.9 Video Quality Experts Group (VQEG)

A growing concern of video researchers and broadcasters is the assurance and maintenance of an acceptable quality of service level for the distribution of video. The Video Quality Experts Group (VQEG) is a group of experts from various backgrounds and affiliations, including participants from several internationally recognized organizations, working in the field of video quality assessment. The group has been working on video quality since its inception in 1997. With the increasing number of digital video and television deployments, new quality assurance systems

are needed to assess digital compression quality and artefacts. The majority of VQEG participants are active in the International Telecommunication Union (ITU) and VQEG combines the expertise and resources found in several ITU Study Groups to work towards a common goal [119].

The long-standing benchmark used for assessment of video images has been subjective assessment. For more than 20 years, researchers world-wide have used the methods outlined in ITU-R Recommendation 500-11,2002 [107] to evaluate video quality in television services. More recently, the ITU-T has developed Recommendation P.930 to standardize methods for multimedia quality assessment [120]. The first goal of VQEG is to provide the broadcast, telecommunications, and research worlds with objective methods for video image quality evaluation. Ten models, one of which is Peak Signal to Noise Ratio (PSNR) were tested in 2000 [34]. None of the nine other models demonstrated statistical significance over PSNR [34]. In subsequent work done in 2003, VQEG believes that some models tested in phase II performed well enough to be included in normative sections of recommendations [35], [36].

3.10 Discussion and Conclusions

In this chapter, an overview of image and video quality assessment was presented. Quality assessment is classified on the degree of human involvement. Subjective measures are by definition based on HVS and may therefore accurately relate to the perceived quality [110]. A formal subjective quality assessment is difficult to perform because it requires special facilities, a large number of human observers and is time consuming. On the other hand, subjective measurements may not produce consistent results as the human visual system is a complex system and human judgement variable.

In the past, simple objective measures of image quality were poorly correlated with perceived picture quality. Recently developed objective quality metrics, such as the picture appraisal rating, claim better correlation with subjective measures [110]. All objective quality models developed have specific strengths and weaknesses. The complexities of the human visual system and perception make the goal of designing

single objective measure that corresponds to human experiences, elusive. Some factors which complicate subjective measurements are the personal preferences and the cultural background of human observers.

There is no international standard for the objective measurement of picture quality and there is a need for an easy-to-use portfolio of test signals designed for codec evaluations.

Chapter 4: Test Pattern Generation for Compression Artefacts

4.1 General Philosophy of Synthetic Test Pattern Design

The research presented in this thesis proposes novel and distinct synthetic test patterns for the evaluation of compression artefacts in codecs. In the PhD proposal prepared in 2002, the author of this thesis proposed the use of synthetic test patterns with known and well defined structural spatial content. The potential of structural details for the evaluation of distortion was subsequently emphasised in the research of Wang [37] reported in 2003.

The framework proposed incorporates four types of objective artefact distortion measures requiring fully known well defined test patterns. One of the aims of this research was to design and synthesise test patterns, preferably programmable, in which the spatial distribution of pixel values emphasises the artefacts due to codec operation. This is achieved by stressing or exercising the codec under test for the artefact to be measured. Hence the spatial distribution of pixel values in the original test patterns are designed and synthesised specifically to emphasise the artefact under study in the reconstructed test patterns.

Many image compressors have a control parameter, essentially a quality factor that can be set by the user to adjust the size of the final compressed image. The compression yield can be expressed as the compression ratio. It is the ratio between the original image file size and the compressed image file size. The level of compression can also be expressed in bits per pixels, the ratio between the size of the compressed image in bits to the total number of pixels within the image. This thesis uses compression ratio to represent the level of compression. In general, the lower the quality factor the higher the compression ratio and the more visible artefacts become. At low compression ratios, the artefacts may not be obvious to the human eye but may be critical in machine vision based measurement applications.

4.2 Blocking Artefact

Blockiness is one of the most dominant compression artefacts. This has been studied extensively and both pre- and post-processing algorithms have been incorporated in recently developed codecs such as MPEG-4.

4.2.1 Qualitative Definition

Blockiness or tiling distortion is defined qualitatively in ANSI T1.801.02-1996 as “*distortion of the image characterised by the appearance of an underlying block encoding structure*” [120]. It is not defined mathematically in any standard. The blockiness can be expressed mathematically as the discontinuity in amplitude at a block boundary. The higher the value of the blockiness, the higher the visibility of block structure. Block edges may appear as an artefact in block-based image coding systems. This defect is not restricted to block-processed discrete cosine transform (DCT) compression. For example blocking artefacts may also appear in the output of wavelet-based codecs when large images are first partitioned into smaller sub-images or tiles. Figure 4.1 shows how blockiness appears in reconstructed images where the original has been compressed using 8x8 block processing with DCT or tiled processing with wavelets.

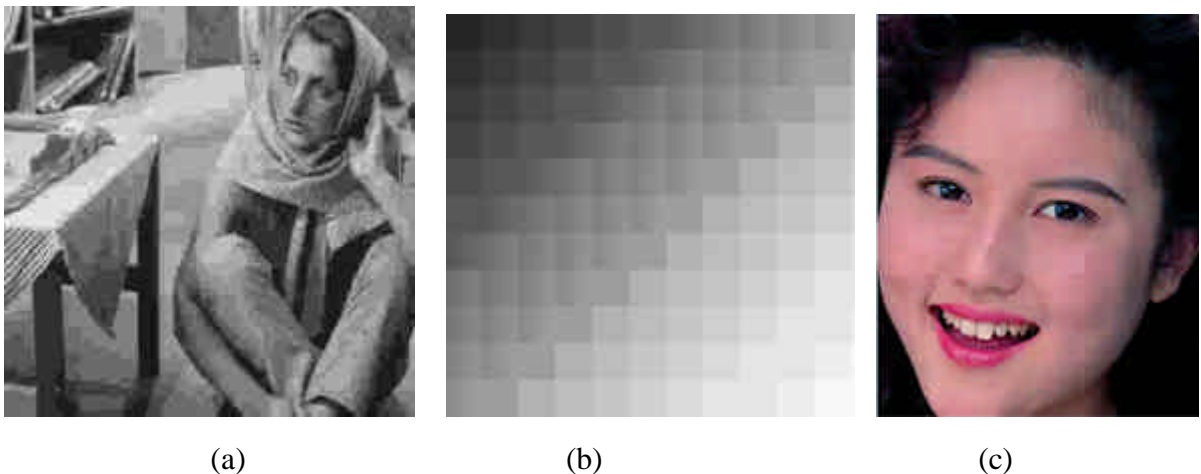


Figure 4.1 Blockiness artefact in reconstructed images. (a) Codec was an 8x8 block processed DCT. (b) Moderate compression using a block processed DCT on an image with no edges. (c) Tile processed wavelet-based codec.

4.2.2 First Generation – Test Pattern ‘sine-squared grey scale – diagonal’

The pixel values and shape of the test patterns need to be chosen so that the algorithms can detect the coding blockiness artefact. To provide a clean measure for the blockiness artefact, it is necessary for the input test patterns to be without edges. To produce edges in the reconstructed blocky-images, it is necessary to have an intensity gradient within the test pattern. A simple horizontal or vertical linear intensity gradient test pattern as shown in Figure 4.2(a) cannot be used to distinguish between edges introduced by block and tile processing from contouring resulting from too few quantisation levels as shown in Figure 4.2(b).

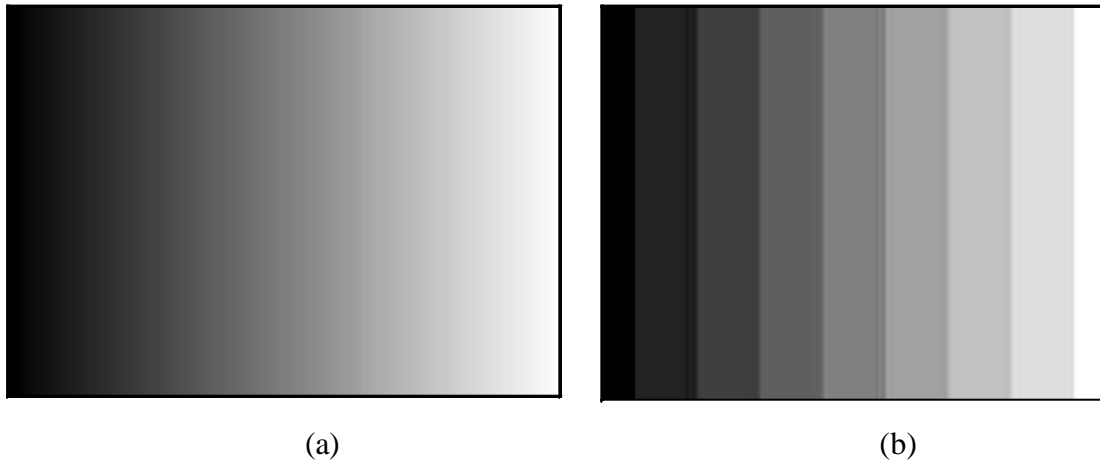


Figure 4.2 (a) Pixel values in horizontal linear intensity gradient test pattern having values from zero to 255 on 8 bits per pixel scale before compression, (b) Contouring induced by a very high level of compression (0.01 bits per pixel = 3 Kbytes) for the pixel.

When the intensity of the pixels within the spatial domain varies diagonally, it introduces spatial intensity gradients in both vertical and horizontal directions. The change of intensity between successive pixels should not be a constant value. If it is constant, the quantisation error within a block will be a special case and each block will introduce the same set of errors. When the pixel values are varied non-linearly, the boundaries between different blocks or tiles will have different quantisation errors. The reconstructed pattern may have a range of block boundary step values over the complete test pattern. This will result in range of quantisation errors spread over the

complete spatial region of the test pattern. Therefore the intensity pattern as shown in Figure 4.3(a) was designed and synthesised [121]. The pixel values vary sinusoidally along the diagonal from the top left corner to the bottom right corner.

The intensity $I(x,y)$ of the pixel at (x,y) on the test pattern in Figure 4.3 (a) as a spatial distribution on x-y spatial domain can be expressed as,

$$I(x,y) = \frac{\left(1 - \cos\left(\frac{(x+y)\pi}{\min(M,N)}\right)\right)}{2} \quad (4.1)$$

where M and N are the dimensions of the test pattern I .

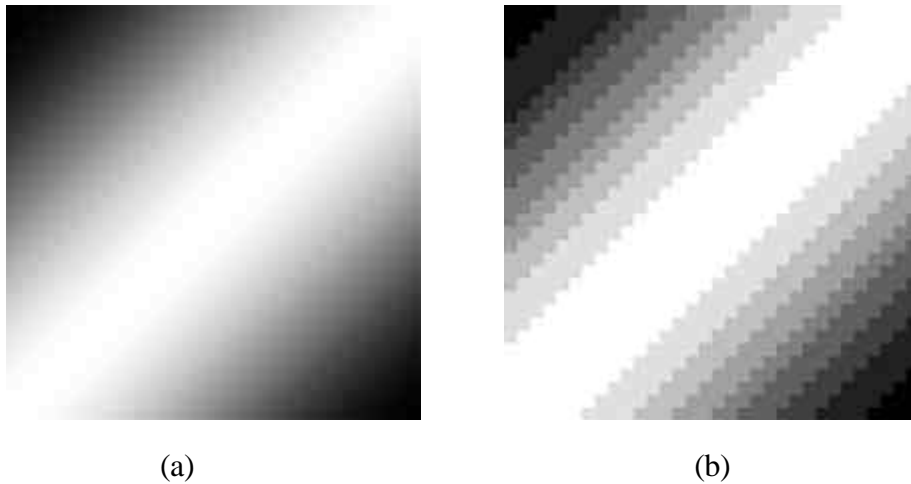


Figure 4.3 (a) The second version test pattern before compression has no perceived edges, (b) The second version test pattern after compression, which has more perceived blocky edges (compression ratio of 90).

Due to the non-uniform variation in pixel values or intensity in different spatial regions, when the test pattern is compressed based on block or tile processing, different blocks of the test pattern are transformed and quantised differently. This is evident in the Figure 4.3(b) where the widths of the bands are not equal. Hence pixels in different spatial regions are stressed differently resulting in a range of quantisation error values.

4.2.3 Second Generation – Test Pattern ‘sine-squared grey scale – radial’

It can be observed in Figure 4.3(b) that there are diagonal bands of uniform grey levels over wide spatial regions. The human eye is sensitive to the orientation of intensity patterns. Hence, it is required to test all possible orientations by stressing in every possible orientation. The test pattern in which the intensity varies diagonally stresses the codec only one orientation. If the intensity is changed in all directions from the centre of circular test pattern, the all possible orientations are stressed. Therefore, the pixel values or the intensity of the pattern was designed and synthesised to vary sinusoidally along the radial lines of the pattern from the centre, as shown in Figure 4.4.(a). In each of the test patterns, the rates of change of intensity values along horizontal and vertical directions are not constant.

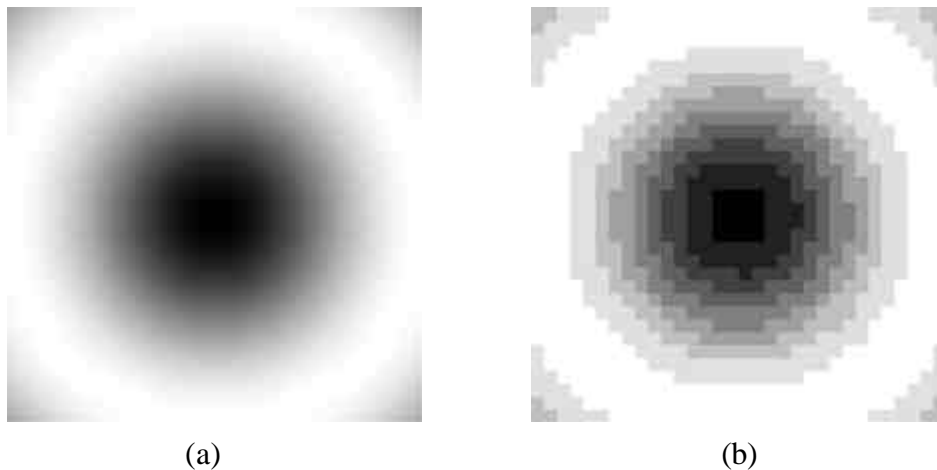


Figure 4.4 The second generation test pattern (a) before the compression which has no perceived edges (b) the test pattern after the compression, which has more perceptual blocky edges (compression ratio of 80).

The intensity $I(x,y)$ of the pixel at (x,y) , where the origin is defined as the centre of the image, on the test pattern in Figure 4.4(a) as a spatial distribution on xy spatial domain can be expressed as,

$$I(x, y) = \frac{\left(1 - \cos \left(2\pi \sqrt{\left(\frac{x}{M} \right)^2 + \left(\frac{y}{N} \right)^2} \right) \right)}{2} \quad (4.2)$$

where M and N are the dimensions of the test pattern I .

The compression characteristics of the two synthetic test patterns using the Matlab™ JPEG codec are shown in Figure 4.5 over the full range of quality factors available.

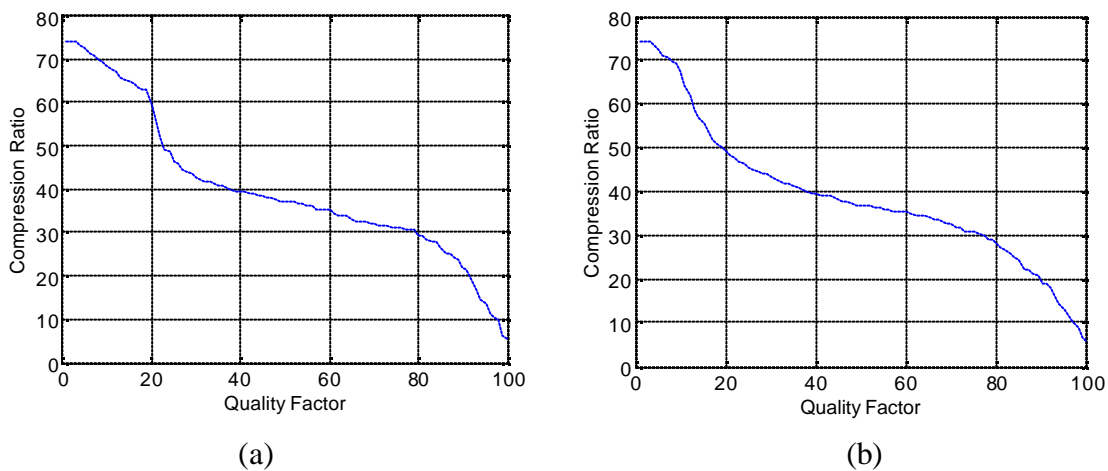


Figure 4.5 The compression characteristics of two test patterns (a) first generation test pattern – *sine-squared grey scale - diagonal*, (b) the second generation test pattern– *sine-squared grey scale - radial* (original size of 512x512).

Both generations of the test patterns have same range of compression ratio with the Matlab™ JPEG codec. The first generation pattern demonstrates a sudden change in compression characteristics around quality factor of 20. The second generation pattern also shows a minor abrupt change around quality factor of 10 however, it gives smoother compression characteristics with respect to quality factor.

4.2.4 Possibility for Sequence Generation

Although spatio-temporal artefacts are beyond the scope of the research presented in this thesis, some of these test patterns can be easily extended to enable the evaluation

of blockiness artefacts due to inter-frame coding. The static test patterns described in 4.2.2 and 4.2.3 can be animated over a virtual image space and then captured at the required frame size to provide an uncompressed test sequence [122]. The movement of the test pattern between frames gives smooth differences that stress inter-frame coding within the codec.

Figure 4.6 shows a video sequence generated by moving the pattern within each frame. The circular pattern is moved within the uniform background.



Figure 4.6 A video test sequence for blockiness [123].

To provide more objects and error pixels, the number of circular patterns can be increased. Figure 3 shows an improved version of a video test sequence with four patterns.



Figure 4.7 Another test sequence for blockiness [123].

The movement of each circular pattern within each frame is controlled by a parameter of the test pattern generation algorithm. The movement can be adjusted to any number of pixels per frame within the range of the frame.

4.3 Blur and Ringing Artefacts

Both blur and ringing occur concurrently. Ringing is an undesirable visible effect around edges and always occurs at edges. Blur generally occurs at edges. Since the

concern is on the blur occurring at edges, the thesis concentrates on edge blur. Many codecs transform the pixel values into the frequency domain where the transformed coefficients are then quantised. Quantisation errors resulting from this approach give rise to ringing around sharp discontinuities in the test pattern.

An ideal step-edge contains components at all frequencies. Any change in the amplitude of any of these components will result in ripples in the test pattern with amplitude corresponding to the error. As explained in chapter 1, as a result of the energy compacting transformation in a codec, many of the coefficients are very small, and get quantised to zero. With frequency based transformations, the loss of high frequency components through quantisation leads to blur in the reconstructed test pattern.

4.3.1 Qualitative Definition

Blurring is qualitatively defined in ANSI T1.801.02-1996 as "A global distortion over the entire image, characterized by reduced sharpness of edges and spatial detail" [120].

The fine details and edges in an input image may have been blurred when the compressed image is decoded as shown in Figure 4.8(b). This blurring causes a loss of edge sharpness in the decoded image, which would be readily apparent by comparing the spatial information of the decoded image with the spatial information of the input image. ANSI T1.801.03-1996 [120] defines a lost edge energy parameter which measures the blurring artefact. This parameter compares the edge energy of the input image with the edge energy of the decoded image to quantify how much edge energy has been lost.

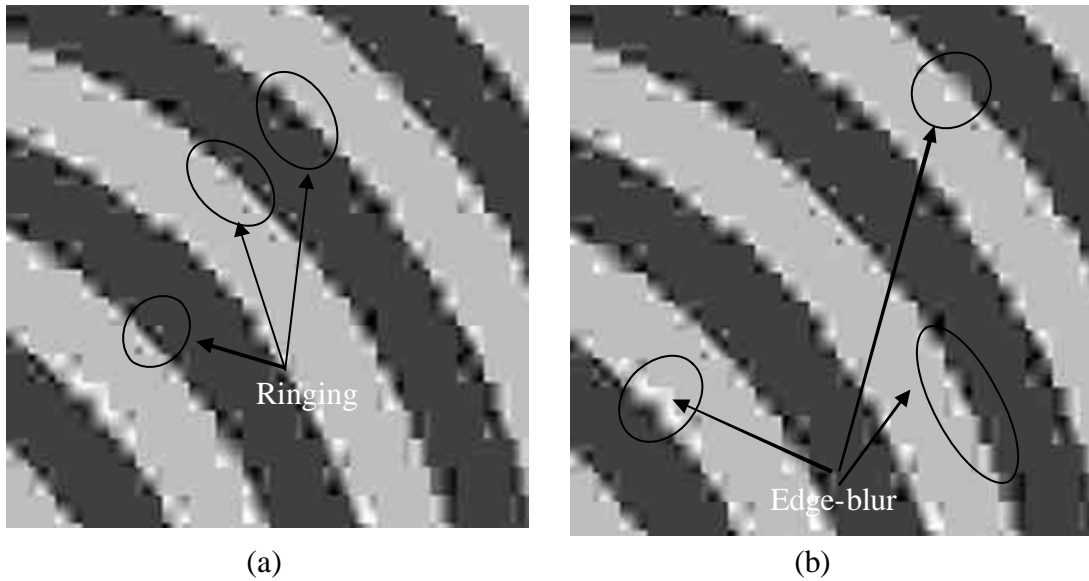


Figure 4.8 An example of (a) ringing artefact and (b) edge-blur artefact that are resulted in a JPEG codec at high compression ratio of 90.

4.3.2 First Generation – Test Pattern ‘monochrome rings’

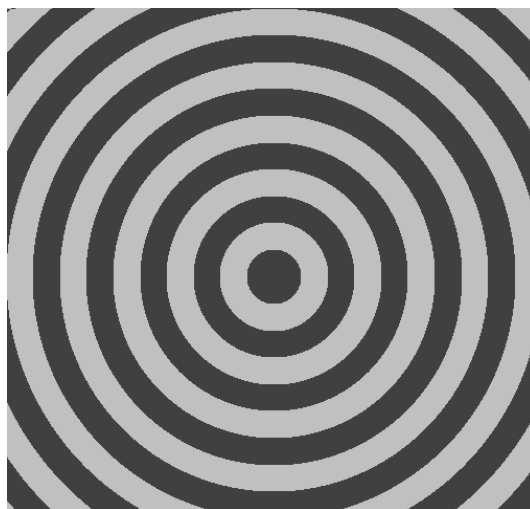


Figure 4.9 The uncompressed *monochrome rings* test pattern [121].

To test and emphasise for the ringing and blur artefacts, it is necessary to have sharp boundaries or step edges (abrupt changes in intensity) within the test pattern. The pixel values and the shape of the test pattern have been carefully chosen and designed so that the proposed algorithm could detect coding edge-blur and ringing artefacts completely, cleanly and adequately. A circular pattern contains edges of every orientation. These should include edges of all orientations in order to detect any

orientation sensitivity inherent in the codec. Pixel values of 64 and 192 with an 8 bit data representation have been chosen on either side of the boundary, so that after reconstruction there is adequate amplitude margin of 64 to allow for the ringing artefact in the reconstructed test pattern. To allow for more edges and resulting error pixels, concentric circles have been incorporated, as shown in Figure 4.9. The width of each monochrome band has been chosen as a prime number so that if block processing is used, the edges fall at different places within the blocks. This gives an average of the effects over all possible relative edge positions with respect to the block boundaries.

Consider an uncompressed colour test pattern $I(x,y)$ having M pixels per row, N pixels per column and three colour primary components R , G and B .

$$I(x,y) = R(x,y); G(x,y); B(x,y) \quad (4.3)$$

For a monochrome image, the values of $R(x,y)$, $G(x,y)$ and $B(x,y)$ in equation (4.3) are all equal. Each ring $Ring(x,y,n)$ is defined as

$$Ring(x,y,n) = ((n-1) \times w)^2 \leq \left(\frac{x}{N_s}\right)^2 + \left(\frac{y}{M_s}\right)^2 < (n \times w)^2 \quad (4.4)$$

where M_s , N_s and w are parameters based on the aspect ratio and the width of the rings w to be formed. For the rest of the research presented in the thesis, M_s and N_s have been chosen as 1 and represent the aspect ratio of 1:1. w is the width of rings and is chosen to be 29.

The criterion on which the intensity value of 64 or 192 is assigned can be expressed as

$$I(x,y) = \begin{cases} 64 & \text{for } Ring(n,x,y) \text{ with } n \text{ odd integers} \\ 192 & \text{for } Ring(n,x,y) \text{ with } n \text{ even integers} \end{cases} \quad (4.5)$$

The compression characteristics of this image are shown in Figure 4.10.

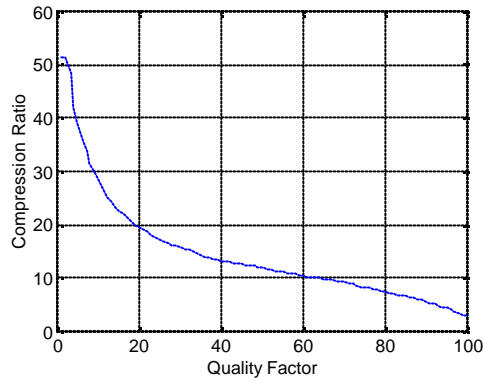


Figure 4.10 The compression characteristics of the Matlab™ JPEG codec that was used in the experiments with the *Monochrome rings* test pattern having dimensions 512x512 with 29 pixel wide bands.

4.3.3 Second Generation – Test Pattern ‘colour rings’

A synthetic colour test pattern has also been designed to emphasise the edge-blur and ringing artefacts. The colours have been chosen from analogue television colour bar pattern and also to have adequate amplitude margin of approximately either 24 or 50 to allow for ringing artefacts in the reconstructed test pattern. However, no floor or headroom can be accommodated for the black and white levels. To allow for more edges and resulting error pixels, multiple colour bands (in this case six) have been incorporated as shown in Figure 4.11.

The value of each colour component depends on the ring number from equation (4.4):

$$R(x, y) = r(n), G(x, y) = g(n), B(x, y) = b(n) \quad (4.6)$$

The assignment of colour components to rings is listed in Table 4.1. The spatial resolution can also be varied to accommodate any aspect ratio based on the application.

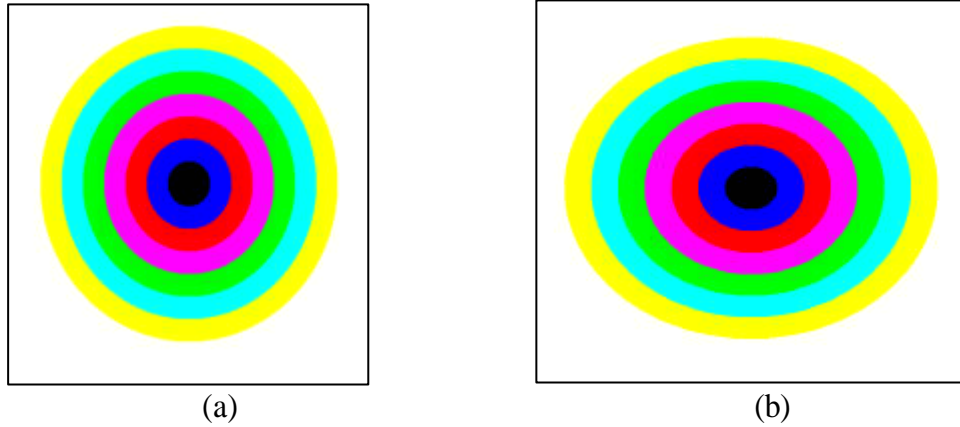


Figure 4.11 (a) The uncompressed *colour rings* test pattern with an aspect ratio of 1:1
 (b) The uncompressed *colour rings* test pattern with elliptical aspect ratio of 4:3. It is a 640x480 colour pattern having 24 bits per pixels. There are six colour bands.

Table 4.1 Eight colour combinations for eight of the n values (assignment of values for r , g and b)

n	Colour	$r(n)$	$g(n)$	$b(n)$
1	Black	0	0	0
2	Blue	0	0	1
3	Red	1	0	0
4	Magenta	1	1	0
5	Green	0	1	0
6	Cyan	0	1	1
7	Yellow	1	1	0
8	White	1	1	1

The luminance component Y of the colour test pattern is calculated based on the human visual system or the human perception as per equation (4.5) below at spatial location (x,y) [11].

$$Y(x,y) = (0.30 \quad 0.59 \quad 0.11) \times \begin{pmatrix} R(x,y) \\ G(x,y) \\ B(x,y) \end{pmatrix} \quad (4.7)$$

Both blur and ringing artefacts are evaluated using the luminance component Y of the uncompressed elliptical colour test pattern as shown in Figure 4.12(a), and the luminance component of its reconstructed elliptical colour test pattern as shown in Figure 4.12(b). The compression characteristics of this test pattern are shown in Figure 4.13. Chrominance components are analysed in colour bleeding chapters to evaluate colour blur and ringing using the same colour test pattern.

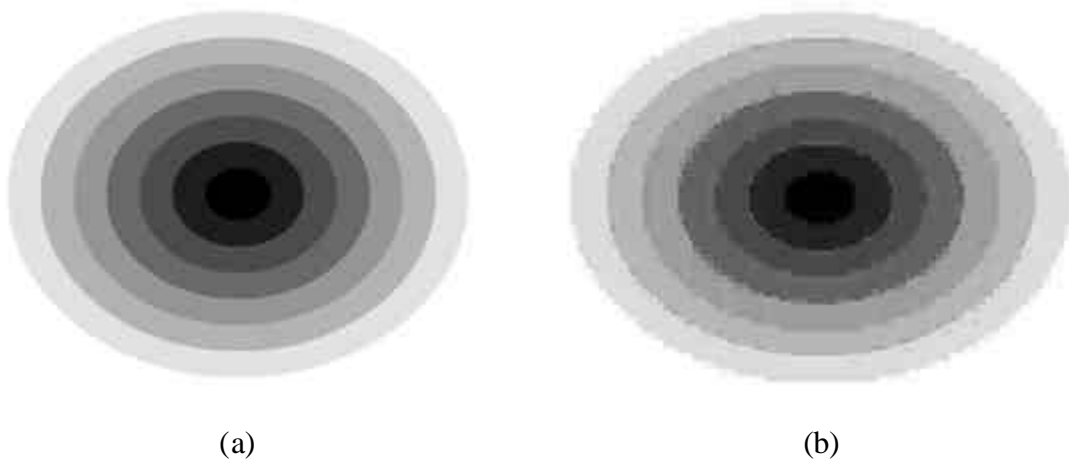


Figure 4.12 (a) The luminance component Y of the uncompressed colour rings test pattern, (b) The luminance component of the reconstructed colour rings test pattern.

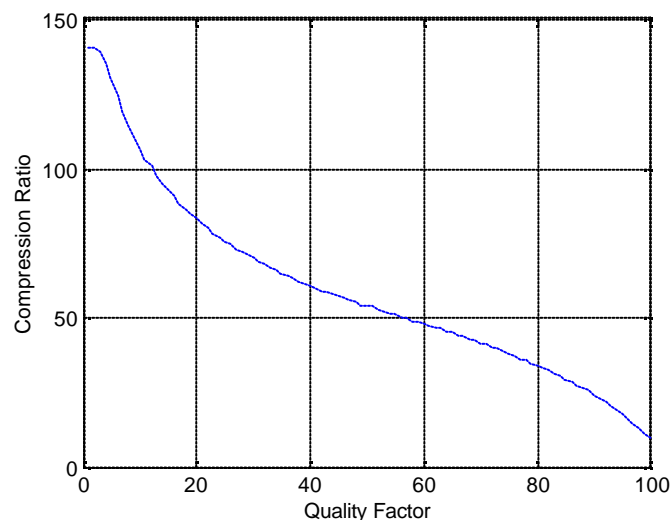


Figure 4.13 The compression characteristics of the Matlab™ JPEG codec that was used in the experiments with the colour rings test pattern having dimensions 640x480 with 29 pixel wide bands. The uncompressed colour test pattern has 24 bits per pixel.

4.3.4 Possibility for Sequence Generation

This thesis focuses on static test patterns generation and due to time constraints no attempts were made to create test sequences for edge-blur and ringing. They will be investigated as future work with mosquito artefacts.

4.4 Colour Bleeding Artefact

In analogue image and video systems, subjective assessments on monitors and objective assessments on measuring instruments enable evaluation of perceptual quality as well as objective measures which are computationally accurate and swift to compute. The traditional colour bar signal or the test pattern shown in Figure 4.14 is a composite test signal and is used in quality evaluation [125].

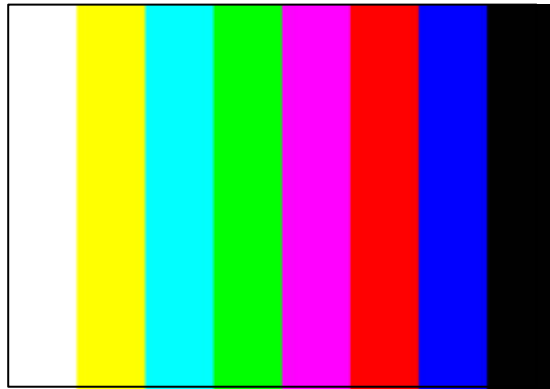


Figure 4.14 Original colour bar static test pattern used in analogue television [12].

This test pattern does not stress a digital codec, since the colour boundaries are only vertical. They are reconstructed with minimal errors as shown in Figure 4.15 for a range of compression ratios (CR). These errors result primarily from the quantisation of the colour component during compression. Therefore, it is necessary to design new test patterns that can stress and measure the colour fidelity of digital codecs.

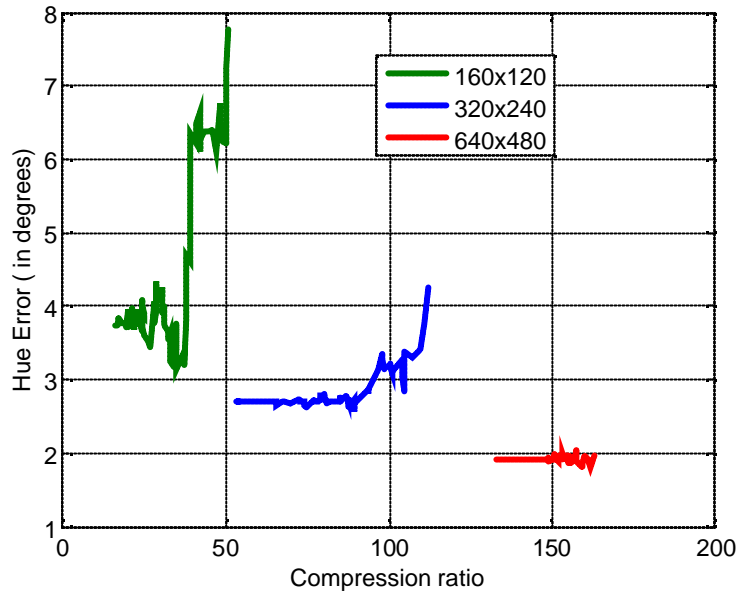


Figure 4.15 Hue errors measured in degrees as a function of JPEG compression ratio with the conventional vertical-bar colour test pattern having 640x480, 320x240, 160x120 pixels.

4.4.1 Qualitative Definition

As its name suggests, colour bleeding occurs when the edges of one colour in the image bleed into or overlap another colour inappropriately. Two common sources of colour bleeding are the excessive saturation in the image at some point and the other as an artefact of digital image and video compression. According to Demtschyna [126] colour bleeding can be demonstrated on a traditional television receiver by simply increasing the colour (tint) control beyond its normal position, beyond a certain threshold the colours in the image begin to bleed into one another as shown in Figure 4.16. This is caused by the saturation of the analogue amplifiers in the image reproduction system.

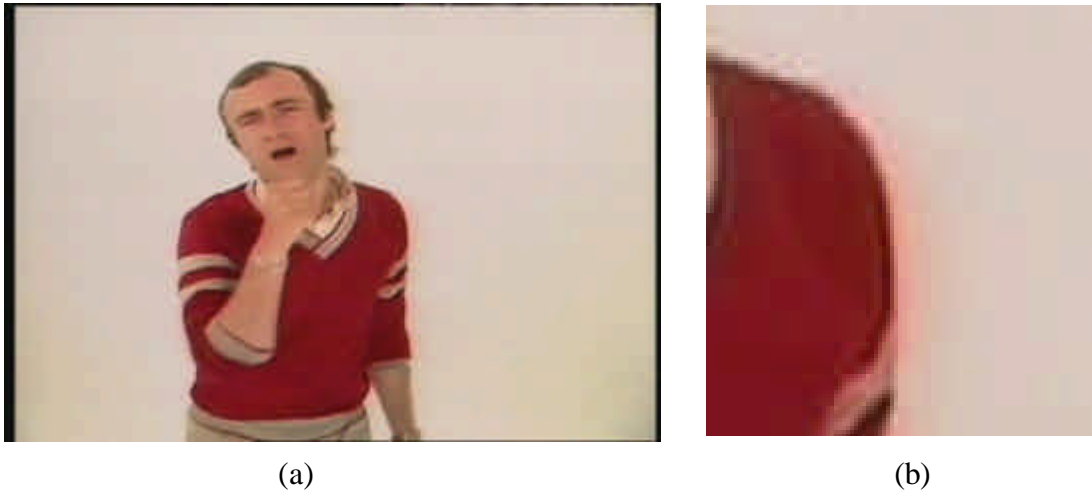


Figure 4.16 (a) A screen shot from television with colour bleeding along colour edges [126], (b) Close up of the shoulder. Note the smearing (bleeding) of the colour red beyond where it should physically be restricted to [126].

Yuen and Wu [27] compare colour bleeding with the blur introduced into the luminance as a result of the smoothing of spatial detail. They argue that the corresponding effect for the chrominance results in a smearing of the colour between areas of strongly contrasting chrominance. As with blurring, colour bleeding results from the truncation of the higher-order coefficients, resulting in the representation of the chrominance components by only lower frequency coefficients. Since the chrominance information is sub-sampled, the bleeding from a JPEG codec is not limited to the typical 8x8-pixel area, as for the luminance, but extends to the boundary of the macro-block for video, usually 16x16 pixels in extent. According to Yuen and Wu [27], for chrominance edges of very high contrast, or where the quantization of the higher order coefficients does not result in their truncation, colour ringing can occur. For example, the blurring of the chrominance component, which leads to colour bleeding, is most evident along the top edge of the arm in Figure 4.17, as well as around the table and the table-tennis paddle. The greenish patches near the red sleeve are a result of colour ringing.



Figure 4.17 From Yuen and Wu [27] illustrate colour ringing and colour blurring of the chrominance: “the reproduction of a frame suffering from colour bleeding and colour ringing from the Table-tennis sequence. Note the high-frequency changes in colour around the table edge, corresponding to the ringing, and the gradual bleeding around the arm”.

Yuen and Wu [27] also describe colour bleeding by its manifestation as spurious coloured oscillations in the vicinity of highly contrasted colour areas of the decoded picture. Coudoux et al. [24], [25], [26] describe colour bleeding as a distortion that appears as a smearing of the colour between areas of strongly contrasting chrominance and results from the quantization of the higher order AC coefficients. Susstrunk et al. [127] and Spampinato et al. [128] define colour bleeding as the “smearing of colour between areas of strongly differing chrominance”.

The three descriptions above are qualitative. One of the challenges is to define the colour bleeding quantitatively, so that it agrees with the above qualitative descriptions. Colour bleeding can be defined as the distortion due to leakage of colour across colour boundaries. With digital codecs, coding colour bleed (CCB) is the result of lossy compression, and includes both blurring and colour ringing.

4.4.2 First Generation - Test Pattern ‘colour rings’

The requirements for the test patterns are derived based on the qualitative definitions of colour bleeding. As colour bleeding occurs over regions having strong colours at the edges, test pattern needs to have discrete colour regions like in the traditional colour bar test pattern. Only six colours have been chosen to enable the use of vectorscope graticule. The colour bar test pattern has only a limited number of colour interactions due to six large colour regions. Codecs using block processing segment the image to 8x8 pixels sub-image blocks aligned with the image boundaries. If the block boundary coincides with the colour boundary the codec can reconstruct the image very well. To stress the codec, it is required to have colour boundaries that are not vertical or horizontal. One possibility is to have diagonal colour boundaries. If the boundaries are made elliptical, then the colour test pattern has boundaries for all possible edge orientations.

The first simple synthetic colour test pattern has been designed with six curved colour regions as shown in Figure 4.18. The curved edges contribute high frequency components to the colour difference signals. The RGB values of pixels have been selected so that they fall within the colour gamut in use. The boundary between the colour regions is curved so that it stresses the codec at all compression ratios as required to emphasise the colour bleeding artefact.

However, the colour elliptical test pattern lacks colour interaction among all possible colours. Having uniform and constant colour over many colour regions gives the ability to measure the extent of colour bleeding cleanly and adequately to have a meaningful measure.

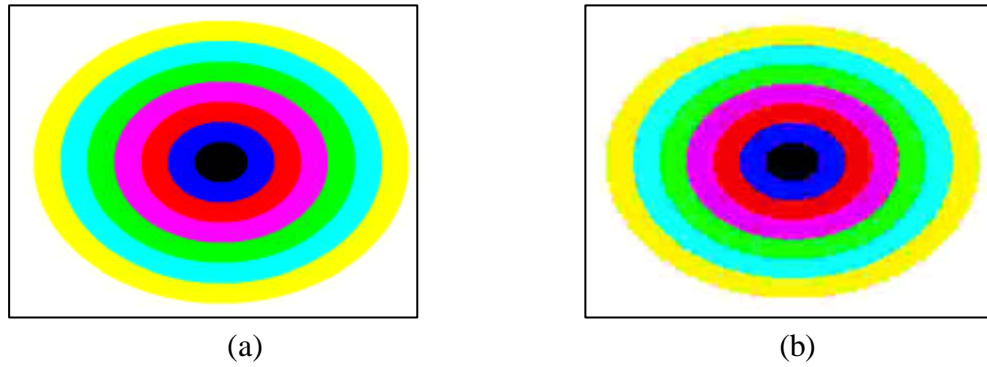


Figure 4.18 This demonstrates the coding colour bleed observed when the test pattern is compressed using a JPEG codec with a compression ratio of 12 (a) *colour rings* (elliptical) test pattern [12], (b) JPEG reconstructed *colour rings* (elliptical) test pattern.

4.4.3 Second Generation – Test Pattern ‘honeycomb’

One of the limitations of the colour rings test pattern is that the colour pixels are not equally distributed among six colours chosen. For a given colour region, it has a maximum of two other colour regions as neighbours. Since there are six colours in the colour bar test pattern, five colour neighbours can be programmed for maximum colour interactions. If colour regions are polygons, they can be connected to each other. To have a tessellation, that is all the regions fit together with no gaps, regular six sided polygons were formed. The hexagonal tiles are tilted so that the boundaries do not align with the image boundaries. The colour test pattern looks like a honeycomb, hence, hereafter it is referred to as the "*honeycomb*" test pattern as shown in the Figure 4.19. As the test pattern was designed manually using an image processing package, the hexagon edges were not sharp colour transitions. This was discovered when hue histogram analysis revealed the contaminated hue in the initial version of the test pattern as shown in Figure 4.20(a). It is important to not use anti-aliasing between the tiles because this will introduce additional colours along the boundaries making it more difficult to identify colour bleeding introduced by the compression. The refined version of honeycomb has clean hue values in each region as shown in Figure 4.20(b). Subsequent experiments of the research used the refined version or test patterns derived from this version.

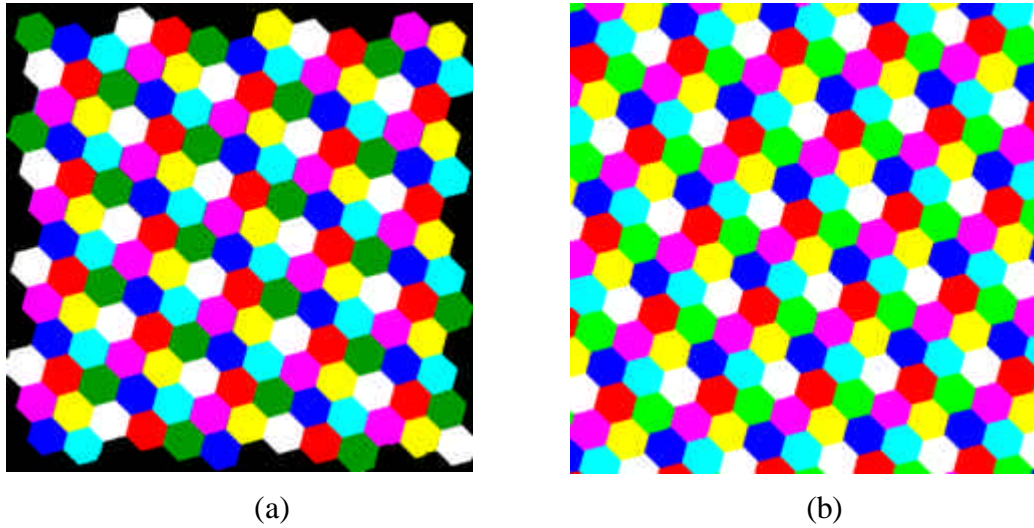


Figure 4.19 The honeycomb test pattern (a) initial version with gaps between colour hexagons and black borders [129] (b) refined version having a tessellation of colour hexagons without black regions [130].

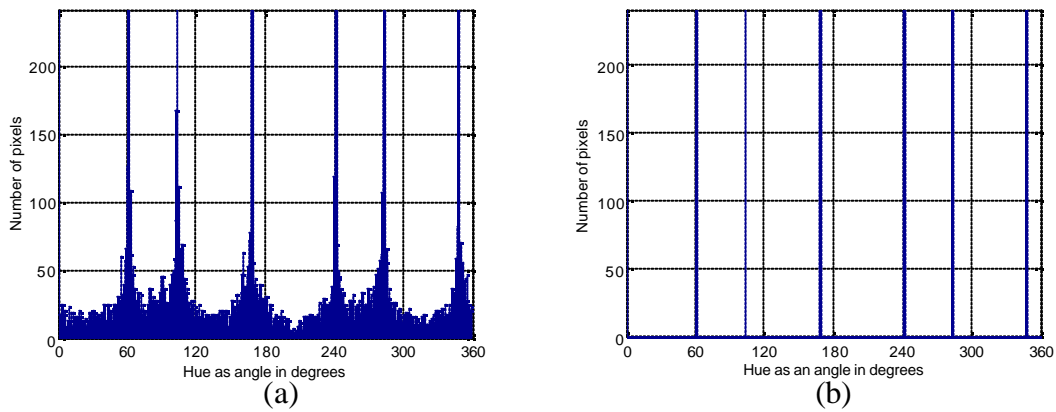


Figure 4.20 Details of the hue distribution of the *honeycomb* test pattern (a) initial version from Figure 4.19(a) (b) refined version from Figure 4.19(b).

4.4.4 Luminance Modulation

The *honeycomb* test pattern was designed and generated with specific hues from the analogue colour bar test pattern in each of the six hexagonal regions. The above test

pattern was transformed to give the same luminance value for each colour region without disturbing the hue and saturation of the original *honeycomb* test pattern as shown in Figure 4.21.

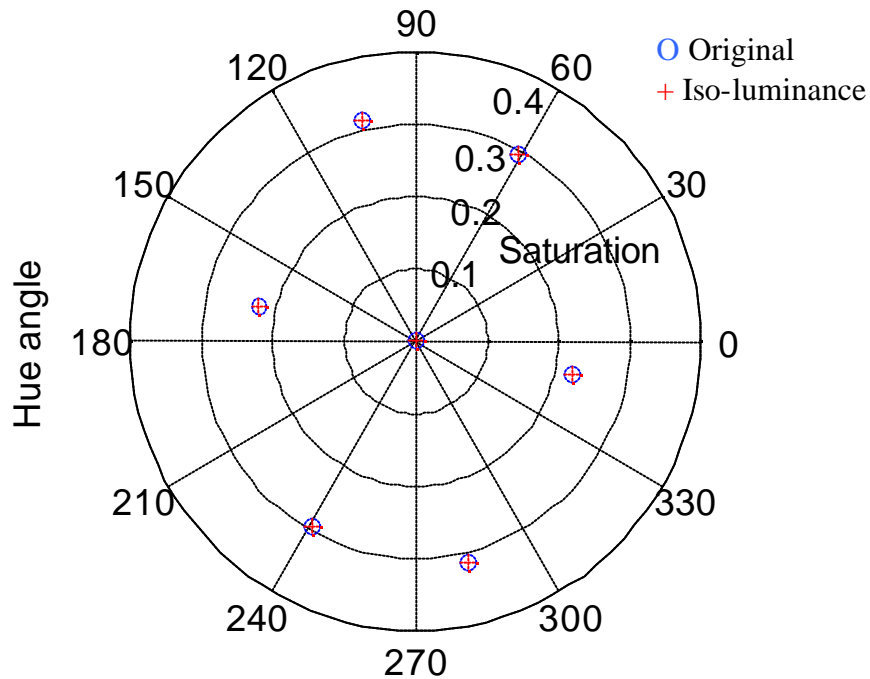


Figure 4.21 Hue (in degrees) and saturation (in normalised units) of honeycomb test pattern; ‘O’ indicates values prior to making iso-luminance and ‘+’ are values of iso-luminance test pattern.

As hue and saturation are the key two parameters needed to define the chrominance, the luminance needs to be kept constant across all the colour regions. Otherwise different luminance levels of six colours would not influence chrominance errors uniformly. Figure 4.22 (b) shows the *honeycomb* test pattern in Figure 4.22(a) adjusted for the same luminance: both test patterns have the same hue angles and saturation as shown in Figure 4.21.

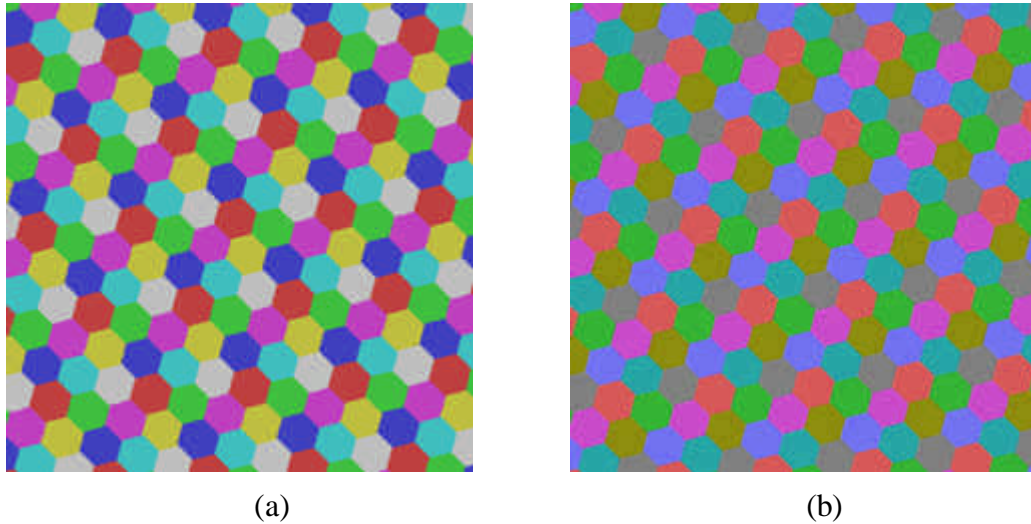


Figure 4.22 (a) *Honeycomb test pattern* that has varying luminance values but with specific hues from the analogue colour bar test pattern (b) *Honeycomb test pattern* having same luminance value and specific hues from the analogue colour bar test pattern.

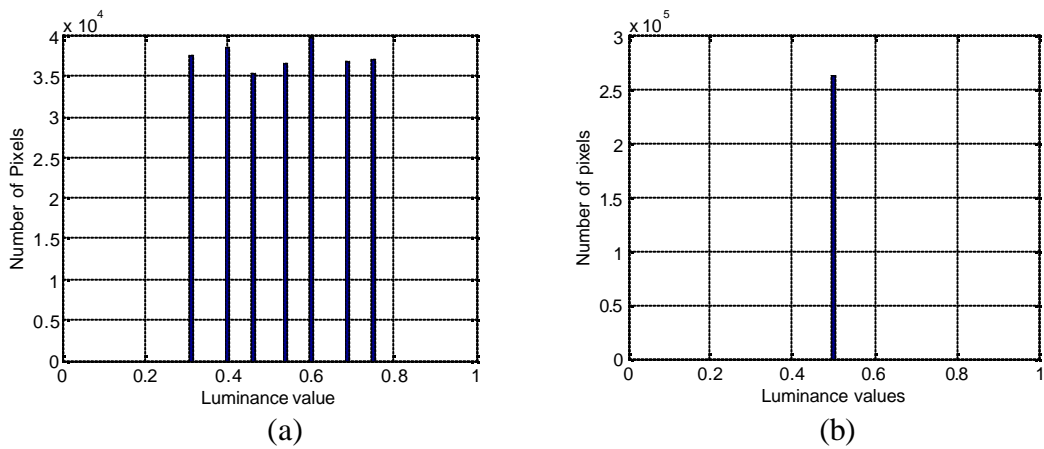


Figure 4.23 The distribution of normalised luminance values of the honeycomb test patterns Figure 4.22 (a) without luminance adjustment (b) with luminance adjustment

4.4.5 Colour Attribute Transformation

The test pattern generator transforms a colour pattern based on the set of primaries defined for the PAL (Phase Alteration by Lines) colour television system. A matrix for conversion from CIE-1931 tri-stimulus values to synthetic-image R, G, B values

based on a knowledge of the PAL system primaries and their CIE-1931 chromaticity coordinates together with the setting of the white point in that system.

$$[R, G, B] = [M][X, Y, Z] \quad (4.8)$$

Where the matrix coefficients of $[M]$ are calculated in accordance with the method outlined in the literature ([131] and [132]). The *honeycomb* and *colour rings* test patterns have been designed using the PAL colour television system hue values. Hue values can be changed to suit other media applications using equation (4.8). A given colour test pattern can be transformed to obtain the colours that can be displayed or printed within a given application. The mapping algorithm transforms the R , G and B values of the captured test pattern with the required colour attribute values as shown in Figure 4.25. This allows using the pattern generator for any colour attributes. Figure 4.24 shows a transformed pattern of a *honeycomb* test pattern. The algorithm maintains the structural information within the test pattern.

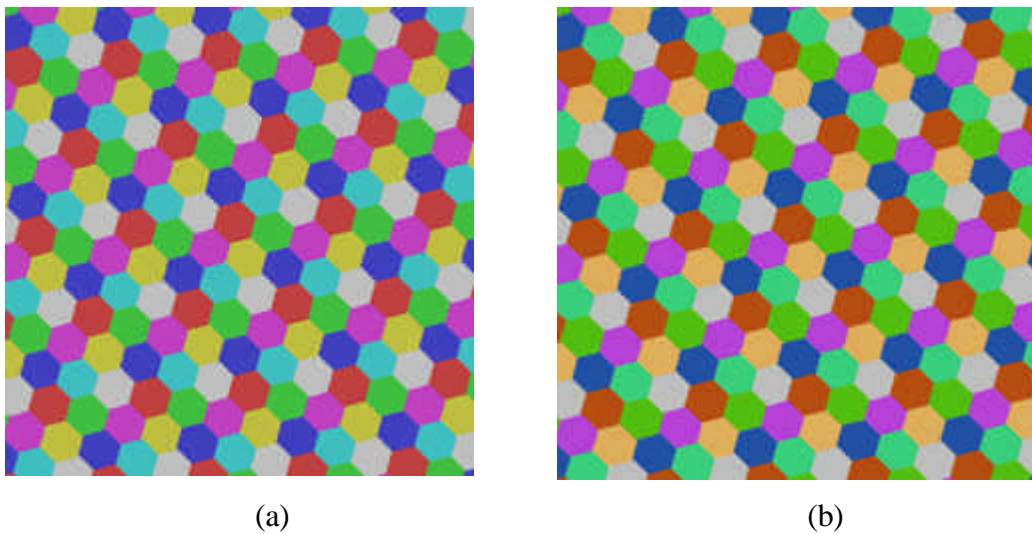


Figure 4.24 (a) A test pattern having hue angles of 0, 61, 104, 168, 241, 284, 348 and
 (b) Transformed test pattern with hue angles of 0, 50, 120, 140, 220, 260, 320

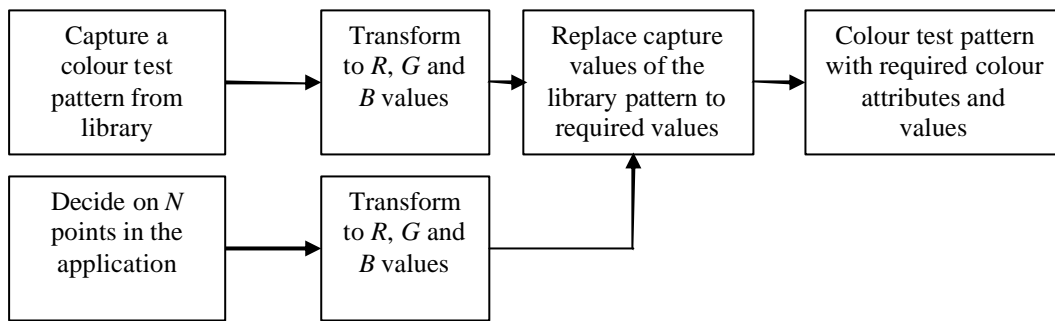


Figure 4.25 Block diagram of the colour pattern conversion algorithm (Adapted from [16]).

The Figure 4.26 shows the hue and saturation values after the hue transformation, which is a special case of colour attribute transformation.

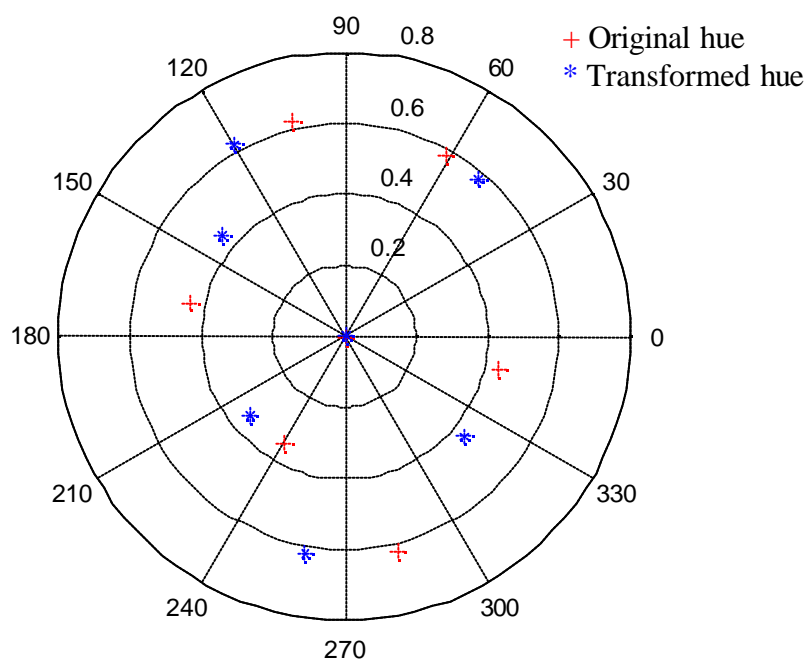


Figure 4.26 original hue angle vector of [0, 61, 104, 168, 241, 284, 348] transformed to another hue angle vector of [0, 50, 120, 140, 220, 260, 320] keeping the saturation the same.

4.4.6 Random Test Pattern Generation

It is also possible to randomly generate colour test patterns to prevent image compression schemes adapting to the test pattern when benchmarking the performance of codecs. In assessing colour bleeding in image codecs sharp colour boundaries are needed. Figure 4.27 shows random colour circles generated to measure colour bleeding composed of discrete circular colour regions within the frame. The size, location and colour of the small circular regions are random.

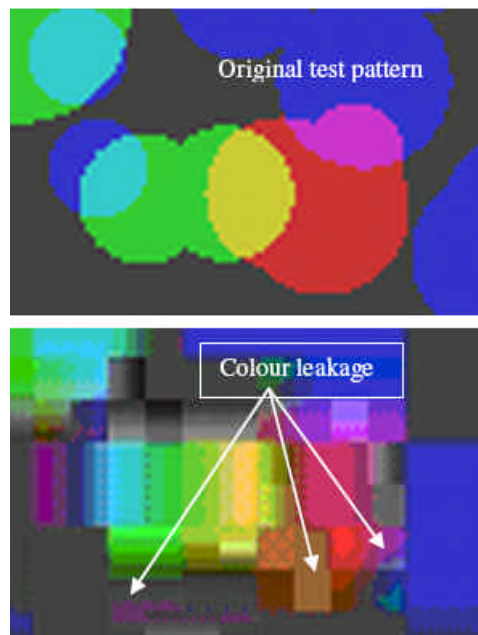


Figure 4.27 Colour leakages in random test pattern, at top the original pattern and at bottom the JPEG compressed test pattern [16].

One of the frames from some sample test patterns generated using the random test pattern generator is shown in Figure 4.27.

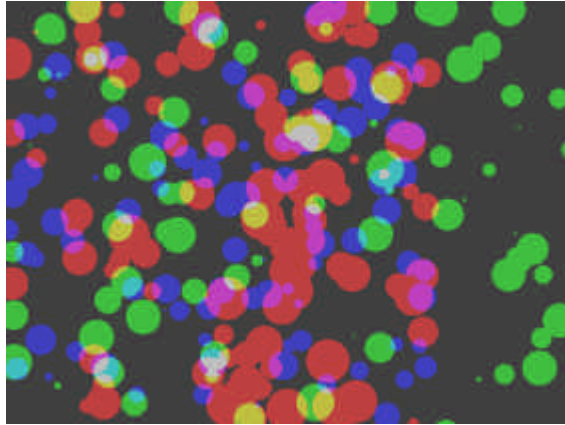


Figure 4.28 A colour test pattern from the colour test pattern generator [16].

4.4.7 Possibility for Sequence Generation

It is possible to generate sequences based on static random colour test patterns, *honeycomb* or *colour rings* test patterns by moving the spatial content with respect to a coordinate system. However, sequence generation and the application of such sequences have not been investigated as motion artefacts are outside the scope of this thesis. The generation of test sequences for spatio-temporal artefact analysis is a major topic for future study.

Chapter 5: Distortion Metrics for Compression Artefacts

Given a set of test patterns that stress the codec, the next step is to define quantitative measures for each of the artefacts.

5.1 Blockiness Artefact Metrics

Bailey et al. [112] proposed an objective no-reference blockiness metric for quality assessment of block-based compressed images and video. The Bailey metric estimates the strength of the blocking artefact by evaluating edge activity, which is a measure of edge strength associated with each row or column spaced at the block size, evaluated using the median value of the first derivative of pixel values vertically and horizontally in the spatial domain. This algorithm needs to be provided with the codec block size as an input parameter. However, it does not require prior knowledge of the original image content. Suthaharan et al. [133] presented a distortion measure for blocking artefacts in digital video. However, this measure does not cope well on images with vertical and horizontal edges. In 1995 Karunasekera et al. [134] presented a perceptual distortion measure for blocking artefacts in images based on human visual sensitivity. In their approach a visual model is used to derive a quantitative error for blocking artefacts and takes into account the variation in visibility of edge artefacts with edge length, edge amplitude, background luminance and background activity. To derive the parameters for the model, they have used synthetic test patterns. They have then carried out subjective tests to verify the model using natural images. This is a pioneering work in the area of perceptual distortion measures. However, this approach is limited to the estimation of blockiness artefact. Generally, an assumption made with other perceptual metrics is that the human visual system response at the visibility threshold can be generalised to distortions above the visual threshold.

5.1.1 Quantitative Definition of Blockiness

Since blockiness is not defined mathematically in the ANSI T1.801.02-19 standard, for the purpose of this research, it is defined as the intensity jump at block boundaries.

This is measured in units of grey scale intensity. Most other researchers [112] have used a similar approach to compute blockiness. If the block size is known, the intensity gradients at each block boundary can be calculated. Since blocks are rectangular in shape and generally square, the gradient values can be calculated in both vertical and horizontal directions. When the intensity steps are over a certain pre-determined threshold, the intensity gradients at those points can be accumulated to compute the average discontinuity or the blockiness. The discontinuity can also be computed based on the error image for the reconstructed test pattern. The intensity gradient at block boundaries can be calculated using the known block size of n or at each pixel. Based on these choices, there are four algorithms that give rise to four blockiness artefact metrics.

It is important to detect blockiness even though it may be below the threshold of perception. When the compression is performed in cascade or with transcoding, concatenated artefacts may result. This is due to the fact that distortions which are not critical or perceptible over one stage of compression may surface due to subsequent compression or processing.

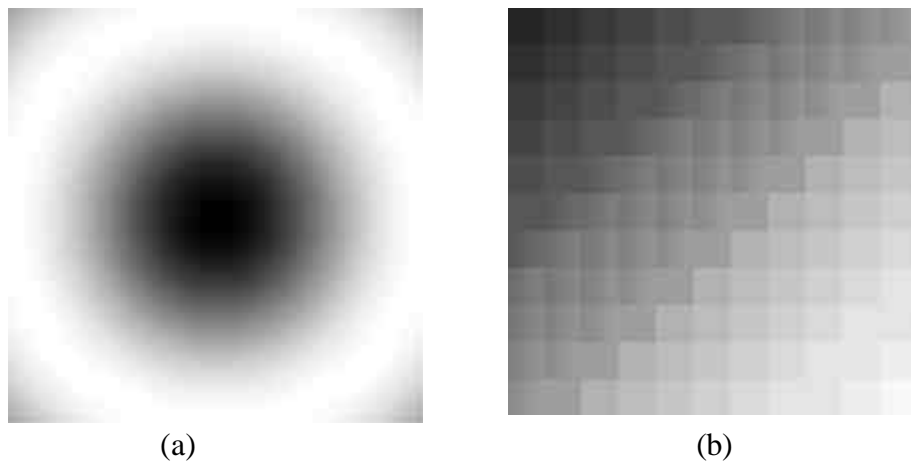


Figure 5.1 (a) Original ‘sinesquared grey scale -radial’ test pattern I and (b) zoomed part of \hat{I} to show vertical and horizontal blockiness.

Consider the reconstruction, \hat{I} , of a $n \times n$ block coded or tiled $M \times N$ test pattern I . As shown in Figure 5.1, both vertical and horizontal edges can be observed at regular

pixel intervals of n , the block or tile pitch. Figure 5.2 shows the algorithm for computing the blockiness metric.

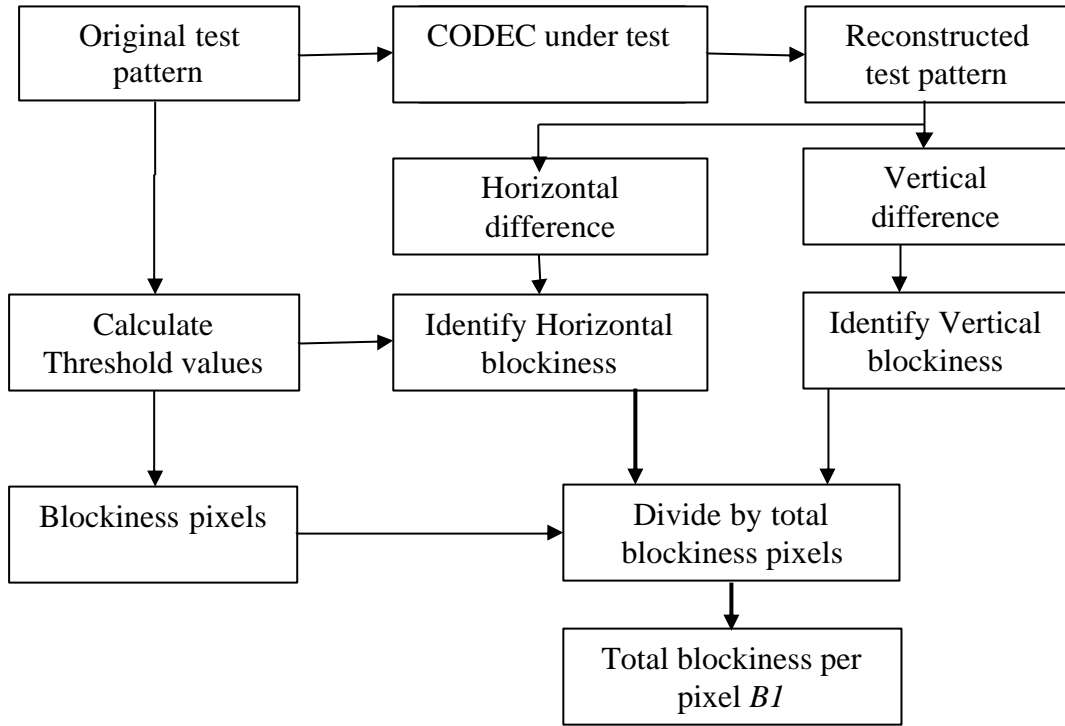


Figure 5.2 Blockiness computation algorithm

First consider the horizontal direction. The horizontal edge strength is calculated as

$$he(x, y) = \begin{cases} \left| \hat{I}[x, y] - \hat{I}[x+1, y] \right| & \text{for } \left| \hat{I}[x, y] - \hat{I}[x+1, y] \right| > \left| I[x, y] - I[x+1, y] \right| \\ 0 & \text{otherwise} \end{cases} \quad (5.1)$$

$he(x, y)$ is thresholded to account for known edges within the test pattern. It also enables edges that are below the threshold of perception to be considered. The horizontal blockiness for a row can then be calculated by adding the edge strength at the columns corresponding to the known block boundaries:

$$hb(y) = \sum_i he(n \times i, y) \quad (5.2)$$

The total horizontal blockiness, thb , then accumulates the horizontal blockiness from all the rows:

$$thb = \sum_{y=1}^M hb(y) \quad (5.3)$$

This results from $\frac{(N-n)}{n}M$ block boundary pixels.

Similarly, the vertical blockiness $vb(x)$ along the column x ,

$$ve(x, y) = \begin{cases} \left| \hat{I}[x, y] - \hat{I}[x, y+1] \right| & \text{for } \left| \hat{I}[x, y] - \hat{I}[x, y+1] \right| > \left| I[x, y] - I[x, y+1] \right| \\ 0 & \text{otherwise} \end{cases} \quad (5.4)$$

$$vb(x) = \sum_i ve(x, n \times i) \quad (5.5)$$

The total vertical blockiness,

$$tvb = \sum_{x=1}^N vb(x) \quad (5.6)$$

results from $\frac{(M-n)}{n}N$ block boundary pixels.

Both the thb and the tvb can be combined and normalised by dividing by the number of boundary pixels. Hence the blockiness per boundary pixel, $B1$, can be expressed as

$$B1 = \frac{thb + tvb}{\frac{N-n}{n}M + \frac{M-n}{n}N}. \quad (5.7)$$

The above computation is performed on the reconstructed test pattern.

An alternative approach, associated with fidelity, is to compute the blockiness on the error image, E , which is defined as

$$E = \hat{I} - I. \quad (5.8)$$

The error image E automatically takes account of any edges within the test pattern, so the thresholding in equations (5.1) and (5.3) is not required. This second blockiness metric is designated as $B2$, and is computed using E instead of \hat{I} in equations (5.1) to (5.7):

$$B2 = \frac{\sum_{x=1}^N |E[x, y] - E[x, y+1]| + \sum_{y=1}^M |E[x, y] - E[x+1, y]|}{\frac{N-n}{n}M + \frac{M-n}{n}N}. \quad (5.9)$$

If the block size is unknown, the blockiness can be calculated at each pixel position. The blockiness metrics $B3$ and $B4$ are computed for reconstructed test pattern \hat{I} and error test pattern E at each pixel ($n=1$) respectively. The need for knowing the block size will be investigated in section 6.1.1 by comparing $B3$ and $B4$ with $B1$ and $B2$ which are computed with the known block boundaries.

5.2 Blur and Ringing Artefact Metrics

Yao et al. presented a blurring distortion measure based on the full reference approach and computed the correlation between the original and error image edges [135]. However the method does not distinguish blur and ringing which, in general, may occur concurrently. A few researchers have developed non-referenced, objective quality metrics for blur in images compressed using either block processing or tile processing [136] [137], [138], [139]. However, search of the literature during 2002 to 2009 did not reveal any objective distortion metric for the edge blur based on synthetic test patterns or in a rapid evaluation tool.

Many researchers have developed non-referenced, objective, quality metrics and mitigation techniques for the ringing artefact in block-based compressed images [141] to [152]. Kusuma's research measured ringing by measuring the busyness or activity increase [141]. Archibald et al. applied a method known as Gegenbauer method to eliminate ringing in MRI images [142]. Some researchers worked on removal of ringing distortions by adaptive filtering methods [143] to [146] and [148] to [151]. None of these works show the efficacy of approach objectively. Marziliano proposed

a perceptual ringing metric defined similar to the approach proposed in this research [147]. However, a search of the literature did not reveal any objective artefact metric for ringing based on synthetic test patterns.

5.2.1 Quantitative Definition of Blur and Ringing

An ideal step-edge contains components at all frequencies. Any change in the amplitude or phase of any of these components will result in ripples in the image with amplitude corresponding to the error. As a result of energy compaction in a codec, many of the high frequency components are very small, and get quantised to zero. This loss of high frequency components leads to blur and ringing in reconstructed test patterns.

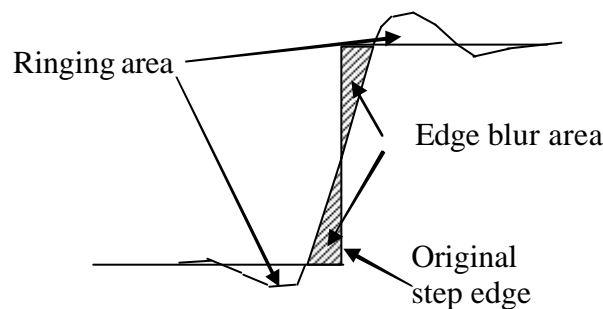


Figure 5.3 The edge blur and the ringing at an edge of a one-dimensional signal [140].

The edge blur is defined using Figure 5.3 as the region between the first crossings on each side of the edge transition as the edge blur region. The crosses in Figure 5.4 are the pixel values near the edge of a reconstructed test pattern from a codec. The transition involves many pixels and pixel values may oscillate around each level of pixel values. By adding all blur areas resulting from each edge pixel and dividing by the total number of edge pixels gives an average blur area. The edge-blur is the blur width which is the ratio between average blur per edge pixel and edge step height.

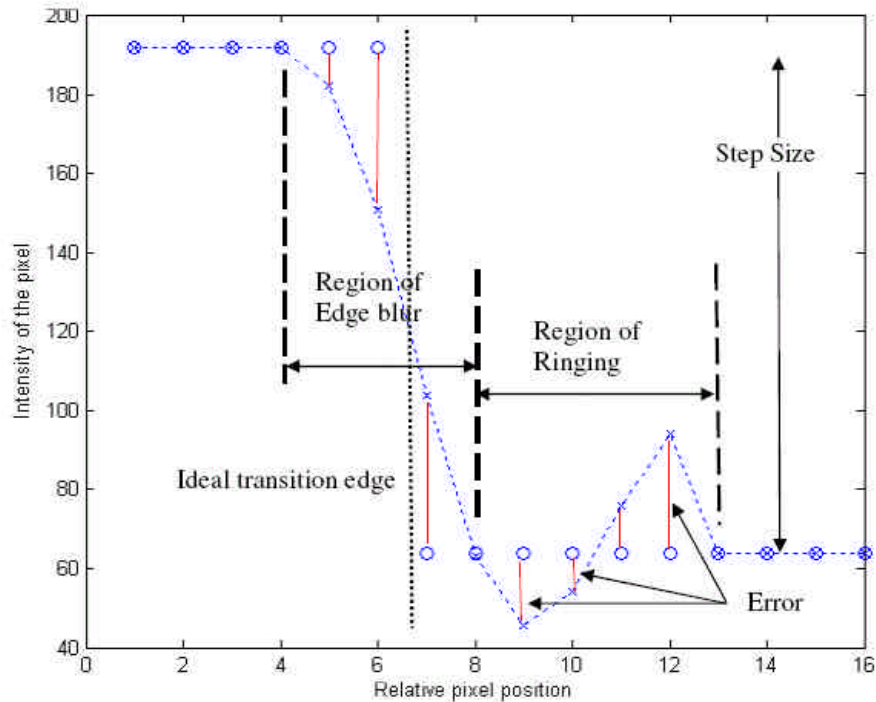


Figure 5.4 The edge blur and the ringing for one-dimensional sampled data. Circles represent original pixel value and crosses represent reconstructed pixel values [121].

Similarly, to obtain a measure of ringing, consider the area marked as ringing in Figure 5.3. The greater the ringing, the larger will be the ringing area. The area between the ringing signal and ideal signal provides a measure of the severity of ringing. By dividing the area by the step height, a measure of the average ringing height can be obtained. With sampled data, an ideal step edge would involve a transition between two pixels, as illustrated by the circles in Figure 5.4. The crosses in Figure 5.4 are the pixel values near the edge of the reconstructed image from a codec. The transition involves many pixels, and the pixel values may oscillate around each level of pixel value.

5.2.2 Algorithm

Using the rings test patterns; either the *monochrome rings* or the luminance component of the *colour rings* test pattern, the edge blur can be evaluated using the equation (5.7). Figure 5.5 shows intensity profile over 3 grey scale rings. The transition from intensity values of 64 to 192 takes place over one pixel in the original

monochrome test pattern. In the reconstructed test pattern the transition occurs over many pixels.

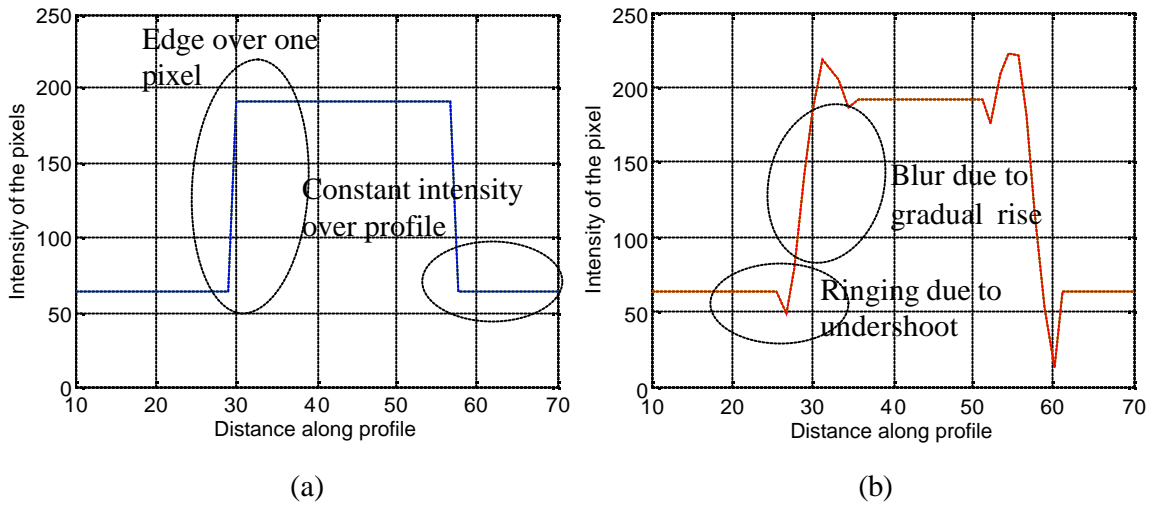


Figure 5.5 (a) An edge of the uncompressed *monochrome rings* test pattern, (b) An edge of the reconstructed *monochrome rings* test pattern with the edge blur and the ringing.

Figure 5.6 shows radial profiles of original and reconstructed *monochrome-rings* test patterns. Profiles are shown starting from the centre of the *monochrome-rings* test pattern to an edge of the test pattern. It can be observed that the edges are of the same step size. Considerable edge-blur and ringing distortions is present at all seven edges.

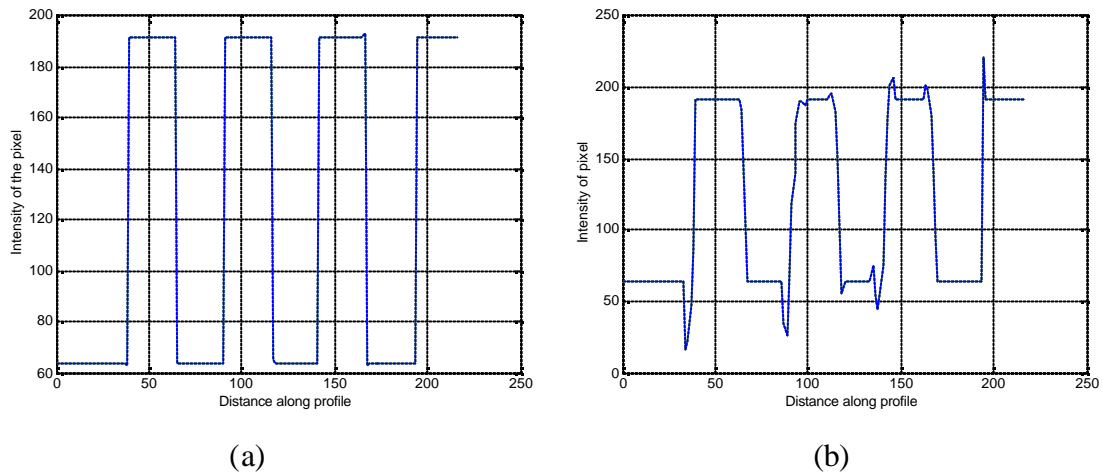


Figure 5.6 (a) The edge along a radial line from centre of an uncompressed *monochrome-rings* test pattern, (b) An edge along a radial line of the reconstructed *monochrome-rings* test pattern.

The algorithm shown in Figure 5.8 computes both edge blur and ringing. It was designed to detect, separate and measure both blur and ringing artefacts. The algorithm utilises some of the key structural features of the rings test patterns for cleaner detection of the ringing artefact.

The challenge is to apply 1-D blur and ringing definitions given in Figure 5.3 to a 2-D test image where there can be some ambiguity as to what is ringing and what is blur. One possibility is to take radial image profiles and to analyse them. However this is complicated by the fact that pixels are at discrete locations, and a profile at an arbitrary angle is not well defined. The approach taken here is to use the Euclidean distance transform of the test pattern to label each pixel with its distance from the original transition. Starting from the edge, connected blur pixels are considered blur rather than ringing if it has at least one neighbour closer to the boundary (determined by the distance transform) also classified as a blur pixel. This is implemented through successive dilations of previously classified blur pixels, adding only those whose distance is equal to the iteration number. For JPEG codecs, a distance of 7 pixels is sufficient to identify all blur pixels. The resultant mask is shown in Figure 5.7(b) and is used to identify blur error from the error test pattern shown in Figure 5.7(a). The

remaining error pixels are the ringing pixels. The uniform grey areas are reproduced with least errors due to the large extent of uniform grey areas.

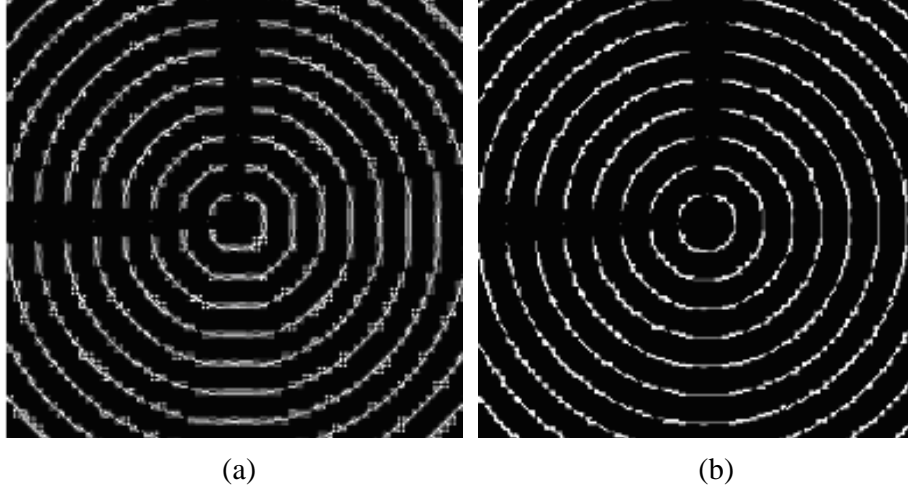


Figure 5.7 (a) The edge blur and ringing errors in a reconstructed *monochrome-rings* test pattern (b) The mask image to obtain the edge blur pixels present in the reconstructed rings *monochrome-rings* test pattern

The blur and ringing are then quantitatively defined according to equations (5.7) and (5.8). Consider a blur pixel (x_b, y_b) . The average edge blur B per edge pixel can be evaluated as,

$$B = \frac{\sum_{\{x_b, y_b\}} \left| \hat{I}(x_b, y_b) - I(x_b, y_b) \right|}{m \times h} \quad (5.7)$$

where m is the number of edge pixels and h is the step height. Similarly, the average ringing per edge pixel R can be calculated as,

$$R = \frac{\sum_{\{x_r, y_r\}} \text{abs} \left(\hat{I}[x_r, y_r] - I[x_r, y_r] \right)}{m \times h}, \quad (5.8)$$

where (x_r, y_r) is a ringing pixel in the reconstructed test pattern.

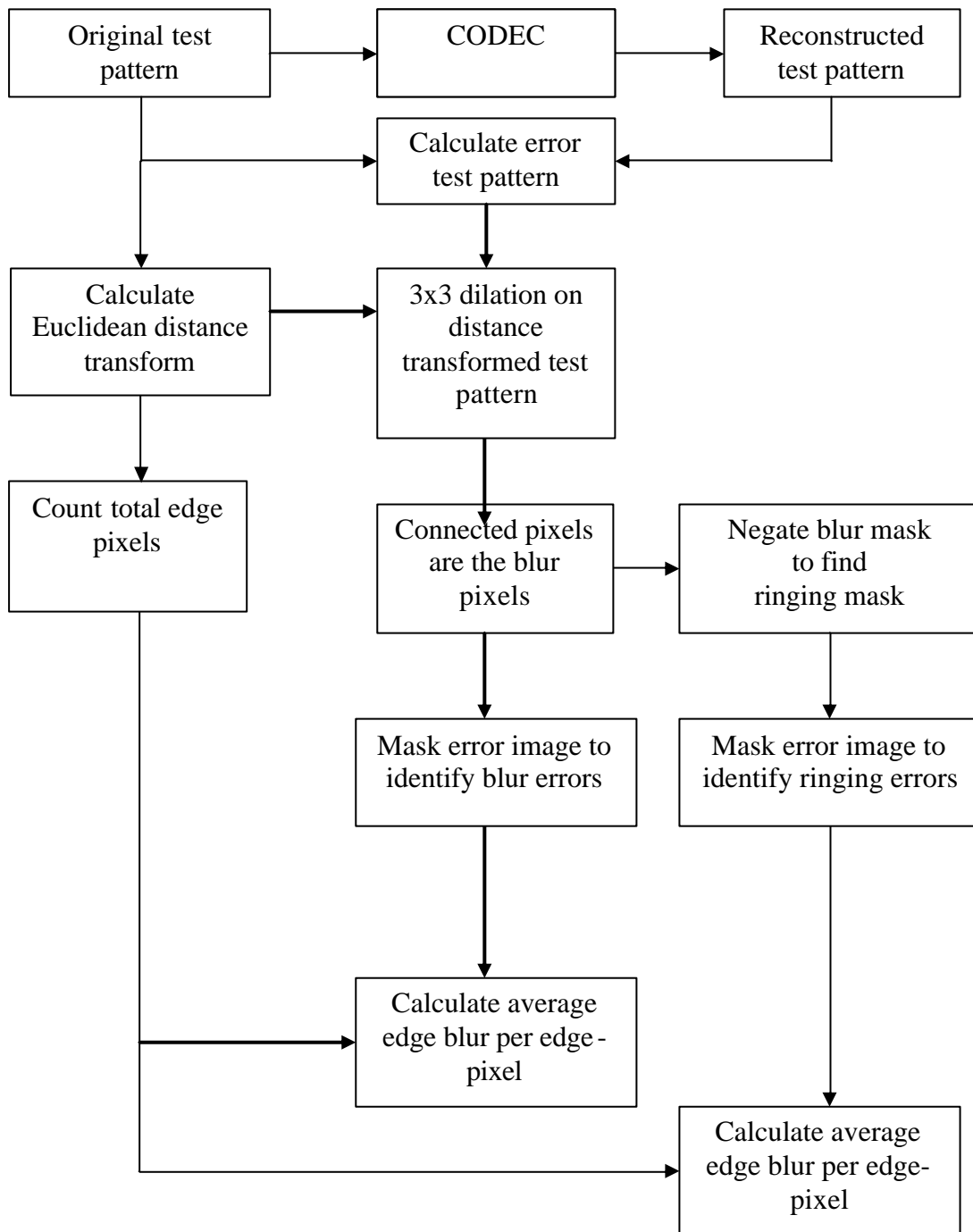


Figure 5.8 The block diagram of the edge blur detection and measurement algorithm.

The ringing artefacts due to colour codecs can also be evaluated using the *colour rings* test pattern. Figure 5.9 shows the luminance components of original and reconstructed *colour rings* test pattern along a radial line.

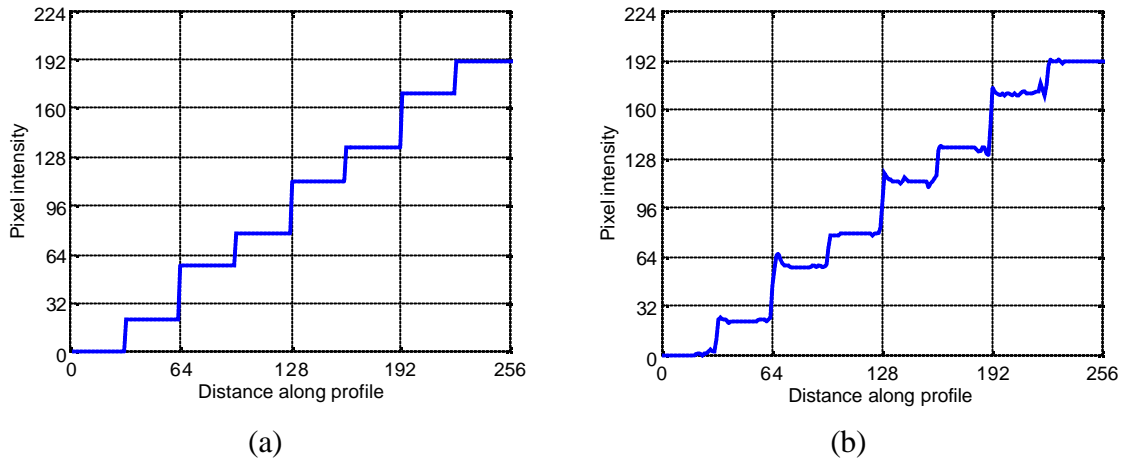


Figure 5.9 (a) An edge profile along a radial line of the luminance component Y of the uncompressed colour-rings test pattern, (b) The profile along the same radial line of the luminance component of the reconstructed colour-rings test pattern.

It can be observed in Figure 5.9(a) that the step heights are not equal so the artefact metric computational algorithm takes this variation into account by applying equations (5.7) and (5.8) to each edge separately. Then blur and ringing artefact metrics for the reconstructed image is calculated by simple averaging the blur and ringing values for all the edges as the intensity step heights are approximately equal.

5.2.3 Influence of Contrast on Blur and Ringing

Under compression the loss of high frequency components in an image results in edge blur and ringing around discontinuities and a spread of the transition region. The edge blur and degree of ringing were investigated by measuring the edge blur metric for a range of step heights and quality settings on a MatlabTM JPEG codec. A general observation is that with increasing quality factor, both blur and ringing demonstrated a decreasing trend with increasing step height, and decrease in absolute values over a decrease in quality factors. The decrease in absolute values is due to the fact that higher quality factors have lower quantisation error, preserving many of the high frequency components. Hence, details around edges can be reproduced while reconstructing the compressed image with the available high frequency components. Figures 5.10 and 5.11 show the blur and ringing metrics respectively, evaluated on the MatlabTM JPEG codec for two quality factors.

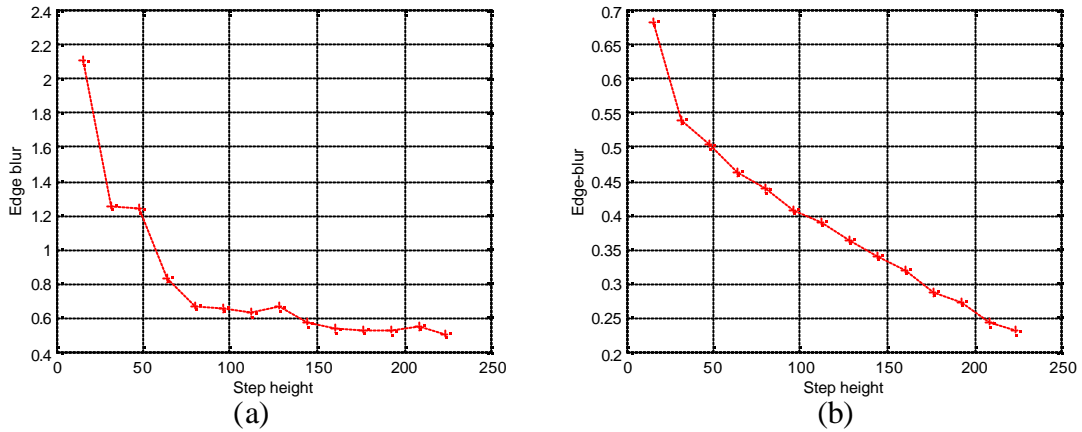


Figure 5.10 The variation of the edge blur artefact metric with step height for a Matlab™ JPEG codec (a) at quality factor of 20 blur ranges from 0.4 to 2.2, (b) at quality factor of 50 blur ranges from 0.2 to 0.7.

The blur varies with the step height. Hence, step height of 128 was selected for the monochrome rings test pattern, which is in the middle of the step-height range. The choice of the step-height value of 128 enables headroom and floor amplitude levels for both when reconstructed so that all error values are preserved without clipping or saturation.

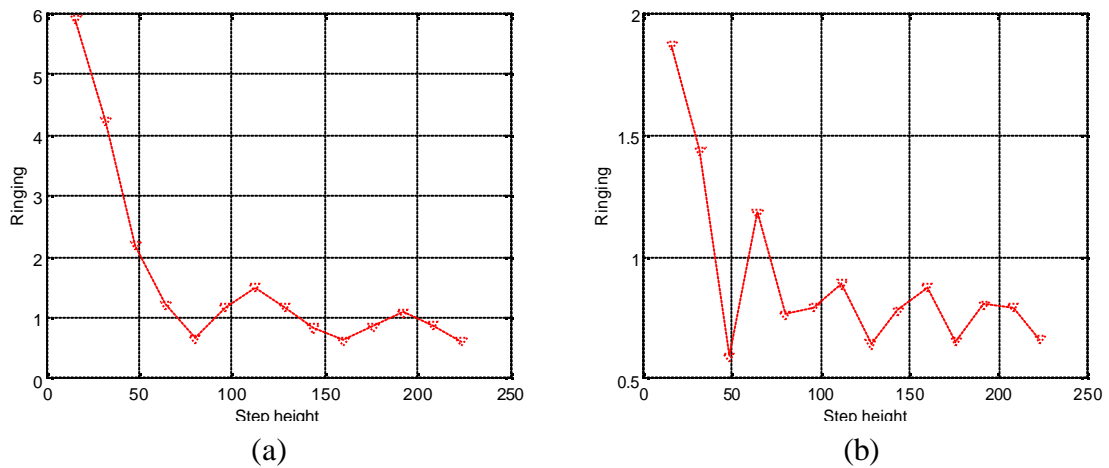


Figure 5.11 The variation of ringing with step height for a JPEG codec (a) at quality factor of 20, and (b) at quality factor of 50 [153].

It was observed that ringing errors are not monotonic. This was attributed to a threshold effect. As the step height is changed, the dominant components move from

one quantisation band to another, with consequent effect on the level of ringing. Smaller step heights resulted in smaller absolute errors. However, because of quantisation, these errors become more significant relative to the step height. When normalised to step height, the ringing shows a slight decreasing trend. For very large steps, there is inadequate range available to adequately represent the ringing in the reconstructed values. For this reason, 64 and 192 were set as suitable pixel intensities for the rings within the *monochrome rings* test pattern.

5.3 Colour Bleeding Artefact Metrics

At the time of writing there are no quantitative metrics defined in the literature for colour bleeding distortion due to image and video compression. Previous research [154] related to colour distortion due to compression used peak-signal-to-noise ratio (PSNR) or mean squared error (MSE) for objective evaluations. They are calculated without identifying the exact pixels having colour distortion.

5.3.1 Quantitative Definition of Colour Bleeding

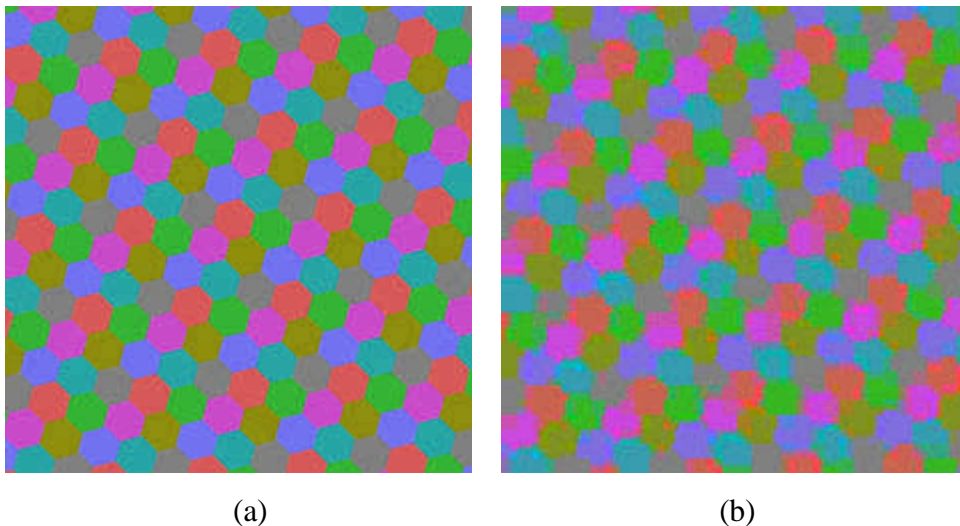


Figure 5.12 *Iso-luminance honeycomb* test pattern (a) Before compression (b) after compression with a compression ratio of 200:1.

In Figure 5.12 (b) it can be observed that after the codec operation, the six colours are no longer distinct as in Figure 5.12 (a). The hue is an important attribute of any

colour. Colour errors can be identified from the hue histogram. As shown in Figure 5.13 (a) the original test pattern has seven colours with hue angles of 0° , 61° , 104° , 168° , 241° , 284° and 348° . In the reconstructed test pattern, the peaks of the hue histogram have spread as a result of colour bleeding, and also shifted slightly, resulting in a perceivable colour shift.

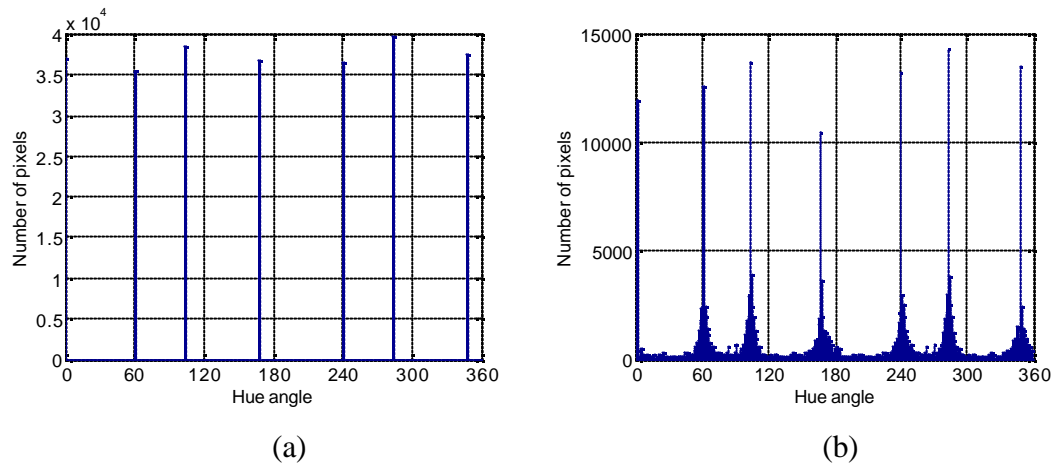


Figure 5.13 (a) The hue distribution of the original *honeycomb* test pattern, (b) The hue distribution of the reconstructed *honeycomb* test pattern [130].

The spreading of hue angle, saturation and luminance is a consequence of colour bleeding. The more the leakage of colour, the higher the visibility of colour error. As an example, consider the distribution of hue of the yellow in the reconstructed test pattern expanded in Figure 5.16.

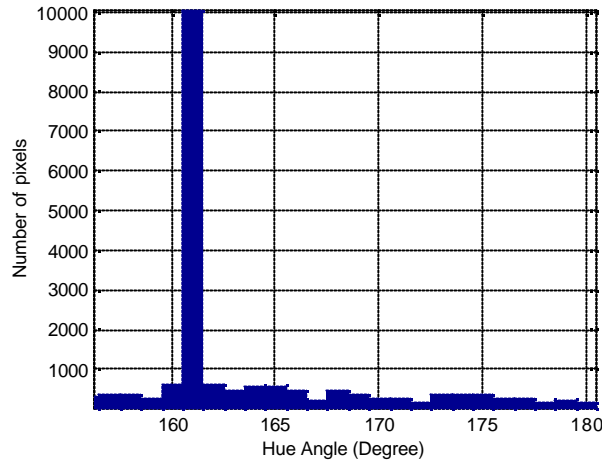


Figure 5.14 A part of hue distribution of the population of yellow regions in the reconstructed test pattern with a compression ratio of 200:1; zoomed to show the shift of yellow from 168° to 161°.

The predominant peak has shifted 7° from the reference value of 168°. A large number of pixels with a shifted hue would make the colour shift perceptible. Hence the above shift would be a measure of colour error due to coding, which is the average hue of a given region. Similarly considering the other two colour attributes, namely saturation and luminance, another two measures can be defined. Coding colour bleed is the spread of colour hence three more measures can be defined, representing the spread of hue, saturation and luminance components.

5.3.2 Algorithms

Since the spread of hue of pixels in each colour region needs to be evaluated separately, the algorithm needs to sort, label and then calculate individual and combined standard deviations to ascertain the hue spread. It is assumed that the RGB colour image has been transformed to hue, saturation and luminance using equations (1.1), (1.2) and (1.3). Then the hue images of the original and reconstructed patterns are processed based on the flow chart given in Figure 5.15.

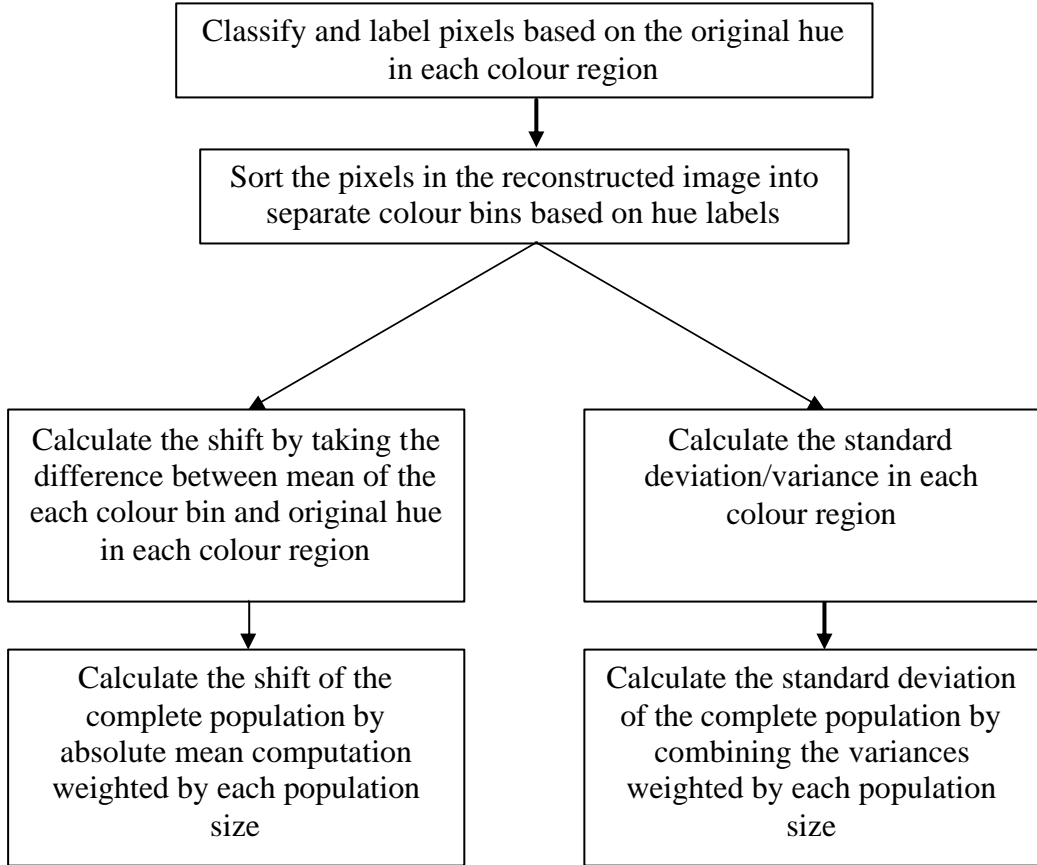


Figure 5.15 Flow chart depicting the spread and shift metrics computation algorithm.

First we consider the colour shift due to coding. Consider a colour test pattern similar to the *honeycomb* test pattern shown in Figure 5.12(a) containing N distinct colours.

Let the mean hue of population of colour region r in the original image be H_r and the mean hue value of the corresponding population of region r in the reconstructed image be \overline{H}_r , then the coding hue shift can be defined as,

$$CHS = \frac{\sum_{r=1}^N |H_r - \overline{H}_r|}{N} \quad (5.9)$$

In a similar way, the coding saturation shift and coding luminance shift can be defined as

$$CSS = \frac{\sum_{r=1}^N |S_r - \bar{S}_r|}{N} \quad (5.10)$$

and

$$CLS = \frac{\sum_{r=1}^N |L_r - \bar{L}_r|}{N} \quad (5.11)$$

Now consider the spread of colour within each of population of colour regions. Let the standard deviation of hue of population of colour region r in the original image be σ_{hr} and the number of pixels in the population of colour region r be P_r . Then the coding hue spread for the whole image can be defined as,

$$CHB = \sqrt{\frac{\sum_{r=1}^N P_r \sigma_{hr}^2}{\sum_{r=1}^N P_r}} \quad (5.12)$$

In a similar way, the coding saturation spread and coding luminance spread can be defined as

$$CSB = \sqrt{\frac{\sum_{r=1}^N P_r \sigma_{sr}^2}{\sum_{r=1}^N P_r}} \quad (5.13)$$

and

$$CLB = \sqrt{\frac{\sum_{r=1}^N P_r \sigma_{lr}^2}{\sum_{r=1}^N P_r}} \quad (5.14)$$

To visualise the values of saturation and hue for the individual colour regions, the mean hue and saturation of each colour regions in both the original and reconstructed test patterns can be calculated and displayed on a same vectorscope style graph, as in Figure 5.16.

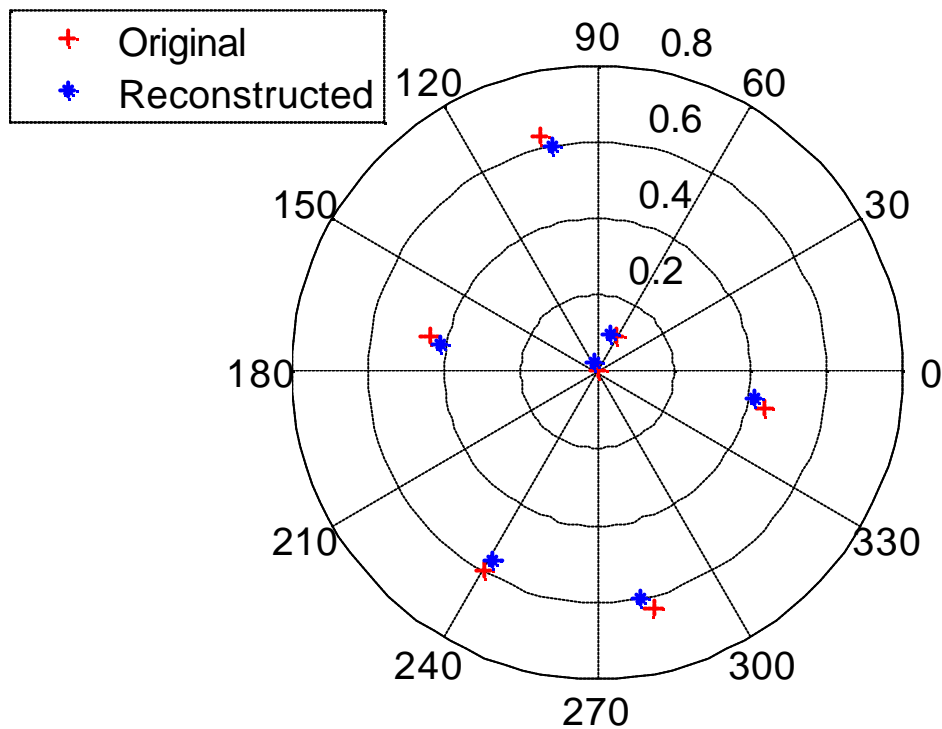


Figure 5.16 As an example of a mean hue and mean saturation on a polar display for each colour of original and reconstructed test pattern having compression ratio of 96:1.

5.3.3 Spatial Scalability of iso-luminance honeycomb test pattern

Image and video data are delivered to wide range of display devices from a 1 inch phone display through to a 40 inch television screen. This implies that it is necessary to assess the spatial domain artefacts under a range of different spatial resolutions. If a single test pattern can be scaled down to the required spatial resolution, the algorithms for test pattern design and artefact distortion metrics can be deployed conveniently.

The parent honeycomb test pattern (512x512) was cropped to create 256x256 and 128x128 test patterns. All three test patterns were compressed and decompressed over the full range of quality factors possible. Hue error was measured as spread of the colour. Figure 5.17 shows the hue error distribution for three spatial resolutions tested.

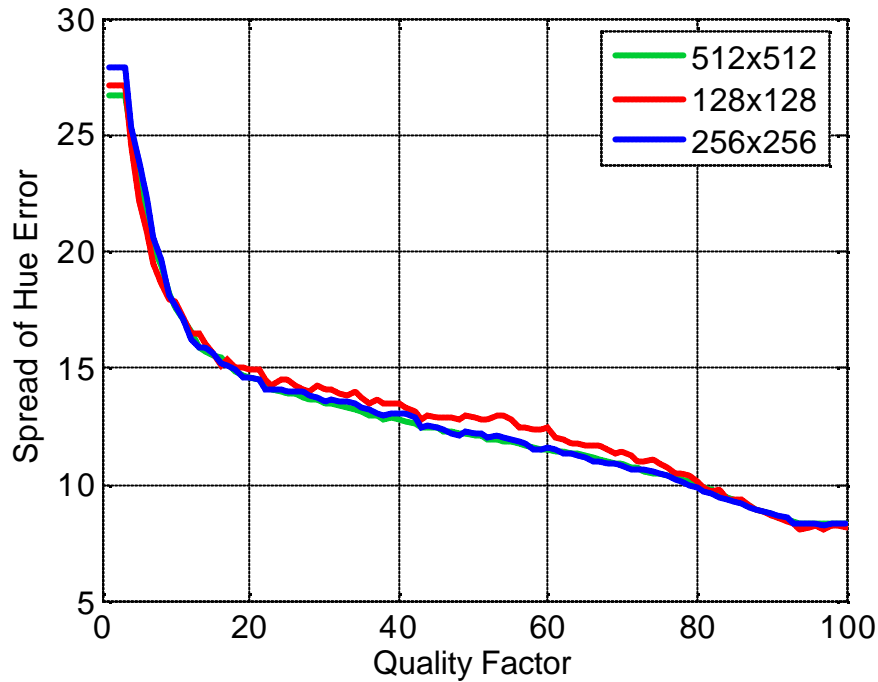


Figure 5.17 Spread of Hue Error (angle in degrees rounded to an integer) plot against the Quality factor for three different spatial resolutions.

It is evident from the Figure 5.17 that varying the spatial resolution of the honeycomb pattern resulted in nearly the same error. Hence, the *iso-luminance honeycomb* test pattern also has the capability to stress the codecs under test with varying spatial scalabilities.

5.3.4 Components of Colour Bleeding

Colour bleeding is defined as the leakage of colour due to distinct colour boundaries. If we analyse the two colour components Cb and Cr, it can be observed that the colour boundaries in the reconstructed image are not as sharp as in the original image, as shown in Figure 5.18. This type of smearing is similar to the edge blur artefact often present in compressed monochrome images with sharp edges. Therefore one component of colour bleeding is isolated and defined as the “*colour blur*” artefact.

Similarly, Figure 5.18 also shows some ringing present in the chrominance of the reconstructed image. This component of colour bleeding is defined as the “*colour ringing*” artefact.

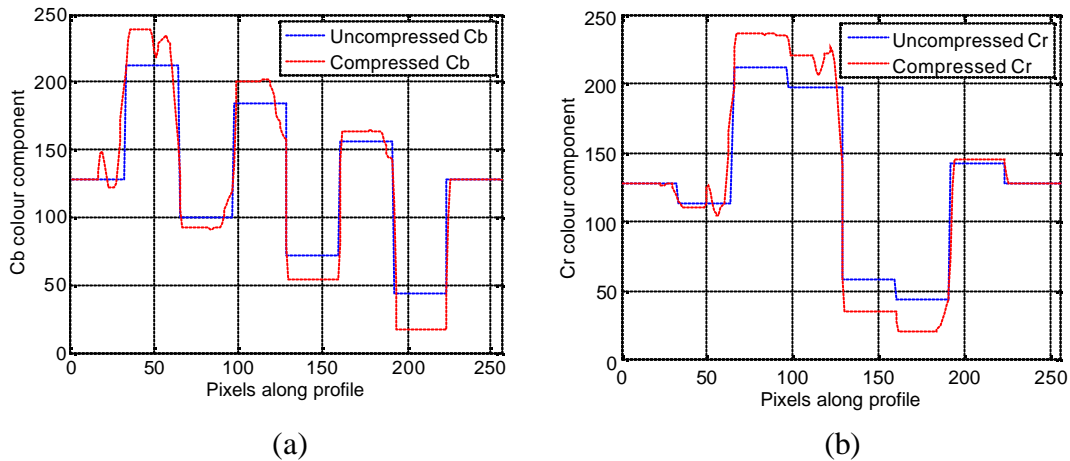


Figure 5.18 Values of colour components Cb and Cr of pixels along a profile of the circular colour test pattern before and after compression using the IrfanViewTM JPEG codec [155].

It is proposed that for the purpose of analysis, we decompose colour bleeding into two colour artefacts: colour blur and colour ringing. Colour ringing is mainly due to quantisation of high frequency components and sub-sampling. Colour blur is mainly due to quantisation and down-sampling of colour information. The definitions and algorithms used for edge blur and ringing can also be used for colour blur and colour ringing by applying 1-D definitions from Figure 5.3 to the chrominance components.

The *Colour rings* test pattern was used to detect and measure colour blur and colour ringing separately. Figure 5.19 summarises the algorithms used to isolate and measure the two components of colour bleeding artefact; colour blur and colour ringing.

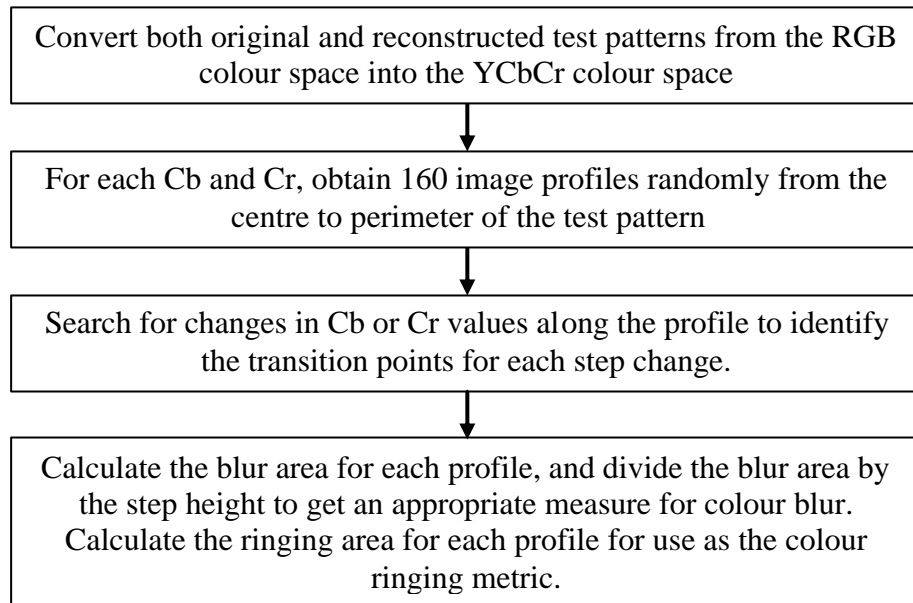


Figure 5.19 Flow chart depicting the colour blur and ringing computation algorithms.

Chapter 6: Evaluation of Metrics for Compression

Artefacts

This chapter evaluates each artefact distortion metric using the accompanying test pattern by carrying out series of experiments using either the MatlabTM JPEG codec or IrfanviewTM JPEG codec as appropriate for the metric. The primary purpose of this evaluation was to determine the range of each metric, and how this was affected over the full range of the quality factor control. A secondary purpose was to relate the metric associated with each artefact with the perceived quality of the compressed images. This will validate the individual artefact distortion metrics proposed in chapter 5.

The next chapter (chapter 7) will then use these metrics to benchmark the performance of different codecs and artefact mitigation algorithms.

Since it was impractical and out of the scope of this thesis to perform formal subjective quality evaluation (for example using the ITU standard test procedures) the structural similarity index (SSIM) was used as a proxy for the mean observer score. The SSIM value provides a HVS inspired quality metric that has been shown to correlate well with subjective assessment [162]. Like the metrics proposed in this thesis, the SSIM is based on a full reference double-ended quality measure.

6.1 Blockiness Artefact Distortion Metrics

6.1.1 Experiment I – Evaluation of Blockiness Distortion Metrics

Aim: The primary aim was to evaluate the efficacy of four blockiness metrics proposed and to investigate the significance of the known block size and the use of the error image in blockiness computation (and hence choose the most useful of the four metrics). A secondary aim was to compare selected blockiness metric with an existing metric proposed by Bailey [112].

Method:

The four blockiness metrics $B1$, $B2$, $B3$ and $B4$ defined in section 5.1.1 were evaluated by stressing an intra-frame coded MatlabTM JPEG codec over its full range of quality factors. The *sine-squared greyscale - radial* test pattern (512x512) described in the section 4.2.3 and shown in Figure 4.4 (a) was deployed. The Bailey metric was also used to evaluate the MatlabTM JPEG codec on the same compressed images, yielding metric $D1$.

Results:

In Figure 6.1, the four blockiness metrics proposed in this thesis are plotted against the compression ratio for the *sine-squared radial* test pattern.

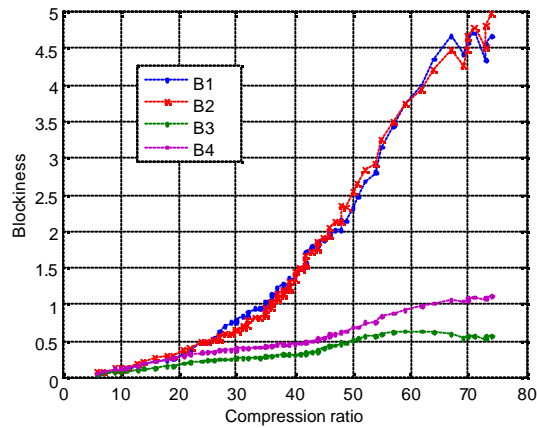


Figure 6.1 The proposed blockiness metrics evaluated on the MatlabTM JPEG codec based on the *sine-squared- radial* test pattern.

It can be observed that the blockiness increases slowly at low compression ratios and then increases rapidly with increasing compression ratio. At high compression ratios the blockiness value is high, where the boundary gradient values are high. This variation is close to what a human observer can see when performing an informal subjective test. In the compression ratio range of 65:1 to 75:1, there is very little variation in the blockiness measure.

It can be observed that both metrics computed at block boundaries from the reconstructed and error images ($B1$ and $B2$) follow each other for increasing compression except for extremely high compression. Blockiness metrics calculated using the intensity gradient at each pixel position ($B3$ and $B4$) deviate from each other for increasing compression. The error image based metric at each pixel location gives a higher value than the metric based on reconstructed image with thresholding. Since thresholding does not accumulate intensity gradient less than the threshold, $B3$ is less than for $B4$ all compression ratios. However, blockiness metrics computed using the reconstructed image after thresholding provides a blockiness measure closer to perception. Thresholding discards gradients not likely to be visible to the human eye based on the threshold test carried out prior to accumulating the horizontal and vertical blockiness.

Both $B3$ and $B4$ are averaged over the complete image resulting in a significantly lower value for blockiness than $B1$ and $B2$ (the denominator of the metric is 8 times larger). They are also measuring other errors not associated with blockiness (for example ringing and blur), making them less suitable as measures of blockiness. $B1$ and $B2$ give almost same value for blockiness, those two are suitable candidates for the blockiness metric for further research work. As $B1$ is computed only on reconstructed image, $B1$ was selected for rest of the work presented in this thesis.

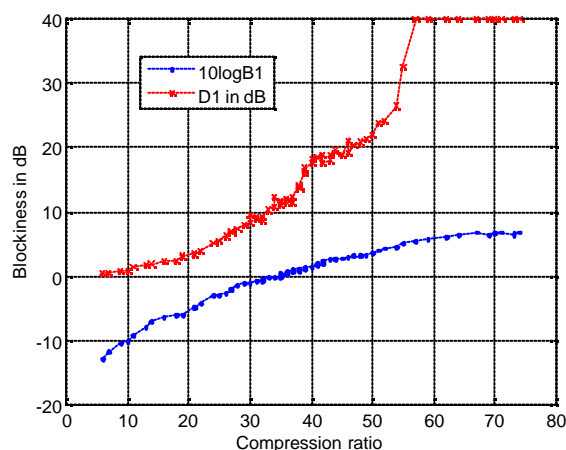


Figure 6.2 The blockiness introduced by MatlabTM JPEG codec evaluated using the Bailey metric $D1$ compared with the proposed metric $B1$ based on *sine-squared greyscale – radial* test pattern as dB values.

In Figure 6.2 the Bailey metric DI was compared against blockiness metric BI in dB for comparison. It can be observed that DI varies over wide range from 0dB from the lowest blockiness to 40 dB for the highest level of blockiness. BI shows that the blockiness measure vary from approximately -12 dB to 7dB. For higher compression, DI rises quite rapidly and saturates. A similar saturation (although less distinct) can be observed for BI .

Conclusions:

The blockiness increases rapidly for high compression ratios above the compression ratio of 35:1 for the sine-squared radial test image. Below that level of compression ratio, the compression process does not produce significant perceptual blockiness both determined from informal tests carried out with the test pattern as well as according to measure BI .

The Bailey metric DI has wider range for its values than the proposed blockiness metric BI . Since the test pattern deployed has no edges, metric BI is a clean measure of average blockiness at block edges. The Bailey metric DI does not show a similar trend to BI . This is due to the fact that DI is computed based on median values of intensity differentials at block boundaries. Hence DI is a representation of median of local blockiness whereas BI is an average blockiness at block boundaries. The two metrics provide different information; BI is a global measure based on the average blockiness and DI is a measure based on the median statistic of local blockiness.

Computation of the blockiness at each pixel yields a smaller value for the blockiness measure as it averages the total blockiness over every pixel in the test pattern or image. Use of the reconstructed test pattern or image resulted in a blockiness measure that reflects high levels of blockiness at severe compression. The proposed test pattern enables a clean measure for the blockiness artefact. The proposed blockiness metrics, together with the proposed test pattern, provide a quick method of evaluating codecs for signal quality with respect to blockiness. As the test patterns stress the codec for the artefact to be evaluated, it possible to detect blockiness artefacts and measure them cleanly.

6.1.2 Experiment II – Validation of Blockiness Distortion Metric

Aim: The aim was to validate the proposed blockiness metric with human perception.

Method:

The SSIM was computed on the same set of images used to calculate the blockiness by exercising the MatlabTM JPEG codec over the full possible range of quality factors from 1 to 100. A scatter plot was made between SSIM and blockiness metric BI as shown in Figure 6.3.

Results:

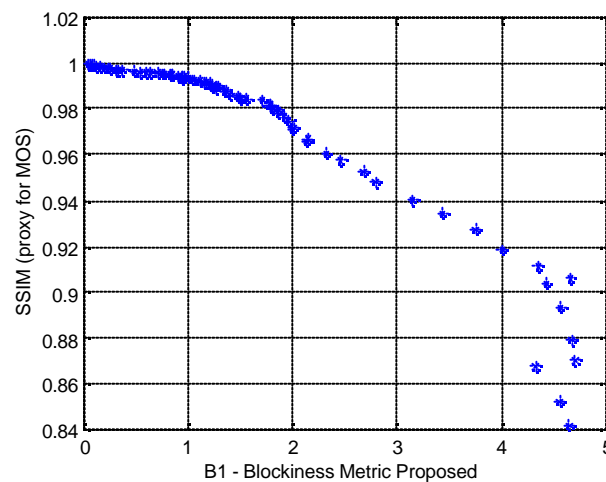


Figure 6.3 Scatter plot of SSIM against the Blockiness metric BI for MatlabTM JPEG codec on sine-squared grey scale-radial test pattern.

Conclusions:

The sine-squared grey scale-radial test pattern was designed to highlight blockiness artefacts due to compression. Figure 6.3 shows that blockiness metric BI has strong correlation to SSIM except for extremely high compression. However, this level of compression is not practical for images as they introduce distortions beyond acceptable levels for image communication. This means that the blockiness metric BI

computed on the test pattern correlates well with human perception (as indicated by the structural similarity index).

6.2 Blur Artefact Distortion Metric

6.2.1 Experiment III – Evaluation of Blur Distortion Metric

Aim: The aim was to evaluate the efficacy of blur metric proposed.

Method:

The Matlab™ JPEG codec was exercised over the full possible range of quality factors from 1 to 100 resulting in a wide range of compression ratios using the monochrome-rings test pattern. The blur metric was calculated for each of the 100 coded test patterns.

Results:

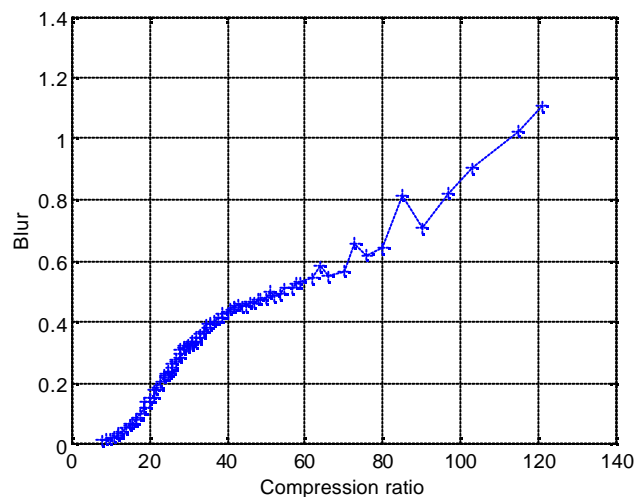


Figure 6.4 The proposed blur metrics evaluated on the Matlab™ JPEG codec based on the *monochrome rings* test pattern.

The blur metric increases with increasing compression except the compression ratios between 60:1 and 90:1. These non-monotonic variations are due to the fact that some quality factors result in lower quantisation error. At higher compressions, due to

coarse quantisation, the blur metric does not demonstrate monotonic variation. As the quantisation levels are shifted by changing the quality factor, there are discrete jumps in error as a coefficient switches from one quantisation level to another. With these switches, the error in the corresponding coefficient changes sign, giving sudden jumps in the error metric, associated with the non-monotonic noisy appearance.

At compression ratios below 40:1, the MatlabTM codec introduces edge-blur at rapidly. Then the rate of change of edge blur with increasing compression drops slightly until 60:1compression. Above the compression ratio 80:1, edge blur increases rapidly again to the increasing level of quantisation. This appears in the reconstructed test pattern as loss of details.

Conclusions:

Increasing compression introduces more blur, which was confirmed in informal subjective tests. As blur metric also demonstrates increasing trend, the proposed metric is a representative measure for blur artefact.

6.2.2 Experiment IV – Validation of Blur Distortion Metric

Aim: The aim was to validate the proposed blur metric with human perception.

Method:

The SSIM was computed on the same set of images used to calculate the blur by exercising the MatlabTM JPEG codec over the full possible range of quality factors from 1 to 100. A scatter plot was made between SSIM and blur metric as shown in Figure 6.5

Results:

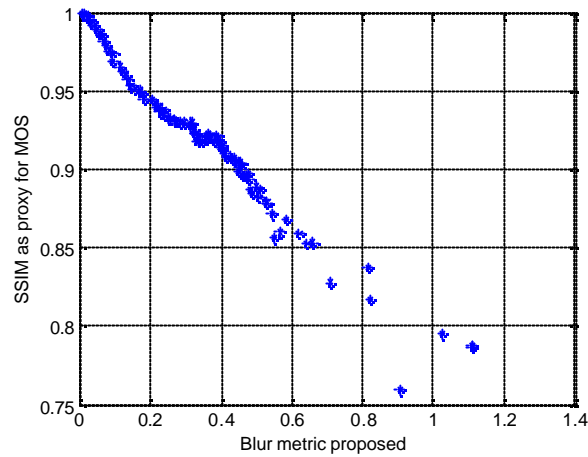


Figure 6.5 Scatter plot of SSIM against the Blur metric for Matlab™ JPEG codec on monochrome-rings test pattern.

Conclusions:

The monochrome-rings test pattern was designed to highlight blur artefact due to compression. Figure 6.5 shows strong correlation between the blur metric and SSIM except for extremely high compression. As the proposed blur metric shows correlation for most of the possible compressions, the blur metric provides a good measure of blurring artefact visible to the human visual system.

6.3 Ringing Artefact Distortion Metric

6.3.1 Experiment V – Evaluation of Ringing Distortion Metric

Aim: To evaluate the efficacy of the ringing metric by exercising the MatlabTM JPEG codec for ringing artefacts.

Method:

The MatlabTM JPEG codec was exercised over a range of compression ratios by varying the quality factor in the range of 1 to 100 at steps of 1.

Results:

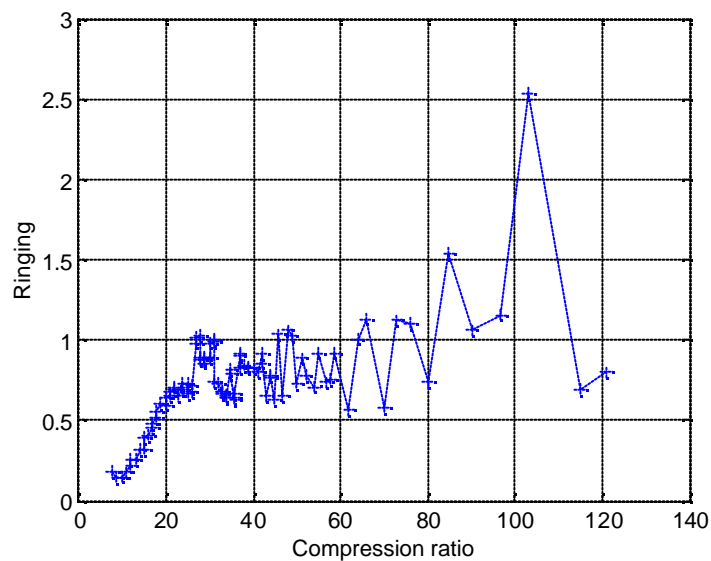


Figure 6.6 The ringing artefact distortion metric as a function of compression ratio on the *monochrome rings* test pattern [153].

It can be observed in Figure 6.6 that there is a high variation of ringing metric with increasing compression ratio. This shows that the ringing metric is much more sensitive to the change in quantisation levels than blur is. As the sign of the error changes, the error can switch between slight blur (because by definition, blur is immediately adjacent to the edge) and significant ringing (because ringing is measured over the whole block, away from the edge).

For the MatlabTM JPEG codec used in the simulations, ringing peaks around compression ratios of 25:1, 55:1, 65:1, 75:1 and 95:1. These peaks are due to quantisation errors that affect the DC component of the pixel values in the reconstructed test pattern around the edge. Due to severe quantisation effects, the ringing artefact distortion metric decreases above the compression ratio of 95:1.

Conclusions:

In informal subjective tests, reconstructed test pattern presented more ringing that appears around edges for increasing compression. The ringing measure has significant variation from the increasing trend with increasing compression. As explained above, the ringing metric is sensitive to the quantisation effects. However, the proposed ringing metric provides a reasonable representative measure of ringing present in the reconstructed test image.

6.3.2 Experiment VI - Validation of Ringing Distortion Metric

Aim: The aim was to validate the proposed ringing metric with human perception.

Method:

The SSIM was computed on the same set of images used to calculate the ringing by exercising the MatlabTM JPEG codec over the full possible range of quality factors from 1 to 100. A scatter plot was made between SSIM and ringing metric as shown in Figure 6.7

Results:

Figure 6.7 shows that the ringing correlates with the SSIM, mainly at lower compression ratios, though the correlation is not as strong as the blur and blockiness metrics.

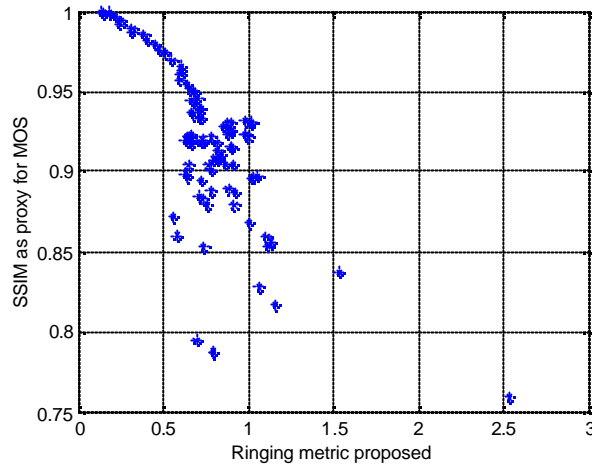


Figure 6.7 Scatter plot of SSIM against the Ringing metric for Matlab™ JPEG codec on monochrome-rings test pattern.

Conclusions:

For low compression, strong correlation can be observed between the SSIM and ringing metric, therefore at these compressions, the ringing metric is valid. One limitation of using the SSIM as a proxy for human perception is that it is not specific to just ringing, and will be measuring the combined effects of blur and ringing on the reconstructed test pattern.

6.4 Colour Bleeding Artefact Distortion Metrics

6.4.1 Experiment VII – Evaluation of Colour bleeding metrics

Aim: The primary goal was to evaluate the efficacy of the *honeycomb* test pattern and colour bleeding metrics using IrfanView™ JPEG codec for colour bleeding artefact. A secondary goal was to identify the key metric for colour bleeding.

Method:

The IrfanView™ JPEG codec was exercised using the *honeycomb* test pattern over a wide range of compression ratios. As shown in Figure 6.8(a), the original *honeycomb* test pattern has an approximately equal distribution of pixels in the ensemble of seven

colour regions. Figure 6.8(b) shows the reconstructed *honeycomb* test pattern at a compression ratio of 96:1.

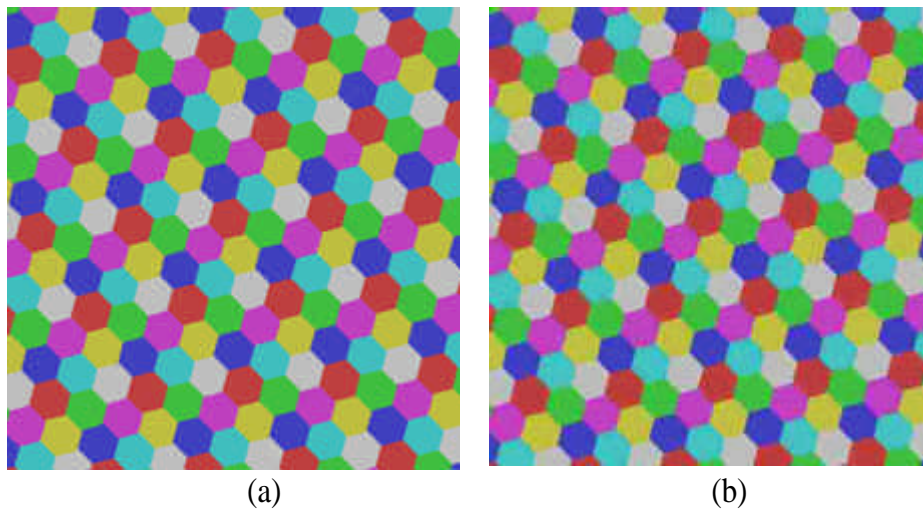


Figure 6.8 (a) The uncompressed version of the *honeycomb* test pattern designed for testing digital codecs [129], (b).The reconstructed colour *honeycomb* test pattern when encoded with an IrfanViewTM JPEG codec with a compression ratio of 96:1

Then the *CHS*, *CHB*, *CSS*, *CSB* *CLS* and *CLB* artefact metrics were evaluated by applying the distortion metrics to the IrfanViewTM JPEG reconstructed ‘*honeycomb*’ test pattern.

Results:

Figure 6.9 provides a plot of two chrominance components, namely the mean-hue of individual regions and the mean-saturation of individual regions, for both the original and the reconstructed honeycomb test patterns. It can be observed that there is a shift of reconstructed colour points from the original colour points. After reconstruction, there is a both saturation error (radial) and a hue error (angle).

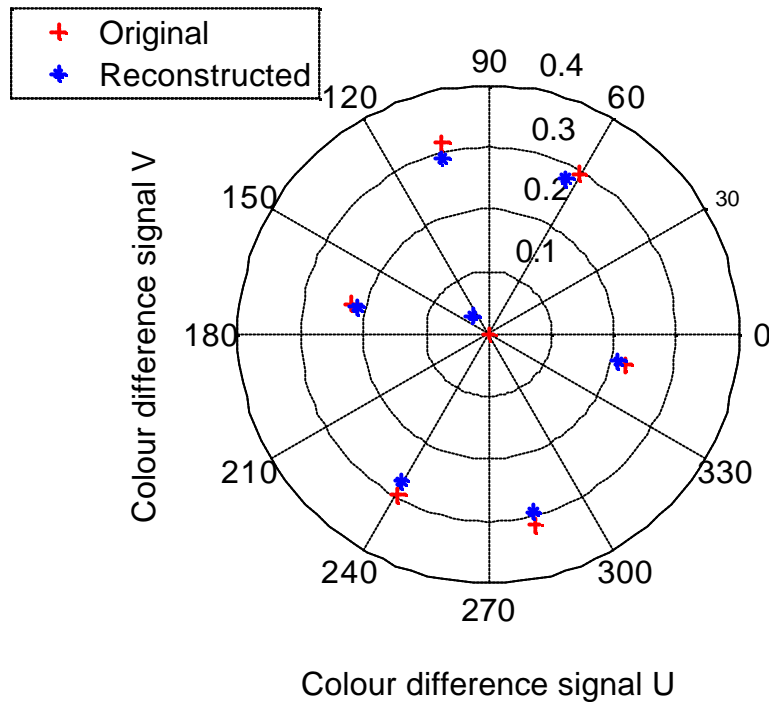


Figure 6.9 Mean-hue and Mean-saturation for each colour of original and reconstructed *honeycomb* test pattern (At compression ratio=96:1) are displayed on a polar coordinate system, which emulates a face of a vectorscope.

Figure 6.10 shows *CHS* and *CHB* artefact metrics that were evaluated by deploying the proposed algorithms and the '*honeycomb*' test pattern. The response of the IrfanViewTM JPEG codec to the *honeycomb* test pattern shows an increasing trend in the coding colour bleed measure with increasing compression ratio as shown in Figure 6.10. This shows clearly that as the test pattern becomes more compressed, the distribution of colour values becomes more spread, with the mean shifted from the original hue. Minor non-monotonic variations can be observed. At some compression levels, for example 80:1, errors may actually reduce for increases in compression, depending on exactly where the quantisation levels fall. The hexagonal shape of the colour boundaries has the result that the block boundaries will not fall on colour boundaries or parallel to them. This stresses the codec to produce more errors.

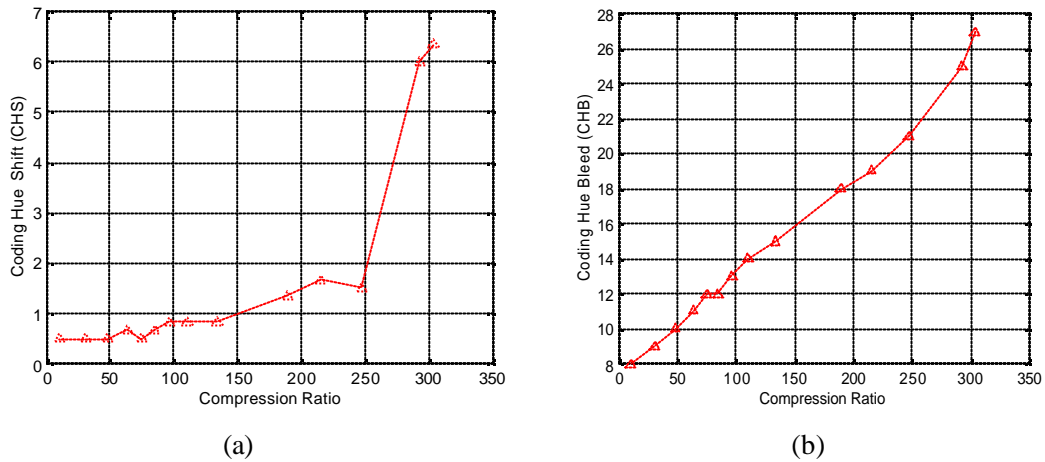


Figure 6.10 (a) Coding Hue Shift (*CHS*) as a function of JPEG compression ratio on the proposed ‘honeycomb’ colour test pattern, (b) Coding Hue Bleed (*CHB*) as a function of JPEG compression ratio on the ‘honeycomb’ colour test pattern [158].

It was observed that the perceived colour errors increase with increasing compression ratio for the ‘honeycomb’ test pattern.

It is evident that the “honeycomb” colour test pattern can be compressed over a wide range of compression ratios between 2 and 240. As shown in Figure. 6.10 to Figure 6.12 the “honeycomb” colour test pattern also resulted in an increasing trend in all three measures of colour artefact metrics defined in (5.9), (5.10) and (5.11), which is in agreement with perceived quality from informal subjective quality assessments. An increasing artefact metric value represents increasing bleeding artefacts. Hence the quality of the reconstructed pattern decreases with an increasing bleeding measure. As the test pattern becomes more compressed, the distribution of colour values becomes more spread. The effect on the luminance is minor in comparison to the effects on the colour.

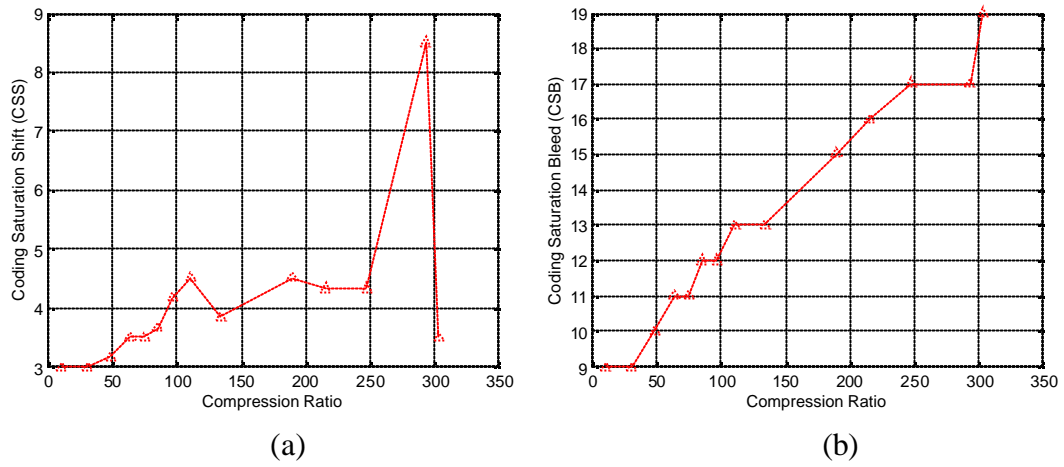


Figure 6.11 (a) *Coding Saturation shift (CSS)* as a function of JPEG compression ratio for the proposed ‘*honeycomb*’ colour test image, (b) *Coding Saturation bleed (CSB)* as a function of JPEG compression ratio on the proposed ‘*honeycomb*’ colour test image.

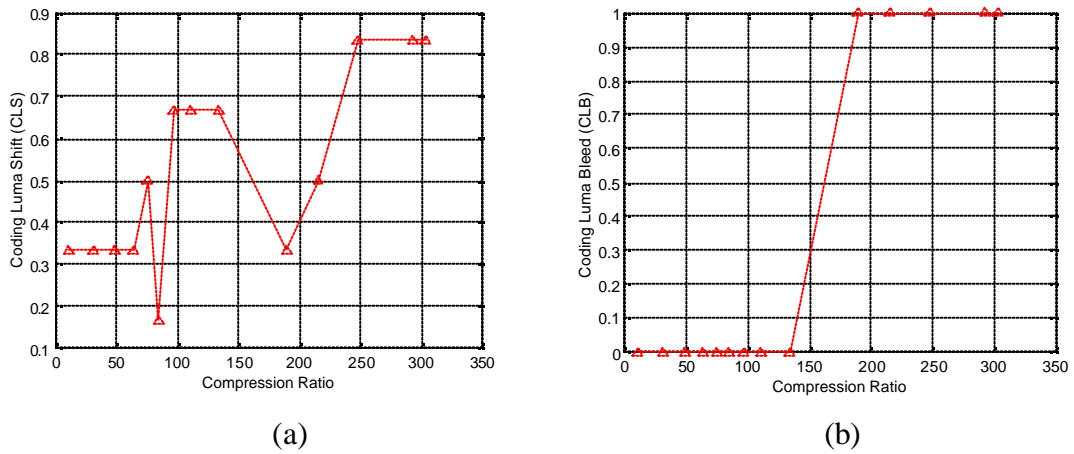


Figure 6.12 (a) *Coding Luminance Shift (CLS)* as a function of JPEG compression ratio on the proposed ‘*honeycomb*’ colour test image, (b) *Coding Luminance Bleed (CLB)* as a function of JPEG compression ratio on the proposed ‘*honeycomb*’ colour test image.

Conclusions:

In addition to the shift and spread in the dominant component of colour - hue, a significant secondary effect of colour bleeding is a loss of saturation. As colours from adjacent regions mix, this tends to make them more grey, reducing the saturation.

The rotated-hexagonal shape of the colour boundaries means that the block boundaries will not fall on colour boundaries or parallel to them. This stresses the codec to produce more errors. The distributed colour regions in a tessellation enable a wide range of compression ratios.

Hue spread was selected as the representative colour bleeding metric as it measure the key attribute of colour, that is, hue. Hue spread will be evaluated with SSIM for validation in the next experiment.

6.4.2 Experiment VIII – Validation of Colour bleeding metric

Aim: The aim was to validate the proposed *Hue Spread* Colour Bleeding metric using SSIM as a proxy for human visual tests.

Method:

The SSIM was computed on the hue component of the same set of images used to calculate the hue spread by exercising the MatlabTM JPEG codec over the full possible range of quality factors from 1 to 100. A scatter plot was made between SSIM and hue spread metric as shown in Figure 6.13

Results:

Figure 6.13 shows the ringing resulted from MatlabTM JPEG codec. It can be observed that values are higher than the values resulted from *monochrome rings* test pattern.

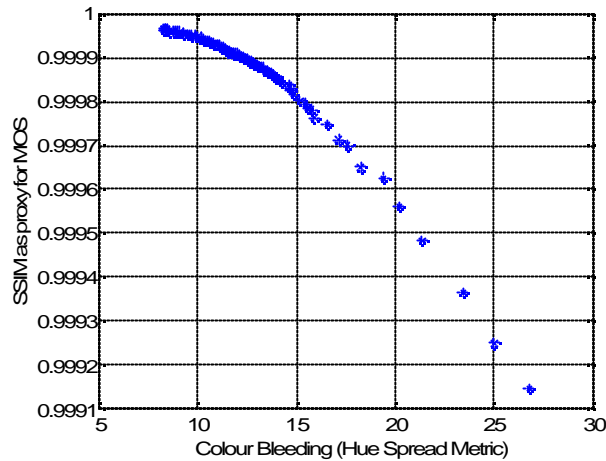


Figure 6.13 Scatter plot of SSIM against the Colour bleeding metric *Hue spread* for Matlab™ JPEG codec on Honeycomb test pattern

Conclusions:

The honeycomb test pattern was designed to highlight colour bleeding artefacts due to compression. Figure 6.13 shows that *hue spread* exhibits strong correlation to SSIM for all possible compressions. This means that, *hue spread* computed on the test pattern provides a good measure of colour bleeding artefacts visible to the human visual system. The wide range of hue spread for small changes in SSIM indicates that the hue spread is very sensitive to even small errors.

6.5 Chapter Summary and Conclusions

Compression artefacts metrics were evaluated using MatlabTM JPEG and IrfanViewTM JPEG codecs. Test patterns: *sinesquared grey scale-radial monochrome, monochrome rings and honeycomb* were deployed to stress the codecs. In the evaluation of artefact distortion metrics, it is observed that distortion metrics increase with an increase in compression ratio. Artefact detection and measurement algorithms compute only the artefact under study. Hence, the artefact metrics provide a reasonable representation of the compression distortions and are readily calculated.

In colour bleeding measurements, the proposed measures clearly distinguish between the hue error and saturation error. The other two artefact metrics presented on a vectorscope provide quick measure against the expected hue and saturation values.

Blockiness, blur, ringing and hue spread distortion metrics shown were validated using the human visual system inspired SSIM. All but the proposed ringing metric show a very strong level of correlation. The ringing metric is good at lower compression ratios, but may be less useful at higher ratios. This enables the proposed test patterns and distortion metrics to be used for codec performance evaluation. The experiments and results are presented in chapter 7.

Chapter 7: Performance Evaluation of Image Codecs

7.1 Benchmarking Codec Implementations

This chapter presents a performance comparison of representative codecs using the proposed framework and the test methodology. Two types of codecs (JPEG and JPEG2000) from two developers (MatlabTM and IrfanViewTM) were evaluated using four test patterns designed and developed (shown in appendix 8 for easy reference) and the related compression distortion artefact metrics.

7.1.1 Experiment –IX Comparison of Blockiness due to JPEG codecs - IrfanViewTM Vs MatlabTM

Aim: To benchmark implementations of two JPEG codecs, that is codecs that use the DCT based processing, for the blockiness artefact. The two codecs were developed by different developers.

Method:

Using the *sinesquared grey scale-radial* test pattern, the two codecs were exercised over a wide range of compressions. The blockiness artefact was evaluated using the blockiness metric *B1*. Since IrfanViewTM and MatlabTM JPEG codecs use fixed size 8x8 block for image coding, the *B1* blockiness metric was the most appropriate for the evaluation.

Results:

The results are shown in Figure 7.1. For compression ratios above 30:1, the IrfanViewTM outperforms the MatlabTM JPEG codec. Since the JPEG standard specifies only the decoder and the syntax for the encoded bit stream, developers can use any technique at the encoder end which complies with the specified syntax. IrfanViewTM is specially designed to handle images; the encoding algorithms may have been optimised for this. MatlabTM is a generic mathematical tool and the JPEG

codec in the image processing tool box provides some capability designed to handle JPEG format image files.

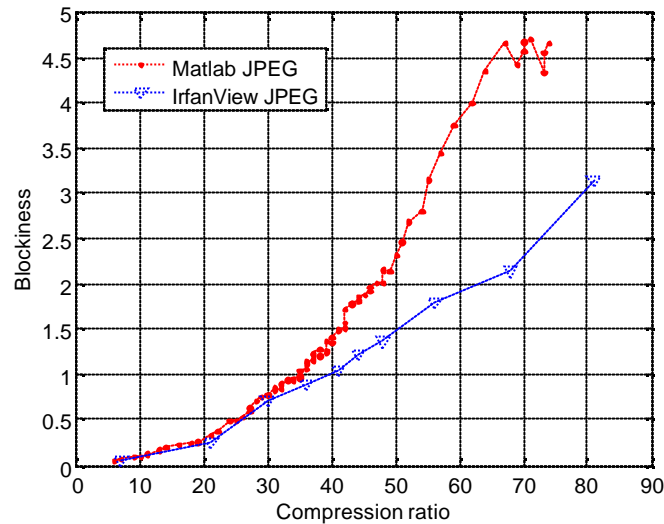


Figure 7.1 Blockiness metric $B1$ measured for on JPEG codecs of MatlabTM and IrfanViewTM [156].

Conclusions:

At low compression ratios, both MatlabTM and IrfanViewTM JPEG codecs perform similarly. For compression ratios above 20:1, the IrfanViewTM JPEG codec significantly outperforms the MatlabTM codec. From this, the IrfanViewTM codec is significantly better than the MatlabTM codec.

7.1.2 Experiment –X Comparison of Blockiness due to IrfanViewTM codecs - JPEG vs. JPEG2000

Aim: To benchmark two different types of codes, that is JPEG and JPEG2000, both developed by IrfanViewTM, for blockiness artefacts.

Method:

The JPEG and JPEG2000 codecs were evaluated to determine the characteristics inherent to frame based and block based coding mechanisms. JPEG2000 codecs use a

wavelet transform generally calculated on complete frames whereas the JPEG codecs use a discrete cosine transform calculated on 8x8 blocks.

Results:

Since JPEG2000 standard based codecs do not use block coding or tiling for moderate size images, the JPEG2000 did not result in blockiness for moderate size images (512x512) and this is confirmed in Figure 7.2. In fact the JPEG 2000 does not introduce any blockiness artefacts over the complete range of compressions used (5 – 70).

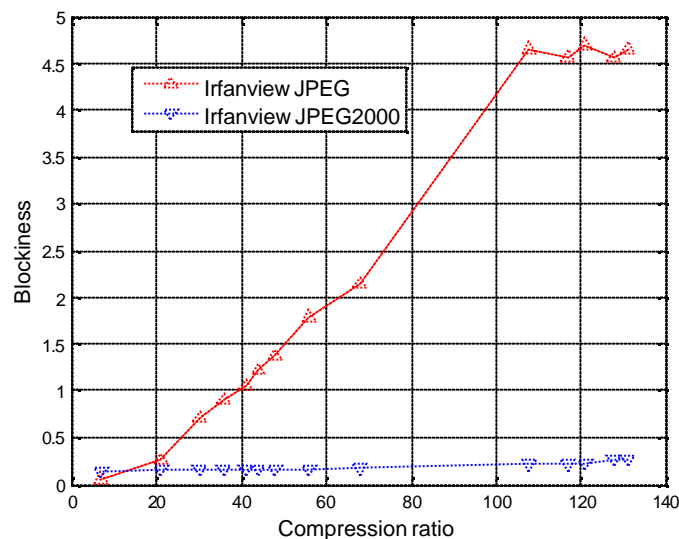


Figure 7.2 Blockiness metric $B1$ measured for the JPEG and JPEG2000 codecs of IrfanView™.

Conclusions:

JPEG2000 codecs use wavelet for transformation, which is generally performed on a sub-image known as a tile. Tiling is not used for moderate size images. When tiling is not used for the IrfanView™ JPEG2000 codec, it does not introduce any blockiness or tiling artefacts. JPEG uses 8x8 block processing for frequency domain transformation. Hence, with increasing compression ratio JPEG demonstrated increasing blockiness.

7.1.3 Experiment –XI Comparison of Blur due to IrfanView™ JPEG and JPEG2000 codecs

Aim: To benchmark the IrfanView™ JPEG and IrfanView™ JPEG2000 codecs for blur.

Method:

IrfanView™ JPEG and JPEG2000 codecs were chosen for evaluation as representative of the two types of codecs based on DCT transformation and wavelet transformations. Each codec was exercised over wide range of compression ratios using the *monochrome rings* test pattern.

Results:

The JPEG2000 codec introduced less blur than the JPEG codec as shown in Figure 7.3. The JPEG2000 codec can compress the test pattern almost twice as much as the JPEG codec before it introduces blur distortion.

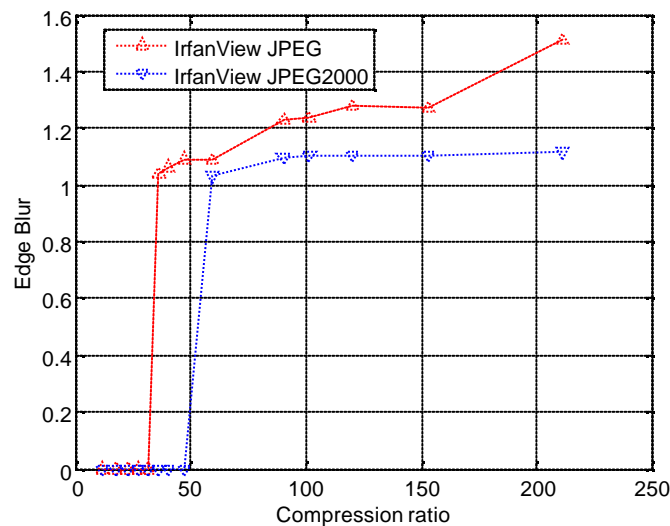


Figure 7.3 Edge blur compared for two types of codecs

It is interesting that the shape of the curve is quite different from that seen in section 6.2.1. Both IrfanView™ codecs display a distinct thresholding effect rather than a smooth increase in blur with compression ratio.

Conclusions:

Though IrfanView™ JPEG2000 codec uses the wavelet transform in compression process, it does not lose details as much as the IrfanView™ JPEG codec. It can be deduced that, based on these implementations, wavelet based codecs may introduce less blur distortion.

7.1.4 Experiment –XII Comparison of Ringing due to IrfanView™ JPEG Vs JPEG2000 codecs

Aim: To benchmark two different types of codecs (DCT based and wavelets based from the same developer) for the ringing artefact.

Method:

IrfanView™ (version 3.0) JPEG and JPEG2000 codecs were exercised using the monochrome rings test pattern over wide range of compressions. Ringing distortion was measured for each reconstructed image and the results are shown in Figure 7.4.

Results:

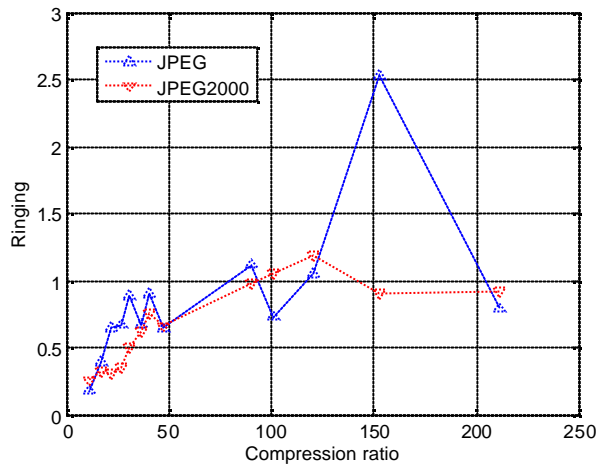


Figure 7.3 The comparison of IrfanView™ JPEG and JPEG2000 codecs for ringing against compression ratio [153].

Figure 7.4 depicts that both IrfanView™ JPEG and JPEG2000 codecs introduce increasing amount of ringing with increasing compression ratio. The two codecs, JPEG and JPEG2000 are from the same codec developer.

Conclusion:

In terms of ringing the IrfanView™ JPEG2000 codec resulted in less compression distortion with respect to ringing.

7.1.5 Experiment –XIII Comparison of Colour Bleeding due to JPEG and JPEG2000 codecs – Using Honeycomb test pattern

Aim: To compare colour reproduction performance of IrfanView™ JPEG and JPEG2000 codecs.

Method:

The *CHB*, *CSB* and *CLB* artefact metrics were evaluated by applying them to the ‘*honeycomb*’ test pattern described in Chapter 4.

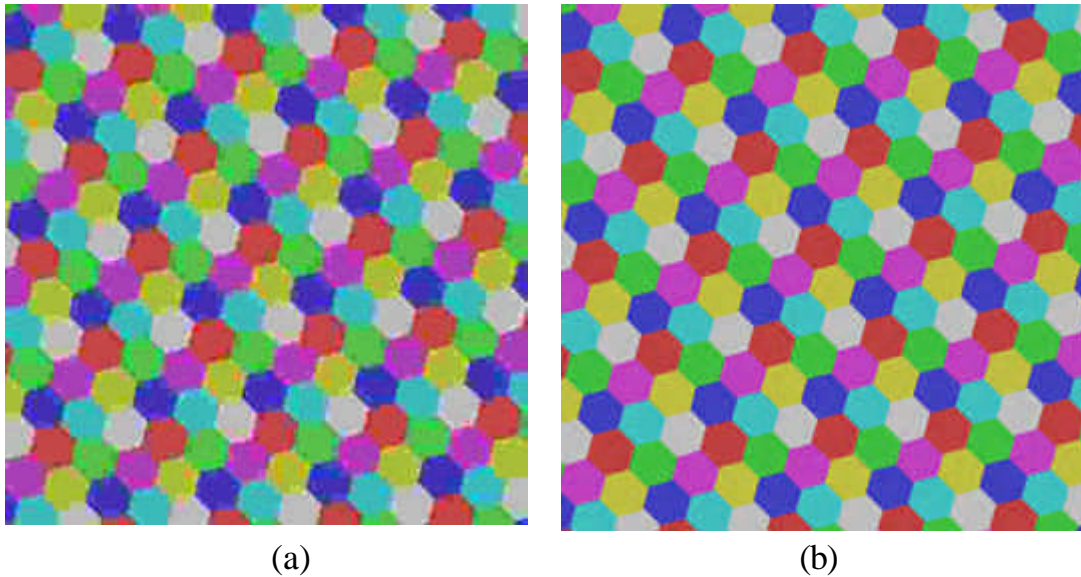


Figure 7.4 (a) The reconstructed colour *honeycomb* test pattern when encoded with a IrfanView™ JPEG codec with a compression ratio of 39:1, (b) The reconstructed *honeycomb* test pattern when encoded with a IrfanView™ JPEG2000 codec with a compression ratio of 39:1.

Results:

The two codecs were tested over a range of compression ratios (CR) with the results shown in Figures 7.6, 7.7, 7.8, and 7.9.

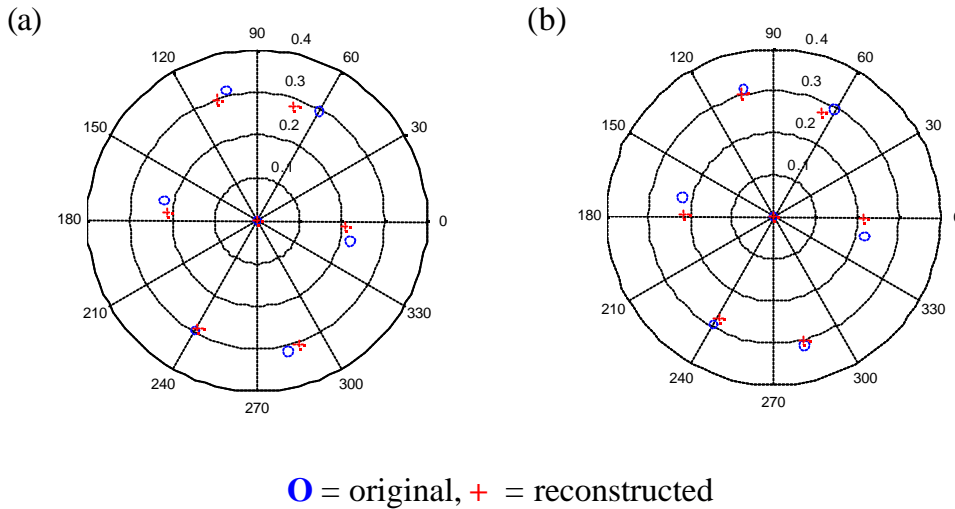


Figure 7.5 Vectorscope plot of mean-hue and mean-saturation for each colour of the original and compressed images (a) JPEG and (b) JPEG2000. (A compression ratio of 39:1 was used).

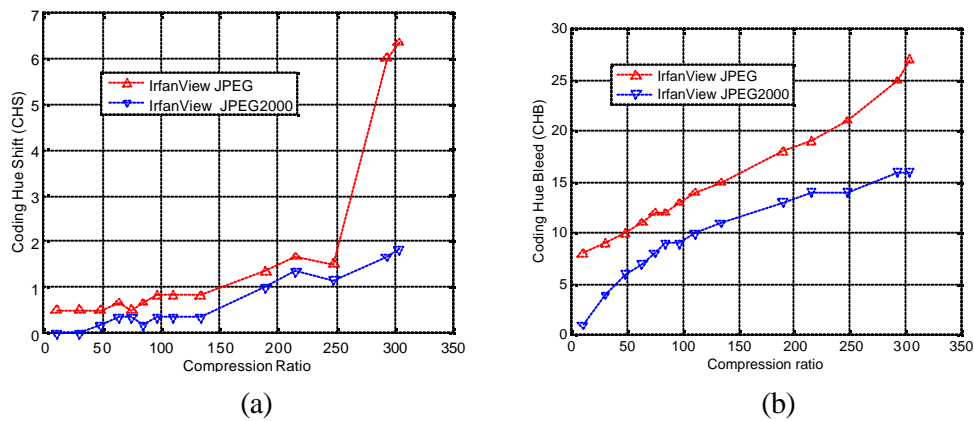
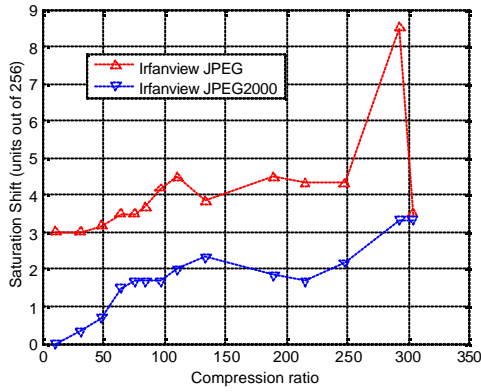
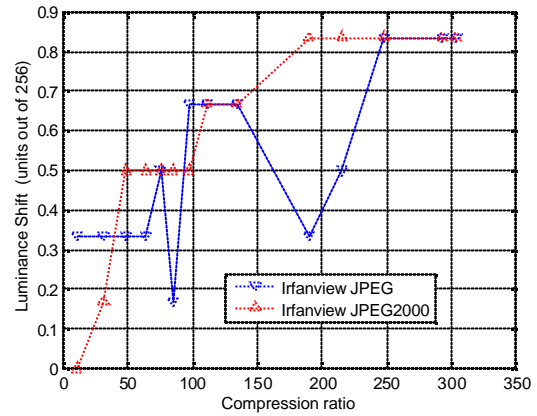


Figure 7.6 (a) *Coding Hue Shift (CHS)* [159], and (b) *Coding Hue Bleed (CHB)* [158] as a function of compression ratio with the ‘honeycomb’ colour test image.

As shown in Figures 7.7 to 7.9 the *honeycomb* colour test pattern resulted in an increasing trend in all six measures of colour artefacts as defined in equations (5.9) to (5.14), which is in agreement with the perceived quality trend. An increasing artefact metric value represents increasing bleeding artefacts though the relationship may not be linear. As the test pattern becomes more compressed, the distribution of colour values becomes more spread. Minor non-monotonic variations can also be observed.

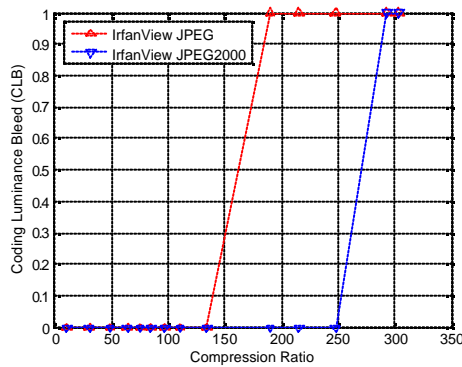


(a)

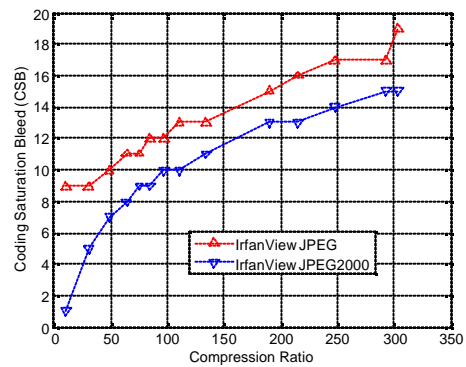


(b)

Figure 7.7 (a) *Coding Saturation Shift (CSS)* and (b) *Coding Luminance Shift (CLS)* as a function of JPEG compression ratio with the ‘*honeycomb*’ colour test image [159].



(a)



(b)

Figure 7.8 (a) *Coding Luminance Bleed (CLB)* and (b) *Coding Saturation Bleed (CSB)* as a function of compression ratio with the ‘*honeycomb*’ colour test image [159].

As colours from adjacent regions mix, in addition to a change of hue, a significant effect of colour bleeding is a loss of saturation. This reduction in saturation as shown in Figure 7.8 tends to make regions more grey. The JPEG2000 codec produces greater luminance shifts than the JPEG codec.

Figure 7.6 provides plots of the two chrominance components, for both the original and the reconstructed images for JPEG and JPEG2000 codecs for the same

compression ratio of 39:1. These graphs are comparable to the vectorscope displays used in television broadcasting facilities. This display provides at a glance a measure of the shift of the mean-hue and mean-saturation values. Though it appears that both reconstructed patterns are degraded to the same extent, in general the JPEG2000 reproduces hue better than JPEG.

Conclusions:

The IrfanView™ JPEG2000 codec out performs the JPEG codec. It can be deduced that that wavelet based JPEG2000 codecs out perform DCT based JPEG codecs for colour reproduction.

7.1.6 Experiment XIV – Comparison of Colour Bleeding due to JPEG and JPEG2000 codecs random colour circles test pattern

Aim: To investigate the influence of random circles on evaluation of colour bleeding artefact due to image codecs.

Method:

Two types of codecs were used to investigate the usability of the random test pattern generator for the evaluation of colour bleeding artefact. IrfanView™ JPEG and JPEG2000 codecs were used to compress an ensemble of randomly generated test patterns from the random generator. The Figure 7.10 shows the reconstructed test patterns to compare colour reproduction performance of IrfanView™ JPEG and JPEG2000 implementations.

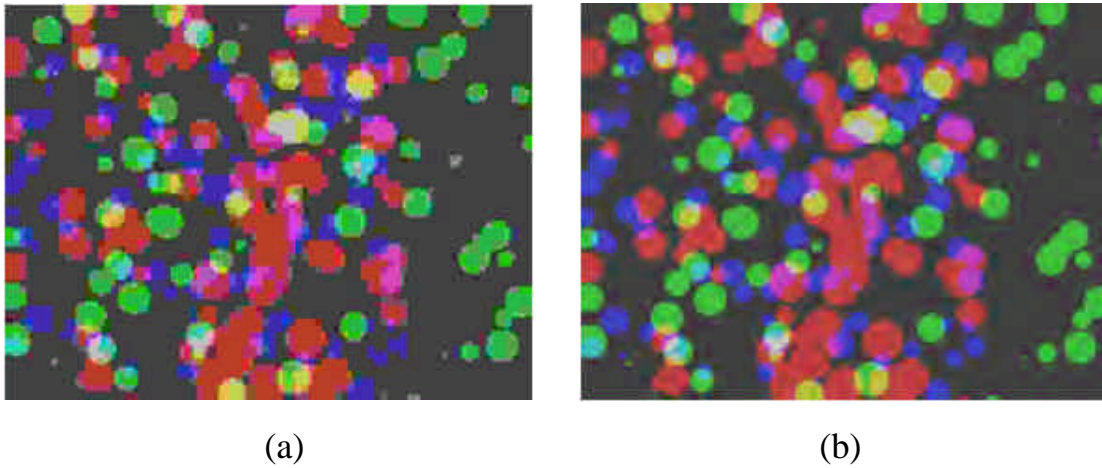


Figure 7.9 (a) JPEG compressed test pattern (b) JPEG2000 compressed test pattern [16]. Both images have a 120:1 compression ratio.

Results:

As a result of the multiplicity of edges present in the test pattern that are neither vertical nor horizontal, both block processing and wavelet based compression techniques introduce errors into the reconstruction process. Figure 7.10 demonstrates the coding colour bleed observed when the test pattern is compressed with the two codecs.

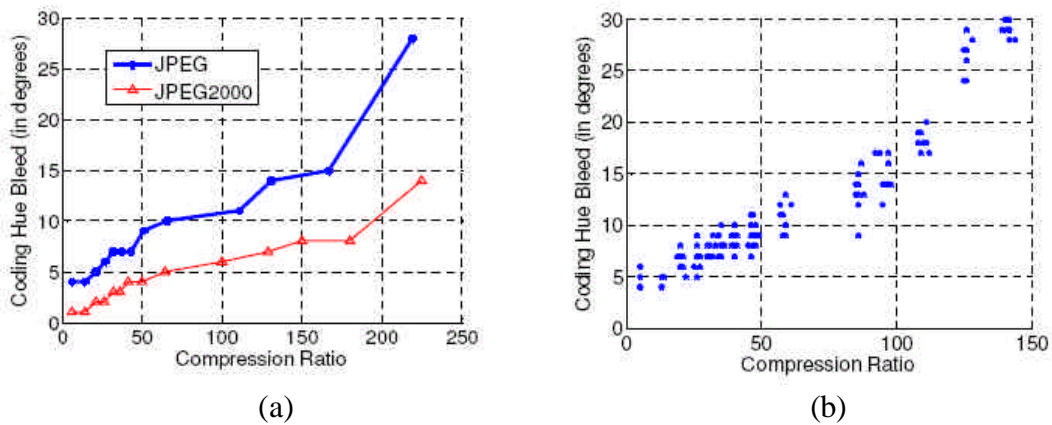


Figure 7.10 (a) comparison of coding hue bleed for JPEG and JPEG2000 codecs (b) Repeated measure for JPEG with different random test patterns generated using the proposed random test pattern generator [16].

A test was carried out to investigate the influence of the random test pattern on coding hue bleed. For the same quality factor nine randomly generated test patterns were coded. This was repeated for ten quality factor values. As shown in Figure 7.11(b) the coding hue bleed (*CHB*) varies with different random test patterns for range of quality factors expressed as the compression ratio. When the test pattern is coded, due to its random nature, pixel contents, colour transitions and boundaries all vary from one pattern to the other. As a result, for a given compression ratio, the coding colour bleed can vary by up to 20%. Hence the random test pattern generator is more useful when benchmarking different codecs where each codec is fed with the same test pattern from each generation. The individual codec performance can be evaluated using the *honeycomb* static test pattern described in chapter 4.4.3 with consistent and reproducible results.

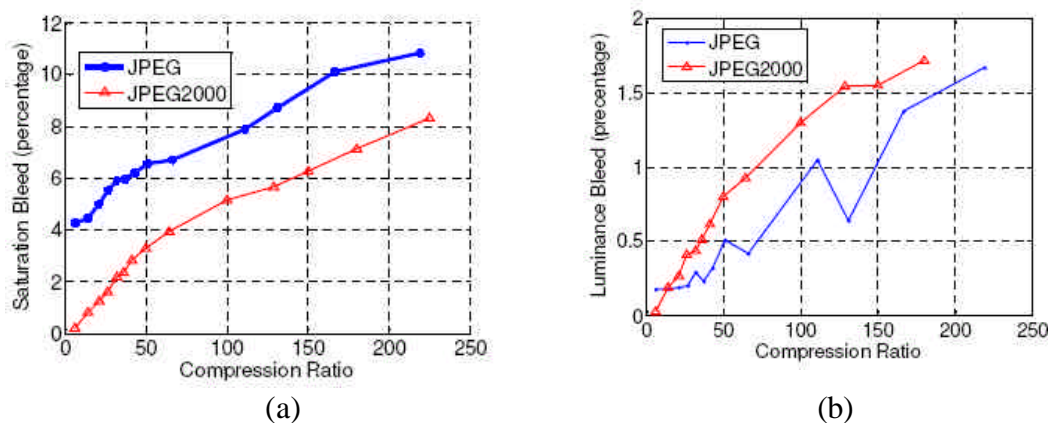


Figure 7.11 (a) comparison of coding saturation bleed (spread) for IrfanView™ JPEG and JPEG2000 codecs (b) comparison of coding luminance bleed for JPEG and JPEG2000 codecs [16].

As shown in Figures 7.11 and 7.12 the random colour test pattern also resulted in an increasing trend in all three measures of coding artefact metrics – *CHB*, *CSB*, *CLB* –, which is in agreement with perceived quality. An increasing coding artefact metric value represents increasing bleeding artefacts. Hence the perceived quality of the reconstructed patterns decreases with an increasing bleeding measure. Coding hue bleed, coding saturation bleed and coding luminance bleed increase rapidly with increasing JPEG compression ratio. As the test pattern becomes more compressed, the

distribution of colour values becomes more spread. Minor non-monotonic variations can also be observed. At some compression levels, errors may actually reduce for increased compression depending on exactly where quantisation levels fall. The circular shape of the colour boundaries has the result that the block boundaries for JPEG will not fall on colour boundaries or parallel to them. This stresses the codec to produce more errors, which are perceivable on a monitor.

Conclusions:

As colours from adjacent regions mix, in addition to the change of hue, a significant effect of colour bleeding is a loss of saturation. There is little loss of luminance which tends to make regions more grey, as shown in Figure 7.12(b). JPEG2000 loses slightly more intensity or luminance than JPEG codecs for very low compression. The losses for both codecs are less than 2% of the original value. The human eye may not be able to make the distinction, hence it can be treated as negligible.

The random colour test pattern can be used to benchmark two or more codecs as long as all are exercised with same patterns. JPEG2000 outperforms JPEG codec for colour reproduction.

7.1.7 Experiment XV - Comparison of Colour Ringing and Blur due to JPEG and JPEG2000 codecs - Using Isoluma colour rings test pattern

Aim: To evaluate the two components of the colour bleeding artefacts, namely colour ringing and colour blur, for IrfanViewTM JPEG and JPEG2000 codecs.

Method:

The *Iso-luma colour rings* test pattern was used to exercise both IrfanViewTM JPEG and JPEG2000 codecs over wide range of compression ratios. Reconstructed test patterns from both codecs were applied to the colour blur and colour ringing algorithms.

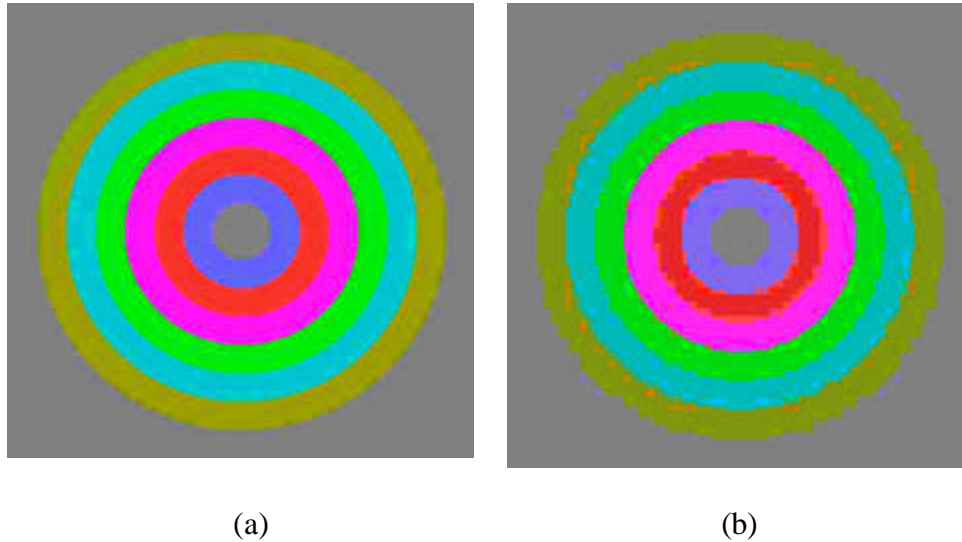


Figure 7.13 Iso-luminance colour rings reconstructed test pattern after IrfanViewTM (a) JPEG codec, (b) JPEG2000 codec compressed with a compression ratio of 180:1. The original test pattern is shown in Appendix 8.

Results:

Figure 7.14 shows the colour blur values calculated for each colour component Cb and Cr using the IrfanViewTM JPEG and JPEG2000 codecs. Figure 7.15 shows very high values for colour ringing. This may be due to level changes in chroma rather than oscillatory changes in chroma.

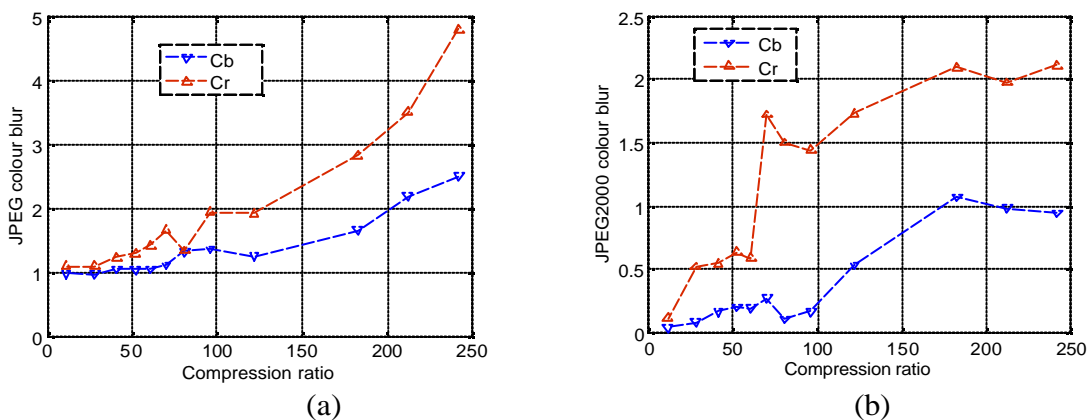


Figure 7.14 Colour blur metric values of colour components Cb and Cr of the reconstructed test pattern – (a) JPEG codec (b) JPEG2000 [155]. The colour component with the higher distortion is plotted in red.

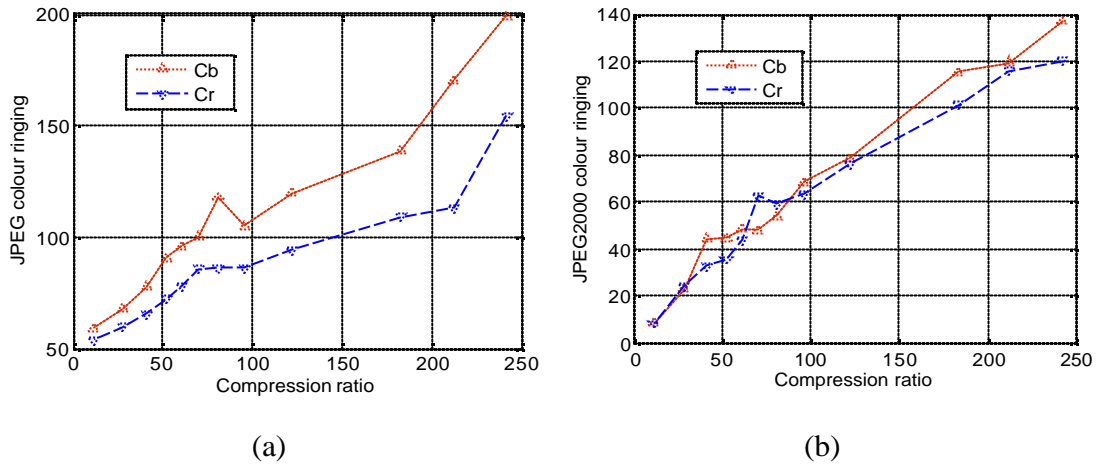


Figure 7.15 Colour ringing metric values for the colour components Cb and Cr of the reconstructed *colour rings* test pattern – (a) JPEG codec, (b) JPEG2000 [155]. The colour component with the higher distortion is plotted in red.

Conclusions:

For the outputs of both codecs, the Cr colour component has a larger blur error compared to the Cb colour component. This is due to larger quantisation error in Cr, which was evident from the clockwise hue shift (see chapter 5.4.1). For all compression ratios, JPEG introduces a colour blur error more than one unit whereas JPEG2000 colour blur errors are below two units. The JPEG 2000 codec introduces an error of less than two units and Cb has an error less than one unit.

Similarly for colour ringing, it can be observed in Figure 7.15 that JPEG2000 introduces less error than JPEG codec. The Cb component has more colour ringing error than the Cr component. This disparity is more evident in JPEG.

7.2 Pre and Post-processing Algorithms

7.2.1 Experiment - XVI De-blocking in an MPEG-4 codec

Aim: Assess the effectiveness of the de-blocking filter deployed within the MPEG-4 codec. However, it was not intended to evaluate the efficacy of de-blocking filter in isolation.

Method:

The test patterns developed can be extended to evaluate video codecs operating in the inter-frame mode as well. The test sequences were compressed for a range of bit rates and average blockiness over the sequence shown in figure 4.7. This was then evaluated using the blockiness algorithm *B1*. Though the work on video is beyond the scope of this thesis, some published work is presented here. Some preliminary results of research work extended to full video codecs are published in reference [123]. These findings validated the possibility of extending the synthetic test pattern design to inter-frame codec video codecs too. Multi format TMPGEnc4.0 XpressTM software based XVID MPEG-4 Part -2 codec deploys a de-blocking filter that is meant to reduce the blockiness compared to MPEG-1 and MPEG-2.

Results:

The goal of the thesis was to develop test patterns to evaluate spatial domain compression artefacts due to still image codecs or motion codecs operating in intra-frame coded mode. Section 4.2.4 briefly described the work in progress as future work to extend the synthetic test patterns to become synthetic test sequences. Figure 7.16 shows the results of the experiment carried out to benchmark three modes of a MPEG software codec using the proposed test sequences.

Conclusions:

It is known among the codec development community that MPEG-4 introduces less blockiness from informal subjective quality evaluations [124]. Due to the pre-

processing performed within the MPEG-4 implementation for deblocking, the blockiness across the range of bitrates tested remains low. MPEG-1 is optimised for low bitrates and MPEG-2 higher bitrates. Figure 7.16 also shows this fact as MPEG-1 outperforms for low bitrates against MPEG-2 with respect to blockiness. However, for high bit rates MPEG-4 is worse than the earlier generation codecs for blockiness artefact with test sequence shown in figure 4.7 [122]. For low bit-rates, the deblocking filter of MPEG-4 is quite effective at mitigating the blockiness artefact.

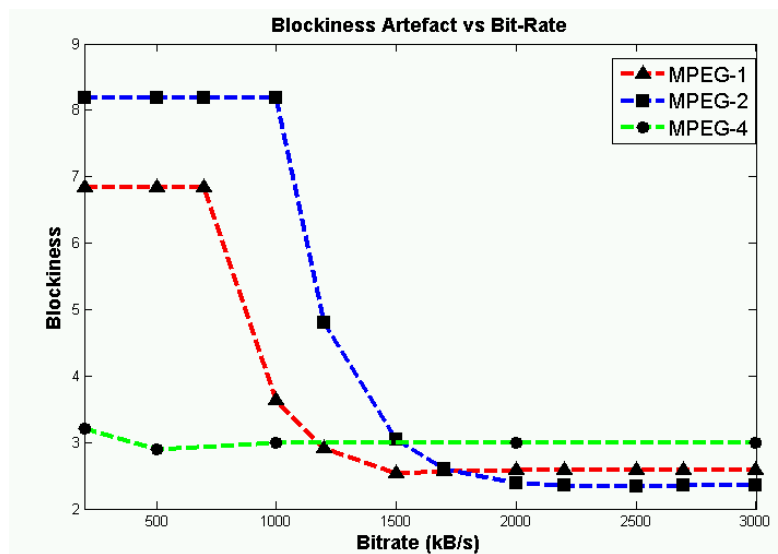


Figure 7.16 Benchmarking MPEG-1, MPEG-2 and MPEG-4 implementations for blockiness artefacts using test sequences [123].

7.3 Integrated Test and Measurement Environment

The framework proposed in this thesis consists of modules for test pattern generation, distortion metric computation algorithms and visualisation modules.

7.3.1 Block Diagram of the Integrated Environment

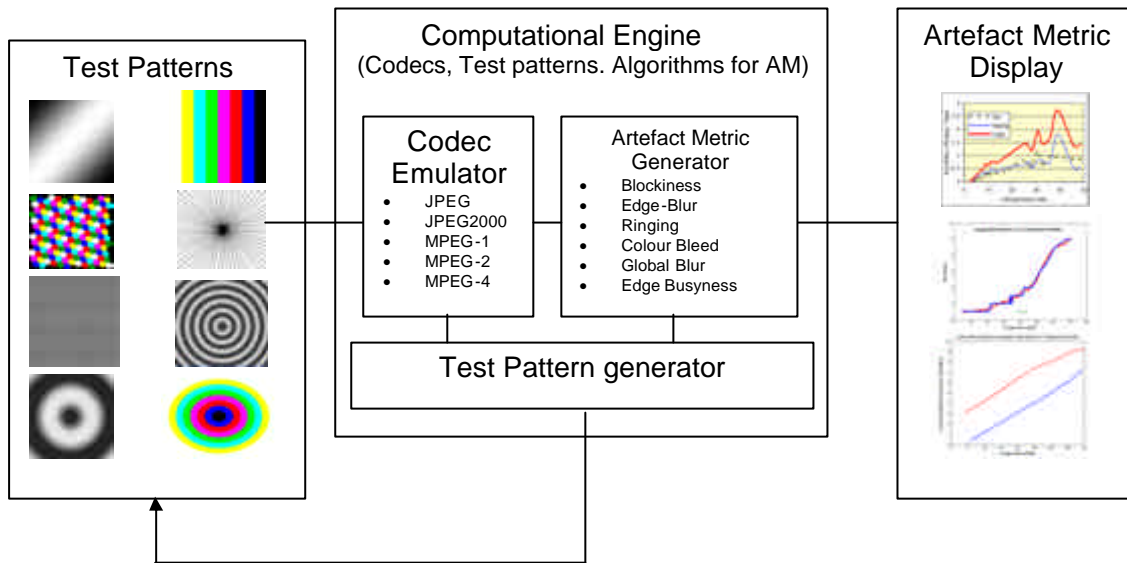


Figure 7.17 Block diagram of the artefact evaluation frame work [160].

Figure 7.17 shows a block diagram of the implementation of the framework. The test pattern generator can access pre-defined test patterns such as honeycomb, monochrome rings, colour rings or sinesquared grey scale – radial test patterns, random colour test patterns or modified colour test patterns for same luminance, chrominance, different colour gamut so on. If a software codec is available, that codec can run within the same environment. Otherwise a collection of compressed and decompressed test patterns can be utilised by passing them to the distortion metric computation algorithms. After applying the artefact distortion metrics, the results can be visualised with the original and reconstructed test patterns for subjective evaluation.

7.3.2 Visualisation

The compression artefact evaluation framework was prototyped within the Matlab™ programming environment. While obtaining objective measures, the evaluation environment can also provide a visual comparison as shown in Figure 7.18. The environment can be extended for the evaluation of other sources of artefacts as well.

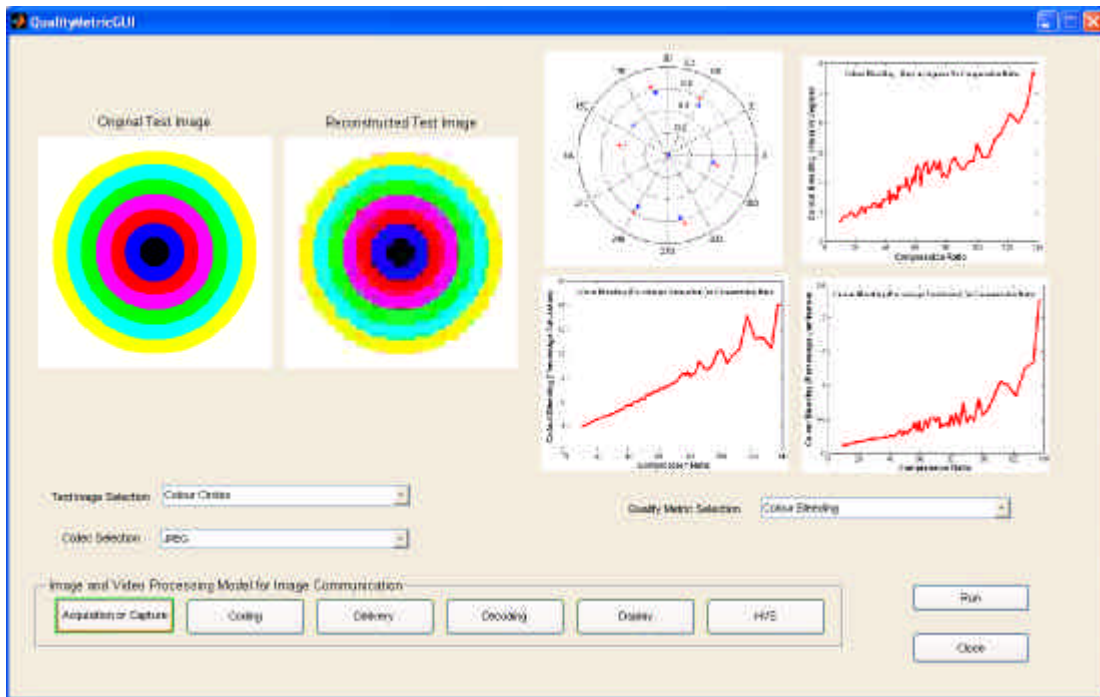


Figure 7.18 The prototype of the GUI of the artefact evaluation framework for image communications.

7.4 Objective Measurement of Artefacts in MPEG-4 and Advanced Codecs

The major challenges of benchmarking image and video coding arise due to the rapid pace of development and the increased complexity of new codecs. New concepts such as scalable and distributed image and video coding are being incorporated into the latest research. Though many of the objective quality metrics developed by other researchers for digital image or video have been developed for natural scenes, images or video, known referenced (synthetic) objective picture quality assessment generally offers swift, economical and uniform evaluation provided that the processing

hierarchy is well represented [161], [115]. To do this we need to design a synthetic picture or sequence. Then to evaluate the compression distortions that appear in the reconstructed picture. The contents are usually designed to stress the codec. The recently evolved MPEG-4 video codec can handle synthetic objects with shape coding and fully functional MPEG-4 may code objects with fewer distortions. This would offer a challenge to the design of a synthetic object to stress this new codec.

Some of the compression technologies used in MPEG-4 are DCT, wavelets, motion estimation, object coding and error resilient coding. Like any other codec standard, MPEG-4 only standardises the decoding process and the bit stream syntax, and many encoder and decoder implementations are possible. This situation makes artefact distortion metric design more complex as we need to evaluate many techniques, architectures and combinations of them. In particular an image source may be encoded in many different ways, with each approach using different object hierarchies and compression technologies, and yet all conform to the MPEG-4 standard. This complicates the design of generic test patterns and sequences.

The segmentation of video into objects is a function of the encoder and is not standardized. Synthetically generated content may already be segmented. In the television studio environment, techniques such as blue-screening (also known as chroma-keying) may be used. Segmentation of video into objects at capture may introduce artefacts such as a borderline around a foreground object.

Since the DCT is applied in block mode, we can anticipate block artefacts. In MPEG-4, such artefacts are mitigated by de-blocking and de-ringing filters, which are included in the post-processing decoder to improve the picture quality. Ringing noise can also be minimised by pre-processing the picture data where processing power is less constrained at the source of data [161], and [115]. The arbitrary shape coding in MPEG-4 may lead to aliasing when the shapes are coded as binary data, which is the simplest approach and indicates whether the object is transparent or opaque at any given point. The edge between the object and the background is abrupt. This leads to a violation of Nyquist theorem, and aliasing is likely to be visible.

In transmission, the objective quality metrics may represent application-level QoS levels where the QoS parameters may include loss of blocks and jitter to reflect the impact on image or video quality. The QoS metric is based on the probability of lost blocks and it can be used to assess performance of a codec transportation module implementation. A new challenge that arises with the introduction of MPEG-4 would be to evaluate the performance of built-in error resilience on IP and other lossy packet networks.

Multimedia content viewed on smaller screens with a progressive scan display may lead to display artefacts such as judder due to the conversion from interlaced scan to progressive scan. This is usually most noticeable in sequences containing motion. As a second example MPEG-4 has the ability to map a static texture onto a varying shape and this is performed at the decoder. The varying shape and the static texture are transmitted as separate objects. The movement of the shape may cause stretching or expansion of the texture far beyond its normal size. Due to poor spatial scaling capability, this can result in artefacts on the final display. Clearly, static-texture-scaling artefacts are content dependent.

MPEG-4 offers greater flexibility in implementation than previous standards but its use results in many challenges to benchmarking its implementations for picture quality, due to rapid improvements, increasing complexity, variability in implementation, and segmentation. Error resilience for transmission is a useful feature in transmission over IP networks. Texture coding and shape coding will introduce new forms of artefacts in MPEG-4. The major challenge to benchmarking picture quality of MPEG-4 is that the standard only specifies the bit stream and decoding process allowing wide range of mature and emerging compression technologies.

7.5 Chapter Summary and Conclusions

The objective artefact measures of blockiness, blur, ringing and coding colour bleed were used to compare the reproduction capability of JPEG and JPEG2000 codecs. JPEG2000 codecs do not introduce any blockiness or tiling for moderate size images. Different implementations may result in different levels of blockiness for JPEG codecs. In general, JPEG 2000 does not introduce blur distortions more than the JPEG codecs. However, poor implementation of JPEG2000 may introduce blur higher than JPEG codec. All three colour components, namely hue, saturation and luminance are degraded in reconstructed patterns. In general JPEG2000 performs better than JPEG in colour reproduction. Based on the colour *honeycomb* test pattern response, it is observed that bleeding increases with increasing compression ratio. The higher the level of compression, the higher the loss of each of the colour components. The artefact metrics provide a good representation of the colour bleeding artefact and are readily calculated. JPEG compression standards use the discrete cosine transform (DCT) whereas JPEG2000 uses wavelets. JPEG resulted in higher colour errors compared with JPEG2000. We may deduce that wavelet based compressors would result in less colour errors compared with DCT based compressors for a given compression ratio. The three artefact metrics clearly distinguish between the individual hue error, individual saturation error and individual luminance error. Individual colour values presented on an emulated vectorscope provide comparisons against the expected hue and saturation values. This is analogous to the conventional vectorscope used in television broadcast and video facilities.

Chapter 8: Summary, Conclusions and Future work

8.1 Summary

This thesis has considered the problem of compression artefact evaluation based on synthetic test patterns. A framework was proposed for the rapid and objective evaluation of blockiness, blur, ringing and colour bleeding compression artefacts.

Compression artefacts are defined as particular visible effects, which are a direct result of some technical limitation. Traditional objective measures for compression distortions such as peak-signal-to-noise ratio (PSNR) and mean square error (MSE) do not correlate well with distortions due to compression. Formal subjective methods of image quality evaluation need more resources and time. There are no tools to ascertain the effectiveness of artefact mitigation techniques. Also there is no standard for objective evaluation metrics or methodology.

Chapter 2 reviews the image communication artefacts. A taxonomy is presented to localise compression artefacts for further studies. Five sources of artefacts for images are presented with a brief account of each source. Capture artefacts are mainly due to optical systems. Delivery artefacts can be of ghosting or lost packets. The display device also plays a major role in the final quality of the image. This chapter also present artefact mitigation techniques proposed by many researchers. However, there are no rapid, objective methods to evaluate the effectiveness of any of the proposed mitigation techniques.

Chapter 3 presents a review of image quality evaluation methods. This chapter reviews signal quality measurement as an indirect image quality measurement method. Picture quality measurement requires human observers to provide a score to evaluate image quality. Such formal subjective methods require time and special resources. Hence, they can not be deployed for rapid measurements in an era where the codec development takes place at a rapid pace.

Chapter 4 proposes the general philosophy in the design of test patterns to evaluate four types of common compression artefacts considered in this thesis. The spatial content of the test patterns are defined to emphasise the compression artefact under study. Each test pattern exercises the codec under test for a single artefact. This enables clean detection and measurement of the respective artefacts.

Chapter 5 defines blockiness, blur, ringing and colour bleeding artefacts quantitatively. It also presents algorithms to detect and measure the respective artefacts. Proposed metrics for the four artefacts under study in this thesis are based on the synthetic test patterns proposed in chapter 4 and the quantitative definitions proposed in this chapter.

Chapter 6 evaluated the proposed metrics and test patterns for their efficacy as tools for artefact assessment. Test patterns and metrics were deployed on Matlab and Irfanview JPEG and Irfanview JPEG2000 codecs. The metrics were validated by comparing them with the structural similarity index, SSIM. This index has been shown to correlate well with subjective human assessment, so strong correlation with the SSIM indicates strong correlation with subjective assessment. The blockiness, blur and colour bleed metrics had excellent correlation with SSIM, and the ringing metric had good correlation at lower compression levels. The ringing metric may therefore require further refinement to give results that relate better to human perception.

Chapter 7 benchmarks two different types of codecs, namely JPEG and JPEG2000 and different implementations – MatlabTM and IrfanViewTM using the proposed test patterns and the metrics. The test patterns and metrics are useful in identifying which codecs perform better with respect to a given artefact distortion. In many cases, the JPEG2000 codec outperformed the JPEG codec. However, implementation variation may result in poor distortion characteristics.

8.2 Conclusions

The main objective of the thesis was to show efficacy and usefulness of the proposed framework for rapid, objective artefact evaluation. The proposed test patterns exercise the codec under study for the respective artefacts. Detection algorithms accurately detect and measure individual artefact distortion based on their characteristics. Artefact distortion metrics can be used to optimise parameters of codecs in the development process. Comparative performance evaluations among different codecs assist the process of codec selection for respective applications. Depending on the applications, compression requirements may differ. Suitable codecs for the required level of compression can be selected based on metrics proposed.

Overall, this thesis has demonstrated that the proposed framework can be used for rapid, objective evaluation of four dominant types of compression artefacts, namely blockiness, blur, ringing and colour bleeding. Colour blur and colour ringing have been defined qualitatively as well as quantitatively for colour image compressions. The framework can be extended to other compression artefacts including spatio-temporal artefacts.

8.3 Future Work

The work presented in this thesis lays a solid foundation for the compression artefact evaluation for video. Test sequences can be generated for spatio-temporal artefacts such as mosquito noise and jerkiness. It is difficult to evaluate the influence of GOP and related parameters for a given codec. The influence of GOP on compression distortions can be investigated through synthetic test sequences.

The robustness of the honeycomb test pattern needs to be further evaluated by rotating the tessellation structure of honeycomb test pattern. Then the spinning honeycomb pattern can be used as a sequence for evaluating colour errors due to video codecs.

The proposed test patterns and metrics can be used in codec performance evaluation, benchmarking and parameter optimisation. One limitation of the proposed metrics is the inability to distinguish between the blockiness and contouring. Future work will focus on improving the detection algorithm and to identify a reasonable threshold point for contouring.

The proposed objective artefact distortion metrics also need to be validated with formal subjective tests to increase the acceptance of metrics for the use in image quality measurement.

Chapter 9: References

- [1] P. Sunna. "AVC/H.264 – an advanced video coding system for SD and HD broadcasting", *The EBU Technical Review Journal*, Volume 302, pp. 1-6, 2005.
- [2] M. Sugawara. "Super Hi-Vision –research on a future ultra-HDTV system", *The EBU Technical Review Journal*, Volume 2008-Q2, pp. 1-7, 2008.
- [3] K. Tanioka, "Integral 3D Television", Broadcast Technology, *Journal of Science and Technical Research Laboratories of NHK*, ISSN 1345-4095 No. 33, p. 19, 2007.
- [4] M. Mark, M. Grgic, S. Grgic, "Scalable Video Coding for Network Applications", *4th EURASIP-IEEE Region 8 International Symposium on Video/Image Processing and Multimedia Communications*, Croatia, pp. 205-211, 2002.
- [5] O. Cohen, Unified Engine for Scalable Video Coding (SVC), *The Proceedings of the Broadcast-Asia 2008 Conference*, Singapore, pp 1-6, 2008.
- [6] A. Kouadio, M. Clare, L. Noblet, V. Botteau, " SVC – a highly scalable version of H.264/AVC", *The EBU Technical Review Journal*, Volume 2008-Q2, pp. 1-7, 2008.
- [7] MPEG Industry forum, "Home Page", <http://www.m4if.org/mpeg4/>, Visited August 2004 and October 2008.
- [8] Centre National Research Technologies in France, "Multimedia page", http://tim.irisa.fr/veille/TVadsl/Broadband%20TV/Broadband%20TVSEM/Presentations/Day%20%20morning/MPEG-4%20Video/H264_broadbandTV.pdf, Visited August 2004 and October 2008.
- [9] D. Wood, Everything you want to know about Video Codecs, *EBU Technical review*, European Broadcasting Union, Geneva, Volume 295, pp 1-8, 2003.
- [10] R. Mausl, Television Technology, Rohde and Schwarz, pp 9-13, 1977.

- [11] Sound and TV broadcasting; CCIR and FCC TV Standards, Rhode & Schwarz, p 3, 1997.
- [12] Rec. ITU-R BT.601-5, section 3.5, *Studio Encoding Parameters of Digital Television for Standard 4:3 and Wide-screen 16:9 Aspect Ratios*, 1982-1986-1990-1992-1994-1995.
- [13] C.W. Brown and B.J. Shepherd, *Graphics File Formats: Reference and Guide*. Greenwich, Connecticut, USA: Manning, pp 124-128, 1995.
- [14] G.A.D. Punchihewa, D. G. Bailey, R. M. Hodgson. “The Development of a Synthetic Colour test Image Subjective and Objective Quality Assessment of Digital Codecs”, *The Proceedings of Asia Pacific Conference on Communications, Perth, Australia*, pp. 881-885, 2005.
- [15] http://www.tek.com/Measurement/App_Notes/NTSC_Video_Msmt/vectorscope.html, visited 17th December 2008.
- [16] G.A.D. Punchihewa, D.G. Bailey, and R.M. Hodgson, “Integrated Test Pattern Generator and Measurement Algorithm for Colour Compression Artefacts in Ubiquitous Spaces”, *Image and Vision Computing New Zealand (IVCNZ'06)*, Great Barrier Island, NZ, pp. 467-472, 2006.
- [17] I. Richardson, *Video Codec: Developing Image Video Compression Systems*, John Wiley Sons Ltd, England, 2002.
- [18] C.W. Brown and B.J. Shepherd, *Graphics File Formats: Reference and Guide*. Greenwich, Connecticut, USA: Manning, pp 174-218, 1995.
- [19] M. Ghanbari, *Standard codecs : image compression to advanced video coding*, London, Institution of Electrical Engineers, p 107, 2003.
- [20] F. Pereira, T. Ebrahimi, *The MPEG-4 Book*, Prentice Hall, 2002
- [21] B. Pank, *The Digital Fact Book*. Berkshire: Quantel Limited, p. 25, 2008.
- [22] M. Kornfeld, U. Reimers. “DVB-H emerging standard for data communication”, *The EBU Technical Review Journal*, Volume 301, pp. 1-10, 2005.
- [23] C. J. Dalton. “Concatenation of compression codecs-The need for objective evaluations”, *The EBU Technical Review*, Volume 271, pp. 31-40, 1997.

- [24] F. X. Coudoux, M. Gazalet, P. Corlay, "An Adaptive Post-processing Technique for the Reduction of Color Bleeding in DCT-Coded Images", *IEEE Transactions on Circuits and Systems for Video Technology*, Volume. 14, No.1, pp 114-121, January 2004.
- [25] F. X. Coudoux, M. Gazalet, P. Corlay, "A DCT-Domain Postprocessor for Color Bleeding Removal", *The proceedings of the European conference on Circuit theory and design*, Ireland, Volume. 1, pp 209-212, 2005.
- [26] F. X. Coudoux, M. Gazalet, P. Corlay, "Reduction of Color Bleeding for 4: 1: 1 Compressed Video", *IEEE Transactions on Broadcasting*, Volume. 51, No. 4, pp. 538-542, December 2005.
- [27] M. Yuen, H. R. Wu, "A Survey of hybrid MC/DPCM/DCT video coding distortions", *Signal processing* Volume 70, Issue 3, pp. 247-278, 1998.
- [28] C.J.V.D.B. Lambrecht, V. Baskarn, A. Kovalick, and M Kunt, "Automatically Assessing MPEG Coding fidelity", *IEEE Design and Test*, Volume 2, Issue 12, pp. 28-33, 1995.
- [29] C. Fenimore, B.F. Field, and C. VandeGrift, "Test Patterns and Quality Metrics for Digital Video Compression", *Proceedings of SPIE: Human Vision and Electronic Imaging II*, SPIE Volume 3016, San Jose, CA, pp. 269-276, 1997.
- [30] C. Fenimore, J. Libert, and P. Roitman, "Mosquito noise in MPEG compressed video: test patterns and metrics", *Proceedings of SPIE: Human Vision and Electronic Imaging*, SPIE Volume 3959, San Jose, CA , pp. 604-612, 2000.
- [31] A. Bilgin, M. W. Marcellin, "JPEG2000 for Digital Cinema", *SMPTE Motion Imaging Journal*, Issue 05 California, pp 1-4, 2005.
- [32] T. E. Litwin, J. N. Maki, "Imaging services flight software on the Mars Exploration Rovers" *2005 IEEE International Conference on Systems, Man and Cybernetics*, Volume 1, pp. 895-902, 2005.
- [33] J. N. Maki, T. Litwin, M. Schwochert, K. Herkenhoff, "Operation and performance of the Mars Exploration Rover imaging system on the Martian

- surface”, *2005 IEEE International Conference on Systems, Man and Cybernetics*, Volume 1, pp. 930-936, 2005.
- [34] Video Quality Expert Group (VQEG), Final report from VQEG on the validation of objective models of video quality assessment, June 2000.
- [35] Video Quality Expert Group (VQEG), Final report from VQEG phase II on the validation of objective models of video quality assessment, August 2003.
- [36] P. Corriveau, Video Quality Expert Group, in H. R. Wu and K. R. Rao Eds. *Digital Video Quality Perceptual Coding* CRC Press, pp 325-333, 2006.
- [37] Z. Wang, A. Bovik, *Modern Image Quality Assessment*, Morgan Publishers, 2003.
- [38] A. Punchihewa, D. G. Bailey: and R. M. Hodgson: ZDomain Analysis of Ghost Cancellation for Television Signals, *Proceedings of the 7th International Symposium on Digital Signal Processing for Communication Systems*, Coolangatta, Australia, pp. 550-556, 2003.
- [39] H. R. Wu, M. Yuen, B. Qiu. “Video coding distortion classification and quantitative impairment metrics”, *Proceeding of the International Conference on Signal Processing*, Volume 2, pp. 962-965, 1996.
- [40] A. Punchihewa, and D. G. Bailey, “Artefacts in Image and Video Systems; Classification and Mitigation”, *Proceedings of Image and Vision Computing New Zealand (IVCNZ’02)*, pp. 197-202, 2002.
- [41] H. Y. Lee, J. W. Park, T. M. Bae, S. U. Choi, and Y. H. Ha, “Adaptive Scan Rate Up-Conversion System Based on Human Visual Characteristics”, *IEEE Transactions on Consumer Electronics*, Volume 46, Issue 4, pp. 999-1006, 2000.
- [42] O. A. Ojo, and H. Schoemaker, “Adaptive Global Concealment of Video Up-Conversion Artefacts”. *IEEE Transactions on Consumer. Electronics*, Volume 47, Issue 1, pp. 40-46, 2001.
- [43] E. Williams, “Educating the broadcast engineer: observations from the field. *Broadcast Magazine*, pp. 1-5, 2001.

- [44] Z. Lei, H. Schroder, "Adaptive Equalisation of Multipath Interference for Mobile Video Signal Reception", *IEEE Transactions on Broadcasting*, Volume 44, Issue 2, pp. 172-181, 1998.
- [45] A. Chini, Y. Wu, El- T. Tanany, and S. Mohmoud, "Filter Decision Feedback channel Estimation for OFDM based DTV Terrestrial Broadcasting System. *IEEE Transactions on Broadcasting*, Volume 44, issue 1, pp. 2-11, 1998.
- [46] R. Negi, and J. Cioffi, "Tone Selection for Channel Estimation in a Mobile OFDM System", *IEEE Transactions on Consumer Electronics*. Volume 44, Issue 3, pp. 1122-1128, 1998.
- [47] C. Dubuc, D. Boudreau, and F. Patenaude, "The Design and Simulated Performance of a Mobile Video Telephony Application for Satellite Third-Generation Wireless System", *IEEE Transaction on Multimedia*, Volume3, Issue 4, pp. 424-431, 2001.
- [48] Y. Chang, T. Carney, S.A. Klein, D. G. Messerschmitt, and A. Zakho, "Effects of Temporal Jitter on Video Quality: Assessment Using Psychophysical Methods", *Proceedings of the SPIE: Human Vision and Image Processing*, Volume 3299, pp. 173-179, 1998.
- [49] A. Punchihewa, D.G. Bailey, R.M. Hodgson, "A Survey of Coded Image and Video Quality Assessment", *Proceedings of Image and Vision Computing New Zealand (IVCNZ'03)*, Palmerston North, New Zealand, pp. 326-331, 2003
- [50] G. de. Haan, and M. A. Klompenhouwer, "An overview of flaws in Emerging Television Display and Remedial Video processing", *IEEE Transactions on Consumer Electronics*, Volume 47, Issue 3, pp. 326-334, 2001.
- [51] W. Zhou, A. C. Bovik, L. Ligang, "Image Quality Assessment: From Error Visibility to Structural Similarity", *IEEE Transactions on Image Processing*, Volume 13, Issue 4, pp. 600-612, 2004.
- [52] R. C. Gonzalez, R.E. Woods, *Digital Image processing*, Pearson Prentice Hall, New Jersey, pp 41-42, 2008.

- [53] M. Nadenau, *Integration of Human Color Vision Models into High Quality Image Compression*, PhD dissertation, Swiss Federal Institute of Technology (EPFL), Lausanne, Switzerland, pp 30-35, 2000.
- [54] W. Zhou, A. C. Bovik, L. Ligang, “Why is Image Quality Assessment So Difficult *Proceedings of the International Conference on Acoustic, Speech, and Signal Processing*, Volume 4, pp. 3313-3316, 2002.
- [55] J. G. Apostolopoulos, and N. S. Jayant, “Postprocessing for Very Low Bit-Rate Video Compression”, *IEEE Transactions on Image Processing*, Volume 8, Issue 8, pp.1125-1129, 1999.
- [56] C. B. Greenberg, “Ghost Cancellation System for the US standard GCR”, *IEEE Transactions on Consumer Electronics*, Volume 39, Issue 4, pp. 928-933, 1993.
- [57] J. Huang, “A Ghost Cancellation System for the NTSC Television”, *IEEE Transactions on Consumer Electronics*, Volume 39, Issue 4, pp. 896-904, 1993.
- [58] P. Appelhans, and H. Schroder, “Ghost Cancelling for Stationary and Mobile Television”, *IEEE Transactions on Consumer Electronics*, Volume 41, Issue 3, pp. 472-786, 1995.
- [59] W.A.A. Al-Saud, M. S. El-Henneyway, and M. T. Boraie, “A New GCR Waveform for Deghosting TV Signals”, *IEEE Transactions on Consumer Electronics*, Volume 42, Issue 4, pp. 920-929, 1996.
- [60] E. Fiallos, J. Harmasz, B. Caron, and B. Ledoux, “An enhanced Ghost Cancellation Reference Signal”, *IEEE Transactions on Consumer Electronics*, Volume 40, Issue 3, pp. 640-644, 1994.
- [61] K. S. Yang, H. M. Park, J. H. Park, and K. B. Kim, “A New GCR Signal and its Application”, *IEEE Transactions on Consumer Electronics*, Volume 40, Issue 4, pp. 852-860, 1994.
- [62] L. Johnson, S. McNay, R. Hill, D. Greene, K. Jostschulte, A. Amei, M. Schu, and H. Schroder, “Perception Adaptive Temporal TV-noise Reduction using Contour Preserving Prefilter Techniques”, *IEEE Transactions on Consumer Electronics*, Volume 44, Issue 3, pp. 1091-1096, 1998.

- [63] C. Min, S. Cho., K. W. Lim, and H. Lee, "A New Adaptive Quantization Method to Reduce Blocking Effect", *IEEE Transactions on Consumer Electronics*, Volume 44, Issue 3, pp. 768-773, 1998.
- [64] H. Paek, R. Kim, and S. Lee "On the POCS-Based Post-processing Technique to Reduce the Blocking Artefacts in Transform Coded Images. *IEEE Transactions on Circuits and Systems for Video Technology*, Volume 8, Issue 3, pp. 358-367, 1998.
- [65] H. Paek, R. Kim, and S. Lee, "A DCT-Based Spatially Adaptive Post-Processing Technique to Reduce the Blocking Artefacts in Transform Coded Images", *IEEE Transactions on Circuits and Systems for Video Technology*, Volume 10, Issue 1, pp.36-41, 2000.
- [66] M. A. Robertson, and R. L. Stevenson, "Reduced-Complexity Iterative Post-Filtering of Video", *IEEE Transactions on Circuits and Systems for Video Technology*. Volume 11, Issue 10, pp. 1121-1127, 2001.
- [67] M. Mancuso, and A. Borneo, "Advanced Pre/post-processing for DCT coded images", *IEEE Transactions on Consumer Electronics*, Volume 44, Issue 3, pp. 1039-1041, 1998.
- [68] B. K. Gunturk, Y.A. Itunbasak, and R. M. Mersereau, "Multiframe Blocking-Artifact Reduction for Transform-Coded Video", *IEEE Transactions on Circuits and Systems for Video Technology* , Volume 12, Issue 4, pp. 276-282, 2000.
- [69] A. J. Patti, and Y. Altunbasak, "Artifact Reduction for Set Theoretic Super Resolution Image Reconstruction with Edge Adaptive Constraints and Higher-Order Interpolants", *IEEE Transactions on Image Processing*, Volume 10, Issue 1, pp. 179-186, 2001.
- [70] C. Liu, C. Wang, and J. Lin, "A New Post-processing Method for the Block-Based DCT Coding Based on the Convex-Projection Theory", *IEEE Transactions on Consumer Electronics*, Volume 44, Issue 3, pp.1054-1061, 1998.
- [71] Y. Jeong, I. Kim, and H. Kang, "A Practical Projection-Based Post-processing of Block-Coded Images with Fast Convergence Rate", *IEEE*

- Transactions of Circuits and Systems*, Volume 10, Issue 4, pp. 617-623, 2000.
- [72] B. Jeon, and J. Jeong, “Blocking Artefacts Reduction in Image Compression with Block Boundary Discontinuity Criterion”, *IEEE Transactions on Circuits and Systems for Video Technology*, Volume 8, Issue 3, pp. 345-357, 1998.
- [73] Y. Kim, J. Jung, K. Choi, and S. Ko, “Post-Processing Technique Based on POCS for Visual Enhancement in HDTV Images”, *IEEE Transactions on Consumer Electronics*, Volume 47, Issue 3, pp. 652-659, 2001.
- [74] T. Meier, K. N. Ngan, and G. Crebbin, “Reduction of Blocking Artefacts in Image and Video Coding”, *IEEE Transactions on Circuits and Systems*, Volume 9, Issue 3, pp. 490-500, 1999.
- [75] S. Yang, Y. H. Ju, T. Q. Nguyen, and D. L. Tull, “Maximum-Likelihood Parameter Estimation for Image Ringing-Artifact Removal”, *IEEE Transactions on Circuits and Systems for Video Technology*, Volume 11, Issue 8, pp. 963-973, 2001.
- [76] Z. Wang, and D. Zhang, “A Novel Approach for Reduction of Blocking Effects in Low-Bit-Rate Image Compression”, *IEEE Transactions on Communications*, Volume 46, Issue 6 pp. 732-734, 1998.
- [77] J. Yang, H. Choi, and T. Kim, “Noise Estimation for Blocking Artefacts Reduction in DCT Coded Images”, *IEEE Transactions on Circuits and Systems*, Volume 10, Issue 7 pp. 1116-1120, 2000.
- [78] Y. Cao, P. P. B. Eggermong, and S. Tereby, “Cross Burg Entropy Maximization and Its Application to Ringing Suppression in Image Reconstruction”, *IEEE Transactions on Image Processing*, Volume 8, Issue 2 pp. 286-292, 1999.
- [79] J. Mateos, A. K. Katsaggelos, and R. Molina, “A Bayesian Approach for the Estimation and Transmission of Regularization Parameters for Reducing Blocking Artefacts”, *IEEE Transactions on Image Processing*, Volume 9, Issue 7, pp. 1200-1215, 2000.

- [80] L. Atzori, F. G. B. Natale, and C. De Perra, "A Spatio-Temporal Concealment Technique Using Boundary Matching Algorithm and Mesh-Based Warping (BMA-MBW)", *IEEE Transactions on Multimedia*, Volume 3, Issue 3, pp.326-338, 2001.
- [81] G. Qui, "MLP for Adaptive Post-processing Block-Coded Images", *IEEE Transaction on Circuits and Systems for Video Technology*, Volume 10, Issue 8, pp.1450-1454, 2000.
- [82] Y. L. Lee, H. C. Kim, and H. W. Park, "Blocking Effect Reduction of JPEG Images by Signal Adaptive Filtering", *IEEE Transactions on Image Processing*, Volume 7, Issue 2, pp. 229-234,1998.
- [83] S. D. Kim, J. Yi, H. M. Kim, and J. B. Ra, "A Deblocking Filter with Two Separate Modes in Block-Based Video Coding", *IEEE Transactions on Circuits and Systems*, Volume 9, Issue 1, pp.156-160, 1999.
- [84] T. Chen, H. R. Wu, and B.Qui, "Adaptive Post-filtering of Transform Coefficients for the Reduction of Blocking Artefacts", *IEEE Transactions on Circuits and Systems for Video Technology*, Volume 11, Issue 5, pp. 594-602, 2001.
- [85] H. Park, and Y.L. Lee, "A Post-processing Method for Reducing Quantization Effects in Low Bit-Rate Moving Picture Coding", *IEEE Transactions on Circuits and Systems for Video Technology*, Volume 9, Issue 1, pp. 161-171, 1999.
- [86] M. Carli, D. Bailey, M. Farias, and S. K. Mitra, "Error Control and Concealment for Video Transmission using Data hiding", *Proceedings of the International symposium on wireless personal multimedia communications*, Honolulu, Hawaii, pp. 812-815, 2002.
- [87] T. Hsung, and D. P. Lun, "Application of Singularity Detection for the De blocking of JPEG Decoded Images", *IEEE Transactions on Circuits and Systems-II: Analogue and Digital Signal Processing*, Volume 45, Issue 5, pp. 640-644, 1998.
- [88] N. C. Kim, I. H. Jang, D. H. Kim, and W. H. Hong, "Reduction of Blocking Artefact in Block-Coded Images Using Wavelet Transform", *IEEE*

- Transactions on Circuits and Systems for Video Technology*, Volume 8, Issue 3, pp.253-257, 1998.
- [89] H. Choi, and T. Kim, “Blocking-Artifact Reduction in Block-Coded Images Using Wavelet-Based Sub band Decomposition”, *IEEE Transactions on Circuits and Systems for Video Technology*, Volume 10, Issue 5, pp.801-805, 2000.
- [90] H. S. Malvar, “Biorthogonal and Nonuniform Lapped Transforms for Transform Coding with Reduced Blocking and Ringing Artefacts”, *IEEE Transactions on Signal Processing*, Volume 4, Issue 4, pp. 1043-1053, 1998.
- [91] W. K. Carey, S. S. Hamami, and P. N. Heller, “Smoothness-Constrained Quantization for Wavelet Image Compression”, *IEEE Transactions on Image Processing*, Volume 8, Issue 12, pp. 1807-1811, 1999.
- [92] S. Nishida, “Human Visual Processing for Surface Qualities of Moving and Stationary Objects”, *The Proceedings of the third International Workshop on Image Media Quality and its Applications*, pp. 92-95, 2008.
- [93] M. C. Q. De Farias, *No-Reference and Reduced Reference Video Quality Metrics: New Contributions*, PhD dissertation, University of California, Santa Barbara, September 2004.
- [94] D. K. Fibush, “Practical Application of Objective Picture Quality Measurements”, *the Proceedings of International Broadcasting Convention*, Amsterdam, pp.504-513, 1997.
- [95] ITU Recommendation P.930, Principles of a Reference Impairment system for Video, 1996.
- [96] M. Craig, *Television Measurements*, Tektronix, United Kingdom, 1992.
- [97] C. J. Van Den B. Lambrecht, *Perceptual Models and Architectures for Video Coding Applications*, PhD dissertation, Lausanne University, Switzerland, 1996.
- [98] C. J. Van Den B Lambrecht, O. Verscheure, J. Urbain, and F. Tassin, “Quality Assessment of Image Features in Video Coding”, *IEEE International Conference on Image Processing*, Santa Barbara, pp. 302-305, 1995.

- [99] W. Gao, C. Mermer, Y. Kim, "A De-Blocking Algorithm and a Blockiness Metric for Highly Compressed Images", *IEEE Transactions on Circuits and Systems for Video Technology*, Volume 12, Issue 12, pp. 1150-1159, 2002.
- [100] K. T. Tan, and M. Ghanbari, "A Multi-Metric Objective Picture-Quality Measurement Model for MPEG Video", *IEEE Transactions on Circuits and Systems for Video Technology*, Volume 10, Issue 7, pp. 1208-1213, 2000.
- [101] Recommendation ITU-T E.800, Terms and Definitions Related to Quality of Service and Network Performance Including Dependability, 1993.
- [102] Recommendation ITU-T M.60, Maintenance: Introduction and General Principles of Maintenance and Maintenance Organization, 1993.
- [103] ITU-R Document 10-11Q/20, Liaison Statement from ITU-T Study Group 9 to ITU-R Joint Working Party 10-11Q, "Quality of Service", November 1998.
- [104] S. Winkler, *Vision Models and Quality Metrics for Image Processing Applications*, PhD dissertation, Lausanne University, Switzerland, 2000.
- [105] ITU-R Recommendation BT.500-3, "Methodology for the subjective assessment of the quality of television pictures." *International Telecommunication Union*, Geneva, Switzerland, 2002.
- [106] A. C. Bovik, *The Hand Book of Video Databases: Design and Applications*, CRC Press, USA, p.1070, 2003.
- [107] ITU-R Recommendation BT.500-11, "Methodology for the subjective assessment of the quality of television pictures", *International Telecommunication Union*, Geneva, Switzerland, 2002.
- [108] ITU-T Recommendation P.910, "Subjective video quality assessment methods for multimedia applications", *International Telecommunication Union*, Geneva, Switzerland, 1996.
- [109] M. Knee, "The Picture Appraisal Rating (PAR) - a single-ended picture quality measure for MPEG-2", *Proceedings of the International Broadcast Convention*, Amsterdam, pp. 1-6, 2000.

- [110] C. J. Van Den B Lambrecht, and M. Kunt, “*Characterization of human visual sensitivity for video imaging applications*”, *Signal Processing*, Volume. 67, pp. 255-269, 1998.
- [111] C. J. Van Den B Lambrecht, , O. Verscheure, J. Urbain, and F. Tassin, “*Quality Assessment of Image Features in Video Coding*”, *IEEE International Conference on Image Processing*, Santa Barbara, pp. 302-305, 1995.
- [112] D. Bailey, M. Carli, M. Farias, and S. K. Mitra, “*Quality Assessment for Block-Based Compressed Images and Videos with regard to Blockiness Artefacts*”, *The Proceedings of the Tyrrhenian International Workshop on Digital Communications* Capri, Italy, pp. 237-241, 2002.
- [113] M.C.Q. Farias, M. S Moore, J. M Foley, and S. K Mitra, “*Detectability and Annoyance of Synthetic Block and Blurry Video Artefacts*”, *Proceedings of XI European Signal Processing Conference*, Boston, pp. 708-711, 2002.
- [114] J. Lauterjung, “*Picture Quality Measurement*”, *the Proceedings of the International Broadcasting Convention*, Amsterdam, pp.1-6, 1998.
- [115] Tektronix, "measurement page", <http://www.tektronix.com/Measurement/>, visited on 10/07/2008.
- [116] ISO/DIS 20462-1, “*Psychophysical experimental method to estimate image quality – Part 1: Overview of psychophysical elements*” *International Organization for Standardization*, 2003.
- [117] ISO/DIS 20462-2, “*Psychophysical experimental method to estimate image quality – Part 2: Triplet comparison method.*” *International Organization for Standardization*, 2003.
- [118] ISO/DIS 20462-3, “*Psychophysical experimental method to estimate image quality – Part 3: Quality ruler method.*” *International Organization for Standardization*, 2003.
- [119] Video Quality Expert Group, "Home Page" <http://www.vqeg.org/>, visited on 10/07/2008.

- [120] ANSI T1.801.02-1996, "American National Standard for Telecommunications - Digital Transport of Video Teleconferencing/Video Telephony Signals - Performance Terms, Definitions, and Examples, 1996.
- [121] G.A.D. Punchihewa, D.G. Bailey and R.M. Hodgson, "Benchmarking Image Codecs by Assessment of Coded Test Images: The development of Test Images and New Objective Quality Metrics", *Journal of Telecommunications and Information Technology (JTIT2006)*, 1/2006, pp 11-16, 2006.
- [122] A. Punchihewa, J. Armstrong, "Benchmarking Video Codecs for Blockiness Compression Artefacts", *Image and Vision Computing New Zealand (IVCNZ'07)*, Hamilton, New Zealand, pp. 467-472, 2007.
- [123] A. Punchihewa, J. Armstrong, "Encoder Artefact Assessment for Visual media: An Engineering Approach", *Proceedings of the BroadcastAsia-2008 Conference*, Singapore, pp. 1-7, 2008.
- [124] MPEG-4 Forum, <http://www.mp4if.org/mpg4>, visited in August 2004.
- [125] M. Robin and M. Poulin, *Digital Television fundamentals*, McGraw Hill Publication Second Edition, p. 126, 2000.
- [126] M. Demtschyna, Web article-"Colour Bleeding", Website visited on 15th April 2008
<http://www.michaeldvd.com.au/Articles/VideoArtefacts/VideoArtefactsColourBleeding.html>.
- [127] S. Susstrunk, S. Winkler "Colour Image Quality on the Internet", *The Proceedings of the SPIE*, volume. 5304, pp. 118-131, 2003.
- [128] G. Spampinato, A. Catorina, A. Bruna, A. Capra, "JPEG Adaptive Chromatic Post-processing", *The proceedings of the International Conference on Image Analysis and Processing*, pp. 202-205, 2007.
- [129] G.A.D. Punchihewa, D. G. Bailey, R. M. Hodgson. "The Development of a Synthetic Colour test Image Subjective and Objective Quality Assessment of Digital Codecs", *The Proceedings of IEEE region-10 Telecommunication Conference, Melbourne, Australia*, pp. 881-885, 2005.

- [130] A. Punchihewa, "Objective Evaluation of Image Codec Encoder Artefact Assessment, *Proceedings of the Visual Information Engineering Conference*, China, pp. 1-7, 2008.
- [131] H. Lang, "Colour Displays", *Colour for Science, Art and Technology*, Elsevier, Amsterdam, pp.453-455, 1998.
- [132] G. J. Braun, M. D. Fairchild, "Gamut Mapping for Pictorial Images", *TAGA Proceedings*, 645-660, 1999.
- [133] S. Suthaharan, H. R. Wu. "A distortion measure for blocking artefacts in digital video", *The International Conference on Information, Communications and Signal Processing*, pp. 1566-1569, 1997.
- [134] S. A. Karunasekera, N. G. Kingsbury. "A distortion measure for blocking artefacts in images based on human visual sensitivity", *IEEE Transaction on Image Processing*, volume 4, pp. 713-724, 1995.
- [135] S. Yao, W. Lin, Z. Lu. EP. Ong and M. Etoh, "Objective Quality Assessment for Compressed Video", *Proceedings of the International Symposium on Circuits and Systems*, pp. 688-691, 2003.
- [136] R. Castagno, S. Marsi, and G. Ramponi, 1998. "A Simple Algorithm for the Reduction of Blocking Artefacts in Images and its Implementation", *IEEE Transactions on Consumer Electronics*, Volume 44, Issue 3, pp. 1062-1070, 1998.
- [137] P. Marziliano, F. Dufaux, S. Winkler, T. Ebrahimi, "A no reference perceptual blur metric", *The Proceeding of the IEEE International Conference on Image Processing*, pp. III-57-60, 2002.
- [138] P. Marziliano, F. Dufaux, S. Winkler, T. Ebrahimi, "Perceptual blur and ringing metrics: application to JPEG2000", *Signal Processing: Image Communication*, Volume 19, pp. 163-172, 2004.
- [139] Z. Devcic, S Loncaric, "Blur identification using averaged spectra of degraded image singular vectors", *The Proceeding of the IEEE International Conference on Image Processing*, pp. 2195-2198, 2000.

- [140] D.G. Bailey, "A rank based edge enhancement filter", *5th New Zealand Image Processing Workshop*, Palmerston North, New Zealand, pp. 42-47, 1990.
- [141] M. Kusuma, and H. Zepernick, "A Reduced-Reference Perceptual Quality Metric for In-Service Image Quality Assessment", *Proceedings of Internet, Telecommunication and Signal processing (WITSP 2003)* conference and workshop, Australia, pp 72-76, 2003.
- [142] R. Archibald, A Gelb, "A method to reduce the Gibbs ringing artefact in MRI scans while keeping tissue boundary integrity", *IEEE Transactions on Medical Imaging*, Volume 21, Issue 4 pp. 305-319, 2002.
- [143] Y. Yang, N.P. Galatsanos, "Removal of compression artefacts using projections onto convex sets and line process modelling", *IEEE Transactions on Image Processing*, Volume: 6, Issue: 10, pp. 1345-1357, 1997.
- [144] S Yang, Y. H. Hu, T. Q. Nguyen, D. L. Tull, "Maximum-likelihood parameter estimation for image ringing-artefact removal", *IEEE Transactions on Circuits and Systems for Video Technology*, Volume 11, Issue 8, pp. 963-973, Aug 2001.
- [145] A. Kaup, "Reduction of Ringing Noise in Transform Image Coding Using a Simple Adaptive Filter", *Electronic Letters*, Volume 34, Issue 22, pp. 2110-1221, 1998.
- [146] M.I. Sezan, AM Tekalp, EK Co, NY Rochester, "Adaptive image restoration with artefact suppression using the theory of convex projections", *IEEE Transactions on Acoustics, Speech, and Signal Processing*, Volume 38, Issue 1, pp. 181-185, 1990.
- [147] P Marziliano, F Dufaux, S Winkler, T Ebrahimi, "Perceptual blur and ringing metrics: application to JPEG 2000", *Elsevier, Signal Processing: Image Communication*, Volume 19, pp. 163–172, 2004.
- [148] S. H. Oguz, Y. H. Hu, T. Q. Nguyen, "Image coding ringing artefact reduction using morphological post-filtering", *IEEE Second Workshop on Multimedia Signal Processing*, pp. 628-633,1998.

- [149] M.Y. Shen, C. C. J. Kuo, "Review of postprocessing techniques for compression artefact removal, Journal of Visual Communication and Image Representation", 1998, *Journal of Visual Communication and Image Representation* , Volume 9, No 1, March, pp. 2–14, 1998.
- [150] J. Li, C. C. J. Kuo, "Coding artefact removal with multiscale postprocessing", *Proceedings of the International Conference on Image Processing*, volume.1, pp. 45-48, 26-29 Oct 1997.
- [151] W. E. Lynch, A. R. Reibman, B Liu, "Post processing transform coded images using edges", *Proceedings of the International Conference on Acoustics, Speech and Signal Processing*, pp.2323-2326, 1995.
- [152] R. Barland, A. Saadane, "Reference Free Quality Metric Using a region-Based Attention Model for JPEG-2000 Compressed Images", *The Proceeding of Signal Processing and IE Electronic Imaging* Volume 6059, pp. 605905-1-10, 2006.
- [153] G.A.D. Punchihewa, D.G. Bailey, and R.M. Hodgson, "Objective evaluation of edge blur and ringing artefacts: application to JPEG and JPEG2000 image codecs", *Image and Vision Computing New Zealand (IVCNZ'05)*, Dunedin, New Zealand, pp. 61-66, 2005
- [154] F. Coudoux, M Gazalet. "An Adaptive Postprocessing Technique for the Reduction of Colour Bleeding in DCT-Coded Images", *IEEE Transaction on Circuit and Systems for Video technology*, volume 14, pp. 114-121, 2000.
- [155] A. Punchihewa, J Armstrong, "Objective Evaluation of Components of Colour Distortions due to Image Compression" *The Proceedings of the Third International Workshop on Image Media Quality and its Applications (IMQA2008)*, Kyoto, Japan, pp 1-6, 2008.
- [156] A. Punchihewa, J Armstrong, "Objective Evaluation of Intra-Frame Coded Codecs for Blockiness Artefact" *The Proceedings of the Electronics Conference in New Zealand (ENZCon2007)*, Wellington, New Zealand, pp. 312-317, 2007.
- [157] A. Punchihewa, "Objective Evaluation of Multiple Artefacts using a Single Synthetic Test Pattern", *Proceedings of the 9th International Symposium on*

- DSP and Communication Systems, (DSPCS'2006) and 5th Workshop on the Internet, Telecommunications and Signal Processing, (WITSP'2006)*, Tasmania, Australia, pp. 1-6, 2006.
- [158] A. Punchedewa, J. Armstrong, "Colour Artefacts in JPEG and JPEG2000 Image Codecs" *The Proceedings of the International Conference in Computer Information and Robotic Applications (CIRAS2007)*, Palmerston North, New Zealand, pp 141-145, 2007.
- [159] A. Punchedewa, D.G. Bailey, and R.M. Hodgson, "Colour Reproduction Performance of JPEG and JPEG2000 Codecs", *Proceedings of the 8th International Symposium on DSP and Communication Systems, (DSPCS'2005) and 4th Workshop on the Internet, Telecommunications and Signal Processing, (WITSP'2005)*, Noosa Heads, Australia, pp. 312-317, 2005.
- [160] A. Punchedewa, D. Salvador, "An Integrated Environment for Objective Evaluation of Digital Codecs using a Small set of Novel Image Quality Metrics and Synthetic Test Images", *The IEEE International Conference on Information and Automation (ICIA 2005)*, Sri Lanka, pp.1-6, 2005.
- [161] P. D. Symes: *Video compression demystified*, pp.194-219, McGraw Hill Publication 2001.
- [162] Z. Wang, A. C. Bovik, H. R. Sheikh, and E. P. Simoncelli, "Image quality assessment: From error measurement to structural similarity" *IEEE Transactions on Image Processing*, vol. 13, no. 4, Apr. 2004.
- [163] T. Skajaa, H. Stephansen, "Applications for JPEG2000 for television contribution and distribution", *The Proceedings of the Broadcast Asia Conference*, Broadcast Asia 2008, Singapore, pp.1-8, 2008.
- [164] N. Komiya, "Ghost Reduction by Reproduction", *IEEE Transactions on Consumer Electronics*, Vol. 38, no. 3, pp 195-199, August 1992.
- [165] M. D. Kouam, J. Palicot, "Frequency Domain Ghost Cancellation Using Small FFT's", *IEEE Transactions on Consumer Electronics*, Vol. 39, no. 3, pp 372-380, August 1993.

- [166] C. B. Greenberg, "Ghost Cancellation System for the US standard GCR", *IEEE Transactions on Consumer Electronics*, Vol. 39, no. 4, pp 928-933, November 1993.
- [167] G. H. Lee, R H. Park, I. Song, J. H. Park and B. U Lee, "Modification of the Reference Signal for Fast Convergence in LMS-based Adaptive Equalizers", *IEEE Transactions on Consumer Electronics*, Vol. 40, no. 3 pp 645-654, August 1994.
- [168] E. Fiallos, J. Jarmasz, B. Caron and B. Ledoux, "An Enhanced Ghost Cancellation Reference Signal", *IEEE Transactions on Consumer Electronics*, Vol. 40, No. 3, pp 640-644, August 1994.
- [169] H. Miyazawa, S. Matsuura, S. Takayama and M. Usui, "Development of a Ghost Cancel Reference Signal for TV Broadcasting", *IEEE Transaction on Broadcasting*, Vol. 35, No. 4, pp 339-347, December 1989.
- [170] K. B. Kim, J. Oh, M. H. Lee, H. Hwang, and D. Song, "A New Ghost Cancellation System for Korean GCR", *IEEE Transaction on Broadcasting*, Vol. 40, No. 3, pp 132-140, September, 1994.
- [171] T. J. Wang, "Complex-Valued Ghost Cancellation Reference Signal for TV Broadcasting", *IEEE Transactions on Consumer Electronics*, Vol. 37, No. 4, pp 731-736, November 1991.
- [172] W. A. A. Al-Saud, M. S. El-Hennawey, and M. T. Borarie, "A New GCR Waveform for Deghosting TV Signals", *IEEE Transactions on Consumer Electronics*, Vol. 42, No. 4, pp 920-929, November 1996.
- [173] A. Punchihewa, *Evolving technologies for 21st Century*, Friedrich Ebert Stiftung, Sri Lanka, pp 15-17, 2000.
- [174] ITU-R BT. 1124 Recommendation of the International Telecommunication Union (ITU) Radio sector, 2001.
- [175] T. J. Wang, "Frequency Division Algorithm for Multi-Path Ghost Cancellation", *IEEE Transactions on Consumer Electronics*, Vol. 42, no. 4, pp 930-937, November 1996.

- [176] Z. Lei, P. Appelhans and H. Schroder, "Image processing Technique for Blind TV Ghost Cancellation", *IEEE International Conference on Acoustics, Speech, and Signal Processing*, Vol.4 pp 2561-2564, 1997.
- [177] P. N. Gardiner, "Ghost Cancellation for 625-line systems", *Proceedings of the International Broadcast Convention*, Conference Publication No. 397, IEE, pp 673-678, 1994.
- [178] L. Johnson, S. McNay et.al. "Low Cost Stand-Alone Ghost Cancellation System", *IEEE Transaction on Broadcasting*, Vol. 40, No. 3, pp 632-639, August, 1994.
- [179] D. R. Case and B. H. Pardoe, "Measurement of Multi-path Effects in Video Signals", *Proceedings of the IEEE Fourth International Conference on Television Measurement*, June 1991, pp 63-68.
- [180] R. S. Sherratt and B. H. Pardoe, " A New Method for Multi-path Channel Characterisation for Terrestrial Transmitted Video", *Radio Receivers and Associated Systems*, Conference Publication No. 415, IEE, pp22-25, 26-28 September 1995.
- [181] B. Ledoux, "Channel Characterisation and Television Field Strength Measurements", *IEEE Transaction on Broadcasting*, Vol. 42, No. 1, March, 1996, pp 63-73.
- [182] B. Caron, "Video Ghost Cancelling: Evaluation by Computer Simulation and Laboratory Testing", *IEEE Transactions on Consumer Electronics*, Vol. 38, No. 3, pp xxvi-xxxiii, August 1992.
- [183] J. D. Wang, T. H.S. Chao, and B. R. Saltzberg, "Training Signal and Receiver Design for Multi-path Channel Characterisation for TV Broadcasting", *IEEE Transactions on Consumer Electronics*, Vol. 36, No. 4 pp 794-806, November 1990.
- [184] P. Appelhans and H. Schroder, "Ghost Cancelling for Stationary and Mobile Television", *IEEE Transactions on Consumer Electronics*, Vol. 41, No. 3, pp 472-475, August 1995.
- [185] D. J. Harasty, and A. V. Oppenheim, "Television Signal Deghosting by Noncausal Recursive Filtering", *Proceedings of IEEE International*

- Conference on Acoustics, Speech, and Signal Processing*, pp 1778-1781, 1988.
- [186] R. S. Sherratt, "Identification and Minimisation of IIR Tap Coefficients for the Cancellation of Complex Multi-path in Terrestrial Television", *IEEE Transactions on Circuits and Systems for Video Technology*, Vol. 6, No 6, pp 703-706, December 1996.
- [187] S. Pao, K. Y. Khoo, and A. N. Willson, "A Programmable FIR Filter for TV Ghost Cancellation", *Proceedings of the IEEE 39th Midwest symposium on Circuits and Systems*, pp 133-136, 1997.
- [188] Tzy-Hong, S. Chao, "Multi-path Equalisation for NTSC Video by using Digital IIR Filter", *IEEE Transactions on Consumer Electronics*, Vol. 34, No. 1, pp 268-278, February 1988.
- [189] M. S. Mousa, K. T. Ibrahim, A. H. Khalil, and A. E. Salama, "Design and Implementation of a TV Ghost Cancelling System using High Level Synthesis Tools", *Proceedings of IEEE Conference on Electrotechnical*, pp 404-408, 2002.
- [190] W. Pora, and P Siriluangtong, "A TV Ghost Canceller using FPGA-based FIR Filters", 2002, *Proceedings of the Asia-Pacific Conference on Circuits and Systems*, pp 289-292, 2002.
- [191] A. M. Dreake, "Television Engineering", McGraw Hill Publication, pp 144, 1979.
- [192] W. Wharton, S. Metcalfe and G. C. Platts, *Broadcast Transmission Engineering Practice*, Focal Press, pp 73-103, 1992.
- [193] B. Grob, C. E. Herndon, *Basic Television and Video Systems*, 6th Edition, McGraw-Hill, p. 292, 1998.

Appendix 1: Ghosting Artefacts: Z-domain Analysis of Ghost Cancellation for Television Signals

This appendix proposes an approach to ghost cancellation for television signals by z -domain analysis [35]. Z -domain analysis estimates the zeros that are added by the reflections in the channel. Section A-1.2 presents a review of techniques for measuring ghosting artefacts due to multi-path and characterising channels in analogue television broadcasting. In section A.1.3 a possible technique is proposed for analogue or digital services which is limited in practice but of theoretical interest. As a direct method, it is sensitive to noise and numerical accuracy effects. The method can be improved by finding a better solution by iteration.

A-1.1 Background

At the frequencies used for terrestrial television broadcasting, signals propagate in straight lines. In addition to the direct path between the transmitting antenna and the receiving antenna, the same signal can also reach the receiver via reflections off nearby buildings and other large objects. Under such conditions, the receiver will display multiple images – a strong, main image and weaker shifted images resulting from the echoes. These secondary images are called ‘ghosts’ because they have the same information as the main image but offset in time, giving the appearance of a ghost. Ghosts can severely distract from the pleasure of television viewing. The propagation path to every receiver has different characteristics so the only practical solution to ghost reduction is to process the signal at the receiver. Ghost reduction can be achieved by characterizing the propagation channel for each receiver. Estimated channel characteristics can be treated as a measure of the ghosting artefact. The same measure can be used to evaluate the effectiveness of mitigation algorithms and deghosting apparatus. Although the channel characteristics usually vary slowly with time, they can be treated as time invariant from frame to frame. Hence an adaptive digital filter can be used to mitigate the ghosting artefact with the filter parameters changed dynamically according to the variations of the propagation channel.

Although digital television is being introduced, the worldwide complete change from analogue television broadcasting will take a few decades. Meanwhile the availability of processing power at the receiver is increasing rapidly. This processing power could be used to reduce ghosting by measuring multi-path delay and characterising the propagation channel where needed in fringe and uneven terrain areas of reception.

Ghosts may also appear in cable television either through impedance mismatches, or as a result of different modes of propagation within the cable. While the causes may be different, the effect on the viewed image is similar. Multi-path is a common problem in communication.

A-1.2 Multi-path Channel Characterisation

The available techniques can be classified as time domain or frequency domain methods based on the domain of analysis. It is also possible to classify the techniques of channel characterisation based on whether or not a reference signal is used. Researchers have developed a number of techniques for modelling, measuring, and mitigating ghosting effects in television broadcasting [164] to [190].

Komiya [164] proposed an adaptive ghost reduction system consisting of a cascaded ghost reduction filter and ghost reproduction filter. The system functions as a blind deconvolution system and to satisfy the reciprocity of transfer functions of these two filters, an adaptive process forces the system output waveforms to coincide with the input waveforms. This is classified as a no-reference, time domain technique.

Kouam et al. [165] developed a method capable of equalising long delays by a method of frequency domain filtering using small FFTs implemented by means of a decimation technique. This technique makes use of temporal windowing, frequency sub-sampling, and automatic selection of the number of filters required. With this technique it is possible to correct echoes even at high sampling frequencies. This is a reference based frequency domain technique.

Most of the research in 1980s and 1990s concentrated on the development of a ghost cancellation reference signal for television broadcasting. Greenberg [166] describes

ghost cancellation using a standard ghost cancellation reference (GCR) signal whereas references [167] to [172] either use another GCR or propose improvements to the referenced signal. The GCR signal consists of a frequency sweep or chirp of constant amplitude as shown in Figure. A-1.1.

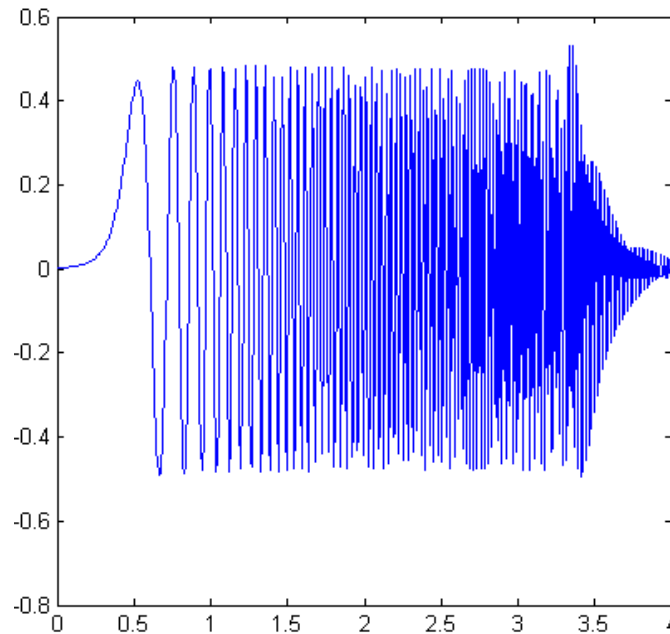


Figure A-1.1 A ghost cancellation reference signal as per standard created within the simulation environment [166]. This is the time domain waveform where x-axis can be mapped to any spatial width. (Units shown on x-axis are time frequency in MHz).

This maximises the energy within the signal while providing a flat frequency spectrum within the bandwidth of interest (DC to 5 MHz for PAL, DC to 4.2 MHz for NTSC). The chirp also has the property that its autocorrelation function is a narrow sinc function, enabling the channel impulse response to be obtained by correlation with a reference signal at the receiver. There are three world standards [173] for the GCR signal, the specifications for which are laid down in ITU-R recommendations [174]. Some television broadcast services transmit the standard GCR signal during the vertical blanking interval. A television receiver equipped with a GCR decoder uses the reference signal to characterise the channel and implement a compensation filter as described in section A.1.3.1. A possible explanation for the poor market response to the implementation of cancellation hardware into television receivers would be the cost of additional hardware in 1980s and 1990s.

Wang et al. [175] propose a frequency domain optimisation technique which requires a large number of FFT and inverse FFT operations to calculate the filters. However, the results are not reliable under high noise and strong ghost conditions. This is a reference based frequency domain technique.

Lei et al. [176] proposed a blind television ghost cancellation technique. Rather than use a special reference signal, the existing vertical edges in the television image are used to estimate the channel characteristics.

Gardner [177] and Johnson et al. [178] proposed ghost cancellation systems based on a ghost cancellation references. These two papers discuss theoretical studies, hardware test beds, laboratory tests and the field trials. Other research work by Case et al., Sherratt et al., Ledoux, Caron, Wang et al., and Appelhans et al. are published in [179] to [184] on ghost cancelling, techniques to measure the multi-path effect or to characterise the multi-path channel so that that information can be used to mitigate the ghosting.

Harasty et al.[185], Sherratt [186], Pao et al.[187], and Tzy-Hong et al. [188] proposed methods of correction filter design for ghost cancellation. Harasty et al. implemented the inverse filter as a non-causal recursive filter which can be realised as a low order filter and equalise both phase and magnitude [185]. Tzy-Hong et al. proposed to use the vertical synchronisation signal as a reference signal to characterise the channel [188].

The work presented in this appendix introduces a new method using z-domain analysis, for multi-path channel characterisation and the estimation of the correction filter. Since the main thrust of the thesis research is coding artefacts, the robustness and the noise performance of the method has not been evaluated. Recent work by Mousa et al. [189] and Pora et al. [190] focuses on the aspects of the implementation and synthesis of the cancellation filters at high level using synthesis tools and state-of-the-art programmable devices such as FPGA. The only recent advancements are on methods of synthesis and implementations but not on processing algorithms.

A-1.3 Analysis in the Z-Domain

This section concerns the z-domain modelling of the channel including the imperfections that give rise to ghosts. First the z-domain characteristics of the channel are investigated. Second, the implications these have on ghost cancellation are discussed. Finally, several techniques for estimating the channel characteristics from the z-domain are proposed. While the details given here relate directly to ghosting in television signals, much of the analysis is also applicable to other multi-path propagation problems in communication.

A-1.4 Channel Characteristics in the Presence of Echoes

The use of z-domain analysis implicitly assumes that the channel is a linear time invariant (LTI) system. While this is not strictly correct, in practice the channel characteristics change sufficiently slowly that a linear analysis provides a useful approximation [165]. The channel behaves as a filter, as shown in Figure A-1.2.

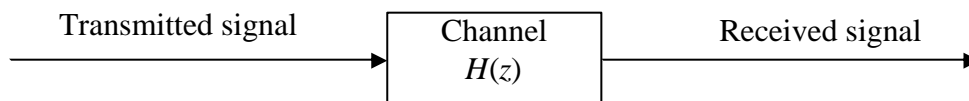


Figure A-1.2 The channel as a filter.

The effect of multi-path echoes is to give the channel an impulse response of the form shown in Figure A-1.3.

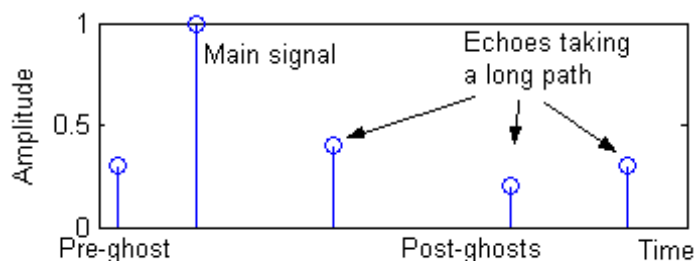


Figure A-1.3 Impulse response of a multi-path channel.

The main signal is defined as the strongest signal component. This is usually the direct signal, although in fringe areas, especially with irregular terrain, one of the reflected signals may be stronger than the direct signal. Each additional path to the receiver, resulting from reflections off buildings or other objects, contributes an extra impulse to the channel impulse response. The ghosts generally have lower amplitude than the main signal because of losses associated with the reflection and scatter and path loss over the extra propagation distance. In some circumstances, for example in the case where a television receiver is located in an area close to the transmitter, the direct pick-up by the receiver input circuit and antenna feeder, or when the main signal is not the direct signal, there may be one or more pre-ghosts [191]. Therefore the channel can be considered as a finite impulse response (FIR) filter because of this finite extent, and isolated impulses. It is necessary to understand the characteristics of this filter in order to develop a compensation filter.

First, consider a single ghost with amplitude of 0.4 relative to the main signal and delayed by one sample, as depicted in Figure A-1.4a. In the z-domain (Figure A-1.4b) the ghost results in a single zero at $z = -0.4$.

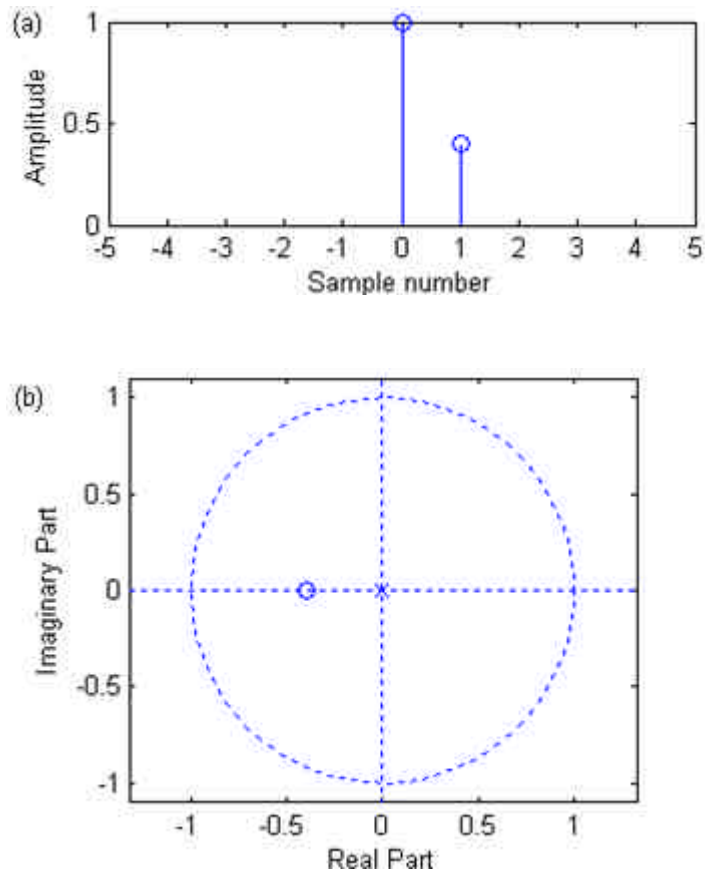


Figure A-1.4 (a) Impulse response of a channel with a single post-ghost with amplitude of 0.4. (b) The pole-zero plot for this channel.

In general, the position of the zero will depend on the amplitude of the ghost. If the channel is

$$H(z) = 1 + az^{-1}; \text{ where } |a| \leq 1 \quad (\text{A-1.1})$$

Then the zero will be located at $z = -a$, where a is the amplitude of the ghost.

This is an over-simplification. There will usually be a significant time delay between the main signal and any ghost, so the ghost will seldom occur in the subsequent sample. To illustrate the effect of such delay, Figure A-1.5 shows the same ghost delayed by 5 samples.

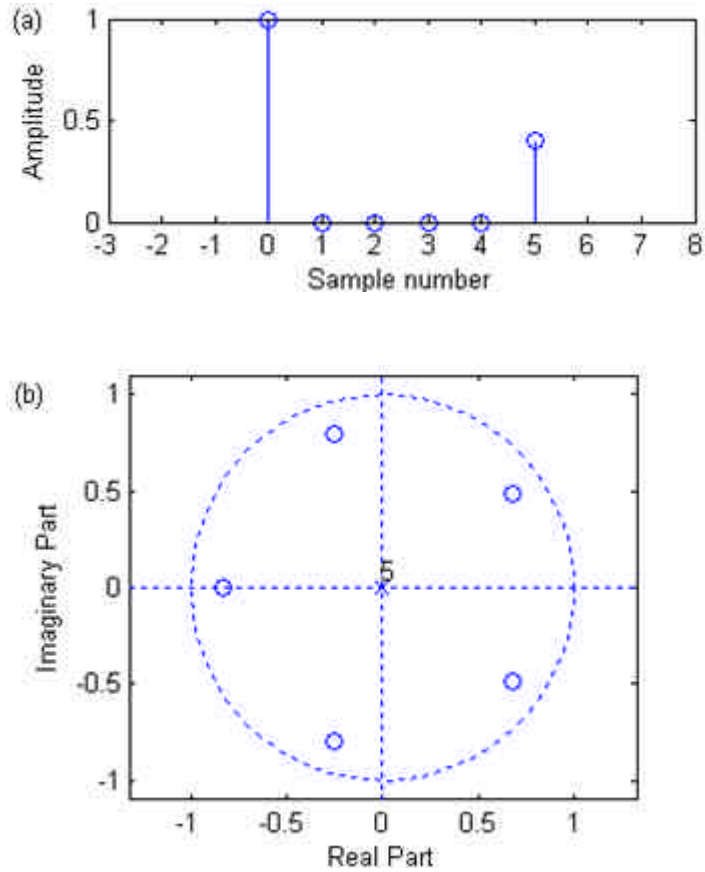


Figure A-1.5 (a) A channel with a single post-ghost delayed by 5 samples. (b) The corresponding pole-zero plot.

As the channel is now a 5th order system:

$$H(z) = 1 + az^{-5} \quad (\text{A-1.2})$$

There will be 5 zeros in the z -domain. Their locations are at

$$z = (-a)^{1/5} \quad (\text{A-1.3})$$

This has the zeros spaced at equal angles and at the same distance from the origin. For a given ghost amplitude, the more the ghost is delayed, the more zeros are introduced, and the closer they will be to the unit circle. Similarly, the larger the amplitude of the ghost a , the closer the zeros will be to the unit circle. Practically a is below 100% of the main signal due to scatter loss at the reflection or diffraction point [192]. When the channel has multiple post-ghosts, the number of zeros in the system depends on

the longest delay present. This is illustrated in Figure A-1.6. With multiple ghosts, the zeros are not all at the same radius or equally spaced. If one (or more) of the ghosts is significantly large then one or more of the zeros may move outside the unit circle. However, for post-ghosts encountered in practise, the ghost amplitude will decrease significantly with increased delay, and all of the zeros are typically inside the unit circle [166].

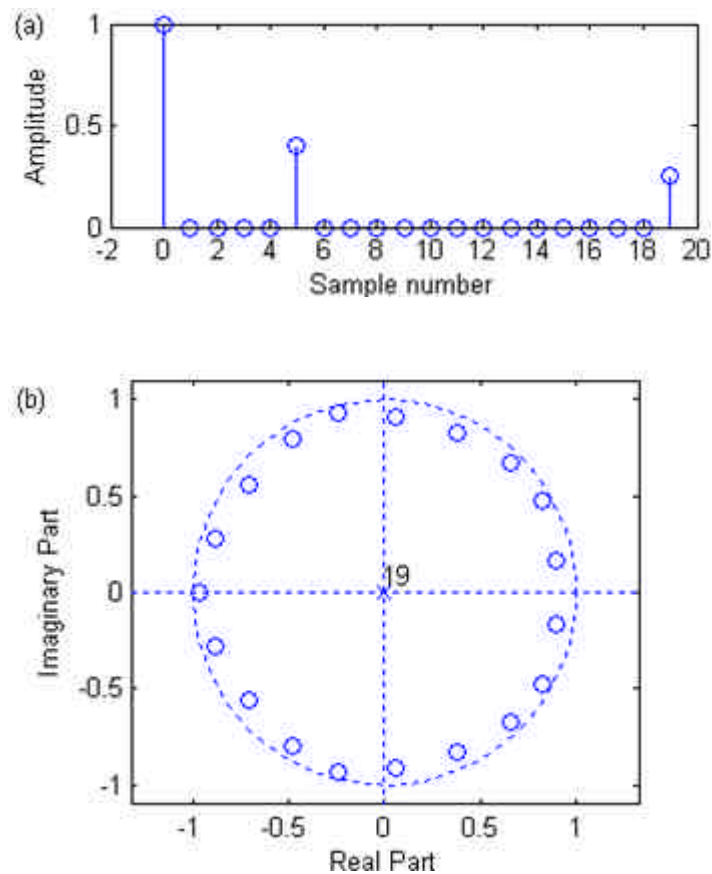


Figure A-1.6 (a) A channel with ghosts delayed by 5 and 19 samples. (b) Pole – zero plot of the channel with ghosts delayed by 5 and 19 samples

In some circumstances a ghost may appear before the main signal rather than after it. The effect of this is shown in Figure A-1.7.

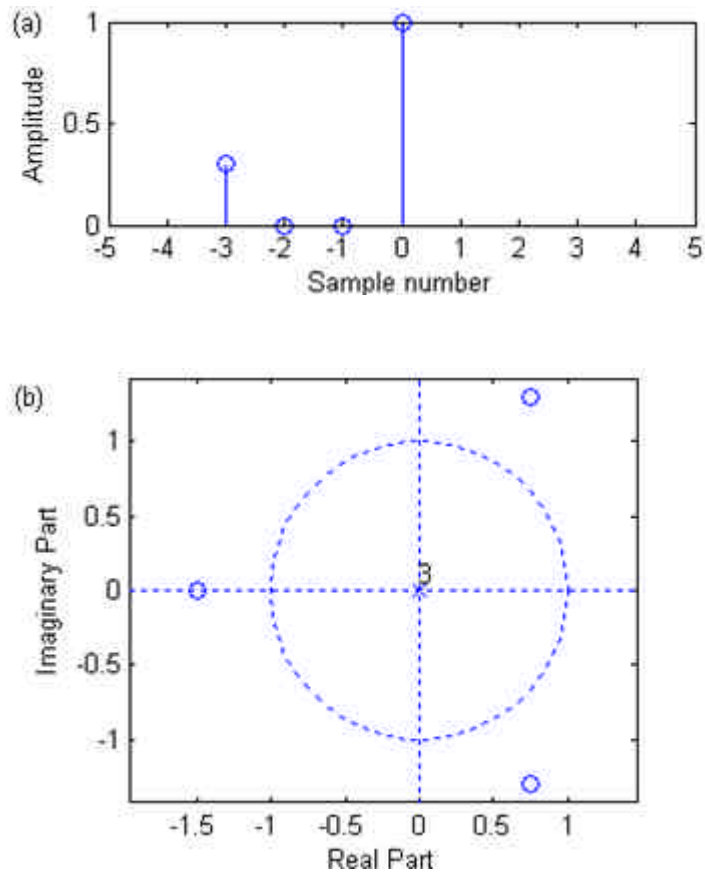


Figure A-1.7 (a) A single pre-ghost channel of 0.3 at -3. (b) The corresponding pole-zero plot.

The effect of ghosts before the main signal is to place the zeros outside the unit circle. This is because the signal is increasing in amplitude with time rather than decreasing. Again, the number of zeros depends on the position of the pre-ghost, and the radius depends both on the position and amplitude.

When pre-ghosts and post-ghosts are combined, the zeros outside the unit circle generally come from the pre-ghost(s) and those inside come from the post-ghosts. This is clearly seen in the example in Figure A1.8. Note that it is not just simple combining of the zeros of the pre- and post-ghost. All of the zeros will be perturbed by the addition of another ghost either before or after the main signal.

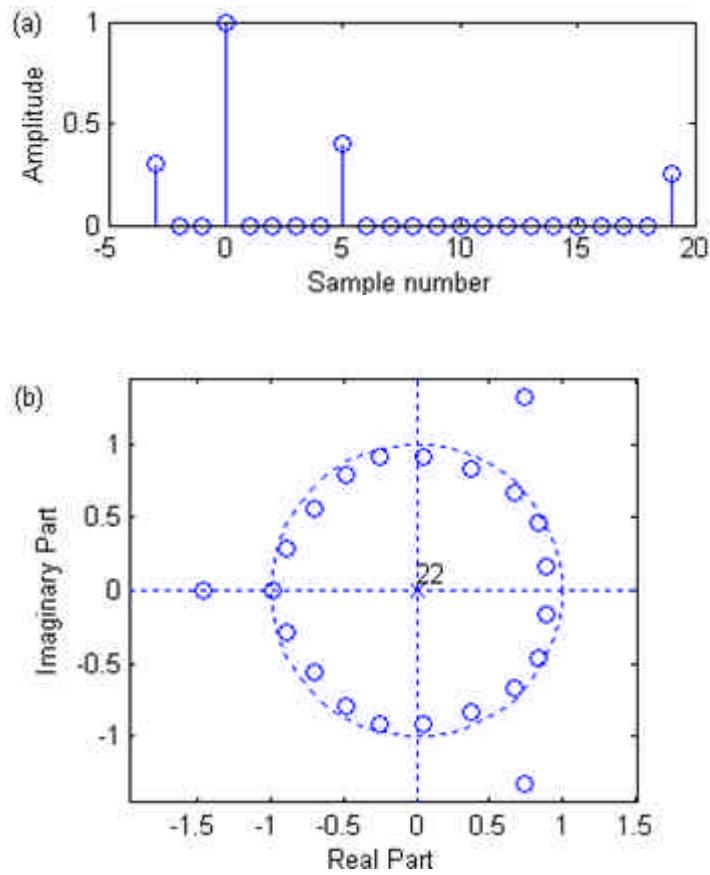


Figure A-1.8 (a) A Multi-path channel. (b) All zeros from the post-ghosts are inside the unit circle, and those from the pre-ghosts are outside.

While the number of zeros outside the unit circle is determined primarily by the position of the pre-ghost, it is possible to have additional zeros outside the unit circle from near post-ghosts, particularly if the post-ghosts have significant amplitude to bring one or more zeros close to the unit circle. This is shown in Figure A-1.9 where an additional post-ghost results in moving one of the zeros outside of the unit circle.

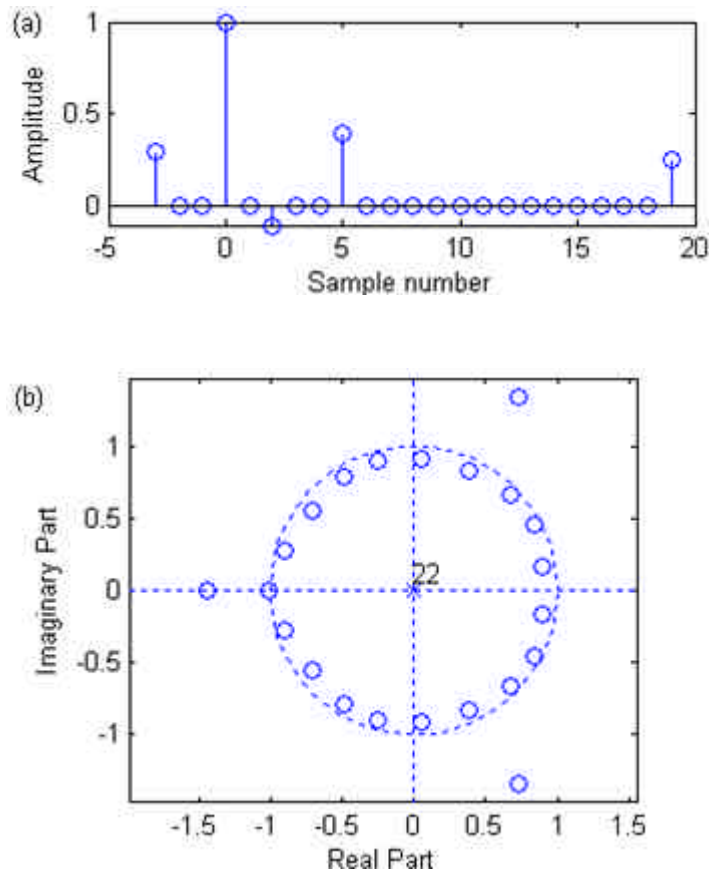


Figure A-1.9 (a) An additional post-ghost with amplitude -0.1 at sample 2. (b) This post-ghost moves an additional zero to outside unit circle.

A-1.5 Echoes and Ghost Cancellation

The ghost amplitudes in a typical channel are below -6 dB relative to the main signal. Pre-ghosts may occur up to 4 μs before the main signal, with post-ghost up to 40 μs after the main signal. When the video signal is sampled at 13.5 MHz, ghosts may be found between samples -54 and +540 [177].

Ghost correction may be accomplished by a correction filter as shown in Figure 4.10. Ideally we require $G(z)H(z)=1$ to completely eliminate the effect of multi-path reflections within the channel.

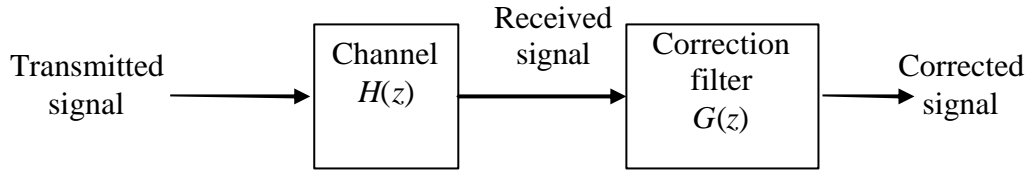


Figure A-1.10 Channel correction using a filter

Ideally, when only post-ghosts are present, all the zeros are within the unit circle. It is then possible to equalise the channel by placing the poles of $G(z)$ on zeros of $H(z)$ to cancel them, thus realising the inverse filter of the channel response. Since all of the poles of the inverse filter are inside the unit circle, this will result in a stable infinite impulse response (IIR) filter.

If the channel response has ghosts with amplitude g_i located at sample n_i , the channel can be represented as

$$H(z) = 1 + \sum_i g_i z^{-n_i} \quad (\text{A-1.4})$$

The correction filter is then given as

$$G(z) = \frac{1}{H(z)} = \frac{1}{1 + \sum_i g_i z^{-n_i}} \quad (\text{A-1.5})$$

Therefore the filter coefficients are given directly from the sampled impulse response. If the ghost amplitudes are sufficiently low that all of the zeros are within the unit circle, which is usually the case, the IIR filter may be safely implemented using its direct form. This does not even require factorising the channel response to locate the zeros.

When the channel introduces pre-ghosts, the same cancellation technique can not be used directly. Since a pre-ghost introduces zeros outside the unit circle, the resulting cancellation filter would have poles outside the unit circle, and would therefore be unstable.

Poles outside the unit circle correspond to a stable infinite anti-causal sequence, which is by definition unrealisable. However, the sequence can be truncated making it finite and then delayed, making it causal. This process is illustrated in Figure A-1.11 for the pre-ghost shown in Figure A-1.7. When both pre- and post-ghosts are present, the correction filter $G(z)$ can be split into two components: a FIR filter to cancel the pre-ghost and an IIR filter to cancel the post-ghosts. If there are no near post-ghosts, the FIR filter can be calculated using only the pre-ghosts. This is then convolved with the channel impulse response to remove the pre-ghost from that response, and the resultant signal used to calculate the IIR filter.

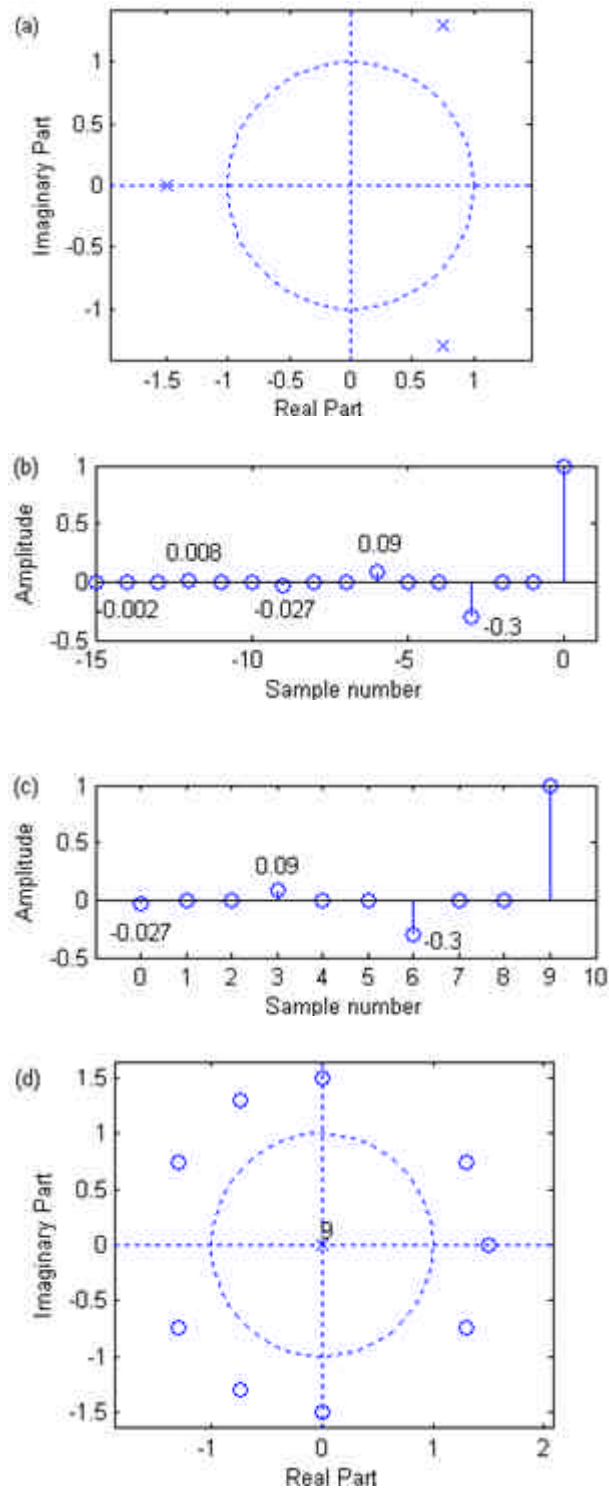


Figure A-1.11 Development of a compensation filter for a pre-ghost. (a) Desired pole locations. (b) Corresponding (stable) infinite anti-causal sequence. (c) Delayed truncated sequence. (d) Its corresponding pole-zero plot.

When there are near post-ghosts, the process will be more complicated because the convolution will result in further impulses before the main signal coming from the near post-ghost. One way around this is to find the roots of $H(z)$ and separate the zeros inside the unit circle from those outside. These can then be used independently for developing the corresponding FIR and IIR compensation filters. This approach is not particularly practical because finding the roots of a higher order polynomial is not trivial, and is very susceptible to round-off errors in the calculations.

An alternate approach is to take the pre-ghost and near post-ghosts within $4 \mu\text{s}$ and develop the FIR filter for cancelling the pre-ghost from this. While this still involves factorising a polynomial, this is more practical. Once the FIR filter has been determined, it can be convolved with the complete signal as before to give the IIR component. Rather than performing factorisation, the FIR filter may also be developed iteratively, by using adaptive filter algorithms [166].

If the channel is such that the post-ghosts are sufficiently large that they result in zeros on or outside the unit circle, cancellation is generally not possible. Zeros on the unit circle will result in loss of information at the corresponding frequency that cannot be recovered. While a zero outside the unit circle may be compensated for, this is generally not practical. Placing a pole just outside the unit circle will require a very slowly decaying anti-causal sequence. Consequently, a large number of coefficients must be used for the generated FIR filter to represent the sequence with any accuracy, making the filter too large for practical implementation.

A-1.6 Characterising the Channel

The analysis in the preceding section assumes that the channel impulse response, or equivalently the locations of the zeros in the z -domain, is known. This may be determined in number of ways, either directly or indirectly.

The direct approach is to periodically transmit an impulse signal, for example during the vertical blanking interval, and measuring the channel impulse response directly. While this gives the impulse response directly, it is limited by how much energy can be placed within a single impulse.

This approach may be extended by transmitting other known signals, and deconvolving the response to calculate the impulse response. The best results will be obtained when the input signal has components over the full range of frequencies. Rather than use dedicated signal, the line synchronisation pulse may be used. While not ideal – the rectangular pulse has a sinc frequency content with nulls – it does have significantly higher energy than a single impulse.

If the channel response to the horizontal synchronisation pulse is considered in the z -domain, there are two components:

$$Y(z) = H(z)X(z) \quad (\text{A-1.6})$$

The horizontal synchronisation pulse is a finite length signal, so $X(z)$ will consist only of zeros (all the poles are at the origin). As shown in section A-1.3.1, $H(z)$ also consists only of zeros. Since $Y(z)$ is the product of the two, it will directly combine the zeros of the two components. Since $X(z)$ is a known signal, with zeros sitting on the unit circle, these zeros may be eliminated from $Y(z)$ leaving only those from $H(z)$. In the case of the horizontal synchronisation signal, this is straight forward as the zeros of $X(z)$ all lie on the unit circle.

From a z -domain analysis, if the zeros of the signal are well separated from those of the channel, the zero locations may be found with more confidence. As all of the post-ghost zeros are close to, and inside the unit circle, if the zeros of the transmitted signal are outside the unit circle, this permits easy identification of the zeros associated with the channel. One signal with such characteristics is a truncated exponentially growing sequence, another simpler signal is a linear ramp.

There is not such problem with pre-ghost zeros since the pre-ghost is relatively close to the main signal and sufficiently low in amplitude that the zeros outside the unit circle can be easily identified.

This approach may be extended to achieve blind channel characterisation. When an arbitrary input signal is applied to the channel, again the zeros of the signal will combine with the zeros of the channel. This time the zeros can not be separated

because the input signal is unknown. However, with multiple independent input signals, the zeros associated with the channel should remain in the same locations, whereas the zeros from the input signals will change. The advantage of this approach is that it requires no additional information so the broadband television signal itself can be used to characterise the channel.

While this approach to blind channel characterisation works in theory, it is subject to three important limitations. First, for most wide band television signals, the z -transform of a single line of video will tend to have zeros spread around the unit circle. This is exactly where channel zeros are also likely to be found. Second, locating the zeros of the z -transform of a line of video is not a straight forward because of the high system order. There are large numbers of zeros spread around the unit circle, and their precise location requires high precision calculations. Round-off errors resulting from limited precision arithmetic can significantly perturb the zeros. Third, the higher the order of the system, the more sensitive the zero locations are to any noise that will inevitably be present on the received signal.

In practice, these limitations mean that this blind channel characterisation approach really only works with short duration signals under relatively low noise conditions.

A-1.7 Summary and Conclusions

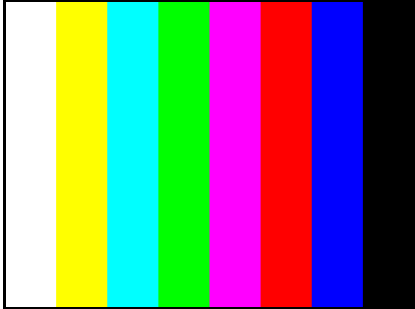
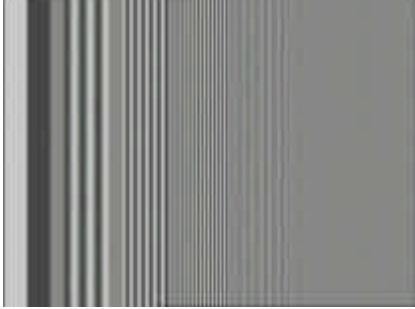

Z -domain analysis can be used to characterise propagation channels in broadcast television. It is shown that a channel may be considered as a FIR system. For channels with only post-ghosts it is possible to devise an equalisation filter that completely corrects for the effects of the channel provided that the zeros from the channel are all within the unit circle. When pre-ghosts are present, an exact stable equalisation filter is not possible. However, an arbitrarily close approximation may be derived using a combination of FIR and IIR filters. It has also been shown that it is possible to use the locations of zeros to estimate the channel characteristics without sending known reference signals specifically transmitted for ghost cancellation.

This appendix proposed an approach to ghost cancellation for television signals by z -domain analysis. Z -domain analysis estimates the zeros that were added by the

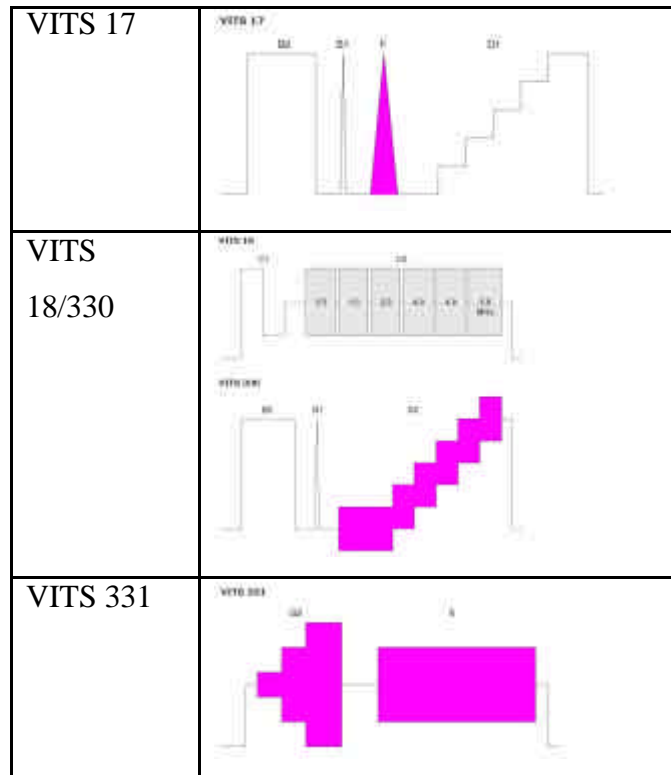
channel. First the z -domain characteristics for different multi-path channels are examined. Post-ghosts give zeros inside the unit circle, while pre-ghosts result in zeros outside the unit circle. From this, the effects of the z -domain characteristics of the channel on ghost cancellations are outlined. The zeros inside the unit circle may be cancelled directly by placing the poles of an IIR filter in the same locations. The zeros outside the unit circle resulting from pre-ghosts must be corrected by using a FIR filter. Several techniques of estimating the channel characteristics from the z domain characteristics are described. The channel estimation can be made without any special reference signal transmitted for this purpose. However the estimates are more reliable based on a known available signal, such as the horizontal or vertical synchronisation signals. A blind channel characterisation method based on matching zeros is proposed. However this new approach is quite sensitive to both noise and rounding errors. More work is required to make this a practical technique. The z -domain analysis performed here can also be applied to other multi-path propagation problems.

Appendix 2: Test Patterns used in Analogue Television Broadcasting:

Colour television has been in use since 1954 [193]. Prior to the adoption of digital codecs, colour television systems used analogue codecs such as NTSC, SECAM and PAL to encode and decode colour signals. When a video signal is coded and decoded, distortions are introduced. The nature of distortions depends on the particular codec used. Colour television information is transformed into the hue-saturation-intensity colour space [10]. The intensity component is a monochrome signal compatible with earlier monochrome television receivers. The chrominance components (hue and saturation) are used to modulate a high frequency sub-carrier. The hue controls the phase of the sub-carrier, and the saturation controls the strength or the magnitude of the sub-carrier. The different analogue television standards use minor variations on this coding mechanism. A composite television signal has both the luminance and chrominance combined into a single signal. In general, low frequency components of the luminance contain most of the energy. Hence the luminance component acts as a bias for the modulated chrominance information by modulating the operating point of the processing amplifiers over the picture. Hence hue and saturation at different spatial positions may be subject to differential gain and differential phase error resulting in distortions to the colour information. These colour errors can be evaluated using static test patterns or signals and the results are expressed as objective measures namely differential gain (DG) and differential phase (DP). As mentioned earlier, for nearly a half century synthetic colour test patterns have been used to evaluate analogue video and television systems [29]. However, the distortions introduced by digital codecs are of quite a different nature to those introduced by analogue codecs. If it is possible to use traditional test patterns or similar test patterns, it may be possible to evaluate image systems incorporating digital codecs.

Name of the Test Pattern	Test pattern	Distortion to be evaluated
Colour bars	 <p>Also called 75% Bars</p> <p>Except in white, each RGB colour component ranges from 0 to 525 mV (75% of 700 mV).</p>	Hue errors, Saturation errors
Multi-burst	 <p>Luminance pedestal at 350 mV across entire active line</p> <p>Reference flag is 420 mV peak-to-peak centred on pedestal</p> <p>6 packets of discrete luminance frequencies, at 0.5, 1.0, 2.0, 4.0, 4.8, and 5.8 MHz</p> <p>Each packet has an amplitude of 420 mV peak-to-peak centred on pedestal.</p>	Frequency response
Modulated ramp	 <p>Colour superimposed on luminance ramp</p>	DG and DP

Vertical Interval Test Signals:



Elements of VITS and usage:

Element	Test Element Name	Test Line Name	Measurements
B1	2T pulse	VITS 17	K Factor
B2	Luminance bar	VITS 17	Bar Line Time, Line Time Distortion
C1	Reference bar (flag)	VITS 18	Multiburst
C2	Multiburst packets	VITS 18	Multiburst
D1	Luminance staircase	VITS 17	Luminance Non-Linearity
D2	Modulated staircase	VITS 330	Differential Gain and Phase
F	Composite pulse	VITS 17	Chrominance to Luminance

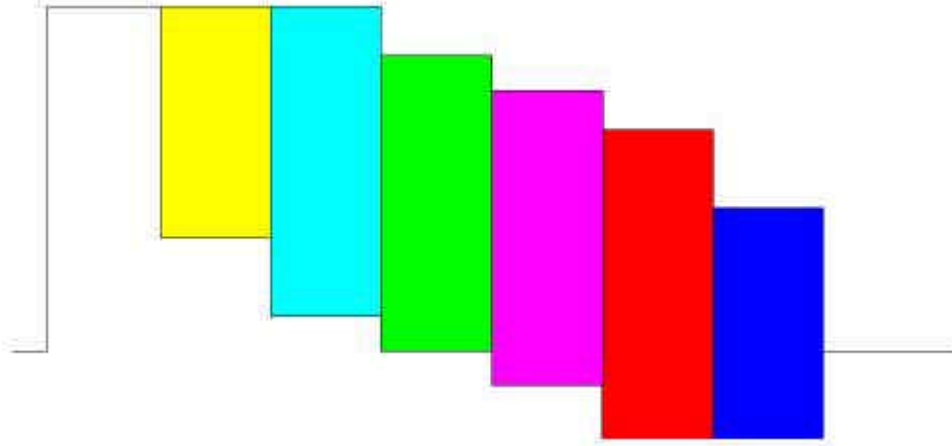
G2	Modulated bar	VITS 331	Chrominance Non-Linearity
–	Field Squarewave	Line Bars	Field Time Distortion
–	Sync and Burst	Any active line	Horizontal Timing
–	75% Colours bars	EBU Bars	Colour Bars
–	Ramp	Ramp	Noise Spectrum, Luminance Non-Linearity
–	Pedestal	Pedestal	Noise Spectrum
–	75% Red	75% Red	Sub-Carrier Frequency, Chrominance AM/PM

Each test element is typically used for a different type of measurement. The waveforms of the active picture region of most of these test lines are shown below. Note that the coloured areas are modulated in a particular colour (e.g. mostly magenta) and the grey areas are luminance frequency packets.

Colour bar signal amplitude values:

Colour	Luma Level (mV)	Chroma pk-pk (mV)	Phase (deg)
White	700.000	0.000	—
Yellow	465.150	470.499	167.11
Cyan	368.025	663.812	283.48
Green	308.175	620.092	240.66
Magenta	216.825	620.092	60.66
Red	156.975	663.812	103.48
Blue	59.850	470.499	347.11
Black	0.000	0.000	—

Colour bar signal waveform:



Appendix 3: ANSI T1.801.02-1996 Definitions of Compression Artefacts:

Blockiness or tiling distortion defined qualitatively as “distortion of the image characterised by the appearance of an underlying block encoding structure”

Blurring is qualitatively defined as "A global distortion over the entire image, characterized by reduced sharpness of edges and spatial detail"

Jerkiness is defined in ANSI T1.801.02-1996 as "Motion that was originally smooth and continuous is perceived as a series of distinct snapshots."

Appendix 4: Abbreviations

AC – Alternative current

ANSI – American National Standard Institute

CCB – Coding Colour Bleed

CHB – Coding Hue Bleed

CHS – Coding Hue Shift

CIE – International Commission on Illuminations

CLB – Coding Luminance Bleed

CLS – Coding Luminance Shift

CODEC – Coder - Decoder

CR – Compression Ratio

CSB – Coding Saturation Bleed

CSS – Coding Saturation Shift

DC – Direct Current

DCT – Discrete Cosine Transform

DCVC – Delay Cognizant Video Coding

DG – Differential Gain

DP – Differential Phase

DPCM – Differential Pulse Code Modulation

DSCQS – Double Stimulus Continuous Quality Scale

DVD – Digital Versatile Disk

EBCOT -

FFT – Fast Fourier Transform

FIR – Finite Impulse Response

FPGA – Field Programmable Gate Array

GCR – Ghost Cancellation Reference

GOP – Group Of Pictures

HVS – Human Visual System

ICT – Irreversible Colour Transform, used in JPEG2000

IIR – Infinite Impulse Response

IP – Internet Protocol

ISO – International Standard Organisation

ITU – International Telecommunication Union

JPEG – Joint Picture Expert Group, also a standard DCT based compression scheme recommended by the JPEG group.

JPEG2000 – A standard wavelet based compression scheme recommended by the JPEG group.

LTI – Linear Time Invariant

MAP – Maximum a Posteriori probability

MC – Motion Compensation

MOS – Mean Observer's Score

MPEG – Motion Picture Expert Group

MRF – Markov Random Fields

MSE – Mean Square Error

NIST – National Institute of Standard and Technology

NTSC – National Television System Committee

OFDM – Orthogonal Frequency Division Multiplexing

PAL – Phase Alteration by Lines

PAR – Picture Appraisal Rating

POCS – Projection On the Convex Set

PSNR – Peak Signal to Noise Ratio

QoS – Quality of Service

RCT – Reversible Colour Transformation (in JPEG 2000)

RGB – Red, Green and Blue

RMS – Root Mean Square

SECAM – *Séquentiel couleur à mémoire*, French for "Sequential Colour with Memory"

SNR – Signal to Noise Ratio

SPIHT -

SVC – Scalable Video Coding

TAE – Total Absolute Error

TV – Television

VQEG – Video Quality Expert Group

WWW – World Wide Web

YIQ – Analogue broadcasting colour space (for NTSC)

YUV – Analogue broadcasting colour space (for PAL)

Appendix 5: Glossary

Artefacts	particular visible effects, which are a direct result of some technical limitation
QoS	The collective effect of service performance which determines the degree of satisfaction of a user of the service.
Colour Bleeding	smearing of colour between areas of strong differing chrominance
Picture Quality	is actually picture degradation through the system and does not imply the intrinsic quality of the picture. Beauty is in the eye of the beholder and not something we can measure.
Jerkiness	represents artefacts of motion rendition in video, for example due to a varying or reduced frame rate chosen by the encoder.

Appendix 6: List of Image and Video Artefacts:

Artefact	Observable in	Cause	Mitigation	Technique used	Researcher
Blockiness	Compressed images	Block processing	Reduction	Block boundary discontinuity criterion	Jeon (1998)
Blockiness	Transform coded images	Transform coding	Reduction	Projection onto convex sets (POCS) -based post processing	Paek (1998)
Blockiness	Transform coded images	Transform coding	Reduction	A DCT-based spatially adaptive post processing	Paek (2000)
Blockiness	JPEG images	block coding	Reduction	Improved equations for JPEG	Lakhani(1997)
Blockiness	visual information transmitted over packet networks after block coding	Loss of data	concealment	A spatio-temporal concealment technique using boundary matching algorithm and mesh-based warping (BMA-MBW).	Atzori (2001)
Blockiness	Block-coded images	Block based processing	reduction	Wavelet-based subband decomposition.	Choi (2000)
Blockiness	JPEG coded images	JPEG coding	de blocking	Application of singularity detection	Hsung (1998)
Blockiness	Block coded images	Block coding	removal	Multilayer perception for adaptive post processing	Qiu (2000)
Blockiness	HDTV decoded images	Block coding	Reduction	Post-processing technique based on POCS	Kim (2001)
Blockiness	Block coded images	Block coding	Reduction	Wavelet transform	Kim N.C. (1998)
Blockiness	Block based coded video	Block processing	De blocking	Post processing using a deblocking filter	Kim S.D. (1999)
Blockiness	Image and video coding	Block-DCT scheme	reduction	Post processing algorithm based on Markov random fields (MRFs)	Meier (1999)
Blockiness	compressed images	Block-transform-coding	restoration	modelling the images as an MRF	Al-Shayka (1999)
Multi frame blocking artefacts	Transform coded video	Block based image or video compression	Reduction	Multi-frame constraint sets and projection schemes	Gunturk (2002)

	transform coded video	transform coding of video	reduction		Gunturk (2001)
	compressed images	image compression	reduction	Adaptive post filtering of transform coefficients	Chen (2001)
	coded images	DCT coding	reduction	noise estimation	Yang J (2000)
Coding artefact	Compressed video	video coding	ameliorate	Multi-channel regularised recovery	Choi (2001)
Ringing artefact	compressed images	compression	removal	Maximum-likelihood Parameter Estimation	Yang (2001)
	low bit rate moving picture coding	quantisation effects	reduction	post processing method	Park(1999)
	transform coded images	transform based coding	reduction	simple adaptive filter	Kaup (1998)
Blocking Artefact	Low bit rate video	video coding	Removal	Adaptive Constrained Least Squares Restoration	Kaup (1997)
Ghosting (Analogue)	TV signals	Multipath signals	Reduction	Reference Signal based - GCR	Greenberg (1993)
	TV signals	Multipath signals	Reduction	3-chip Digital Filter	Huang (1993)
	TV signals	Multipath signals	Reduction	An enhanced GCR	Fiallos (1994)
	TV signals	Multipath signals	Reduction	A new GCR	Yang K.S. (1994)
	TV signals	Multipath signals	Deghosting	A new GCR waveform	Al-Saud (1996)
	Transmitted video	Multipath signals	Reduction	Complex-value GCR	Wang (1991)
	Anlogue and Digital TV transmission	Multipath signals	Deghosting	Frequency division algorithm	Wang T.J. (1996)
	TV signals	Multipath signals	Cancellation	Small FFT's in Frequency domain	Kouam (1993)
	TV signals	Multipath signals	Cancellation	LMS iterative algoritms for filter coefficient calculation	Yong (1994)
	HDTV systems	Multipath signals	Cancellation	using a derivation of OLS learning algorithm	Pantsios (1995)
	TV signals	Multipath	Removal	Modification of th reference signal for fast convergence in LMS-based adaptive equalisers	Lee G.H. (1994)
	Stationary and Mobile	multipath signal	equalisation	blind equalisation	Appelhans (1995)

	Television				
	Advanced compatible TV systems	multipath	De-ghosting	Complementary sequences as a GCR	Roy (1992)
	TV signals	multipath signals	Canceller	an advanced single chip digital filter	Suzuki M. (1993)
	transmitted signals	multipath	elimination	a digital video equaliser	Kurita (1991)
	TV signals	Multipath signals	ghost canceler	using a digital processing IC	Kume (1992)
Ghosting (Digital)		Multipath signals	reduction	Adaptive filtering	Chini (1998)
Ghost	Analogue television	Multi path signals	Ghost cancellation	adaptive filtering using a reference signal	Greenberg (1993)
Multipath	TV signals	multipath signals	channel equalisation	Training signal and receiver design (precisely characterising the multipath channel)	Wang J. D (1990)
Ghost	Television and VCR	Multipath	cancellation	Special considerations	McNay (1995)
Ghosting	TV signals	Multipath signals	Simulator	Time domain TV ghost canceling	Markhauser (1993)
	TV signals	Multipath signals	Simulation	video ghost cancelling: evaluation by computer simulation and laboratory testing	Caron (1992)
	TV signals	Multipath signals	cancellation system	low cost stand-alone 3-IC system	Johnson (1994)
Ghost	TV signals	Multipath signals	Generator	a compact TV ghost generator	Tang (1990)
Ghost	TV signals	Multipath	canceling	Performance of TV ghost canceling systems under field test conditions	Tawil (1992)

Appendix 7: Vectorscope Graphs:

In television and video applications, a vectorscope provides a monitor for the purpose of measuring and testing television signals, regardless of format (NTSC, PAL, SECAM or any number of digital television standards). Broadcast engineers can measure the overall characteristics of a video signal, a vectorscope is used to visualize chrominance, which is encoded into the video signal in analogue television as a subcarrier of specific frequency. The vectorscope locks exclusively to the chrominance subcarrier in the video signal (at 3.58 MHz for NTSC, or at 4.43 MHz for PAL) to drive its display. In digital applications, a vectorscope instead plots the Cb and Cr channels against each other (these are the two channels in digital formats which contain chroma information).

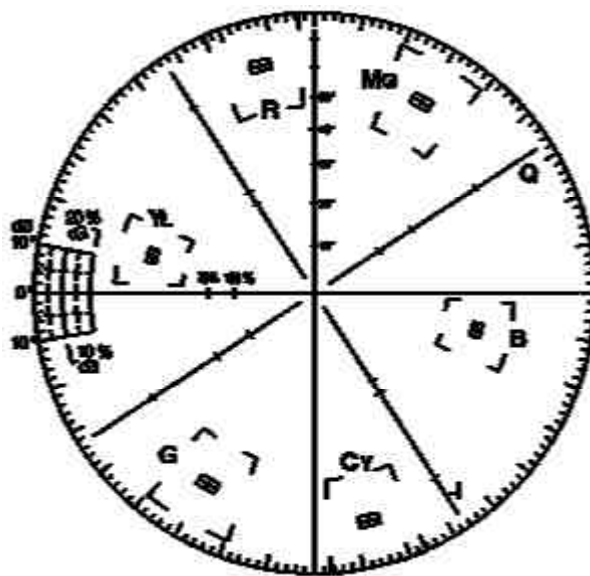


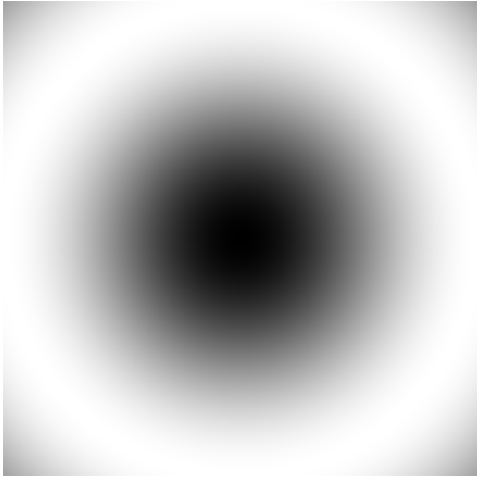
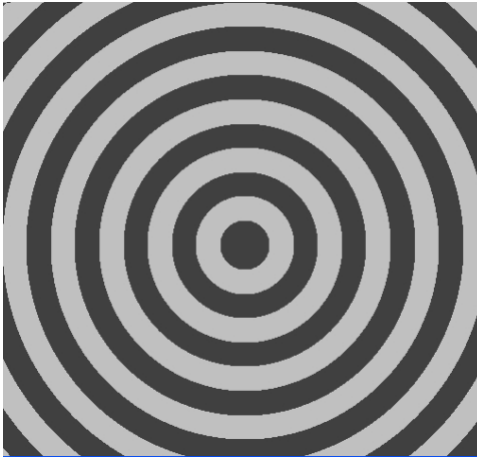
Figure A-7.1 The vectorscope graticule (reproduced from [15]).

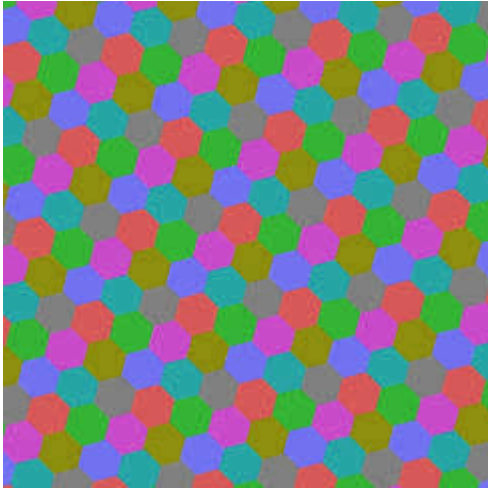
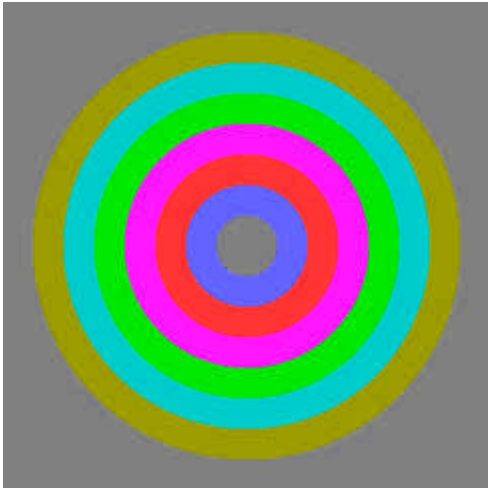
A vectorscope uses an overlaid circular reference display, or *graticule*, for visualizing chrominance signals, which is the best method of referring to the QAM scheme used to encode colour into a video signal. The actual visual pattern that the incoming chrominance signal draws on the vectorscope is called the *trace*. Chrominance is measured using two methods—colour saturation, encoded as the amplitude, or gain, of the colour red, subcarrier signal, and hue, encoded as the subcarrier's phase. The vectorscope's graticule roughly represents saturation as distance from the centre of the

circle, and hue as the angle, in standard position, around it. The graticule is also embellished with several elements corresponding to the various components of the standard colour bars video test signal, including boxes around the circles for the colours in the main bars, and perpendicular lines corresponding to the U and V components of the chrominance signal (and additionally on an NTSC vectorscope, the I and Q components). NTSC vectorscopes have one set of boxes for the colour bars, while their PAL counterparts have two sets of boxes, because the R-Y chrominance component in PAL reverses in phase on alternating lines. Another element in the graticule is a fine grid at the nine-o'clock, or -U position, used for measuring non-linear chrominance distortions due to luminance known as differential gain and phase.

Colour	Hue Angle - colour phase angle
Magenta	61°
Red	104°
Yellow	168°
Green	241°
Cyan	284°
Blue	348°

**Appendix 8: Test Patterns (uncompressed) that are
Designed and Used in this Thesis:**

Name of the Test Pattern	Test pattern	Image and Video Compression Distortion to be evaluated
Sine-squared grey scale - radial		Blockiness
Monochrome-rings		Edge blur and ringing

<p>Honeycomb (isoluma)</p>		<p>Colour bleeding – hue shift, hue spread, saturation shift, saturation spread, luminance spread, luminance shift</p>
<p>Colour rings (isoluma)</p>		<p>Colour ringing and colour blur</p>

Appendix 9: Bibliography:

This appendix provides a list of additional literature studied not referenced in the body of the thesis.

- [1] H. R. Wu and K. R. Rao, Eds. Digital Video Quality Perceptual Coding CRC Press, 2006.
- [2] D. S. Taubman, M. W. Marcellin, JPEG2000: image compression fundamentals, standards, and practice, Boston, Kluwer Academic Publishers, 2002.
- [3] R. C. Gonzalez , R. E. Woods, S. L. Eddins, Digital image processing using MATLAB, Upper Saddle River, N. J., Pearson Prentice Hall, 2004.
- [4] K. R Rao, Z. S. Bojkovic, Multimedia communication systems : techniques, standards and networks, Upper Saddle River, N.J. ; London, Prentice Hall PTR, 2002.
- [5] Multimedia communication technology: representation, transmission and identification of multimedia, Berlin; New York, Springer, c2004.
- [6] E. G. H.264 and MPEG-4 video compression : video coding for next-generation multimedia, Chichester, Wiley, 2003
- [7] A. E. Mohammed, C. N. Canagarajah, D. R. Bull, Video coding for mobile communications : efficiency, complexity and resilience, San Diego, Calif. ; London, Academic, 2002.
- [8] J. Ozer, Jan, Video compression for multimedia Effelsberg, Wolfgang, 1995.
- [9] W. Effelsberg, R. Steinmetz, Video compression techniques, Heidelberg Germany, Dpunkt-Verlag, 1998.
- [10] Z. N. Fundamentals of multimedia, Upper Saddle River, NJ, Pearson Prentice Hall, 2004.
- [11] T. Acharya, P. S. Tasi, JPEG2000 standard for image compression: concepts, algorithms and VLSI architectures, Hoboken, N.J., Wiley-Interscience, 2005.

- [12] R. C. Gonzalez, R. E. Woods, Digital image processing, Harlow : Prentice Hall, 2008 3rd Ed.
- [13] K. R. Castleman, E. Cliffs, Digital image processing, N.J., Prentice Hall, 1996.
- [14] W. K. Pratt, Digital image processing, New York, Wiley, c1991, 2nd ed
- [15] R. C. Gonzalez, P. Wintz, Digital image processing, Addison-Wesley, 1987.
- [16] B. Jähne, Digital image processing, Berlin: Springer, 2005, 6th revised and extended edition.